

The Cryogenic Storage Ring CSR



electrostatic storage ring with
circumference ≈ 35 m
first beam stored: March 2014
cryogenic operation: since April 2015
first electron cooled ion beam: June 2017

Manfred Grieser

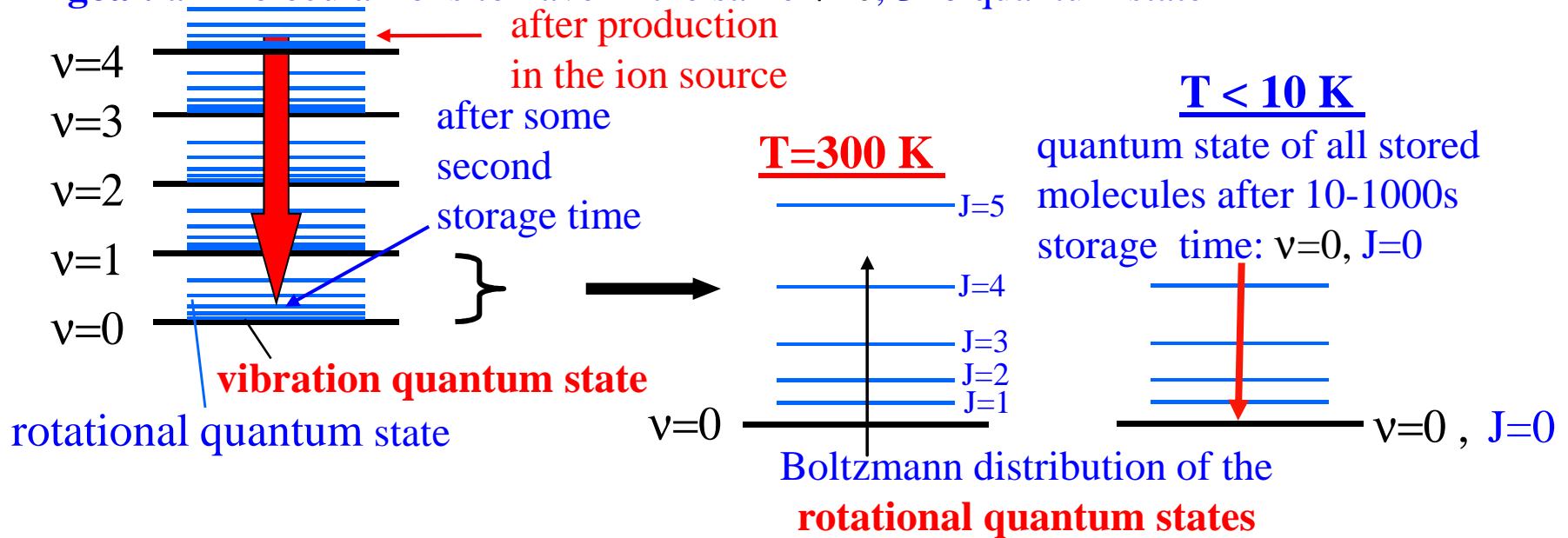
Max Planck Institute for Nuclear Physics

Jülich , January 25th, 2018

Purpose of the CSR

main research field: molecular ion physics

goal: all molecular ions to have in the same $v=0, J=0$ quantum state

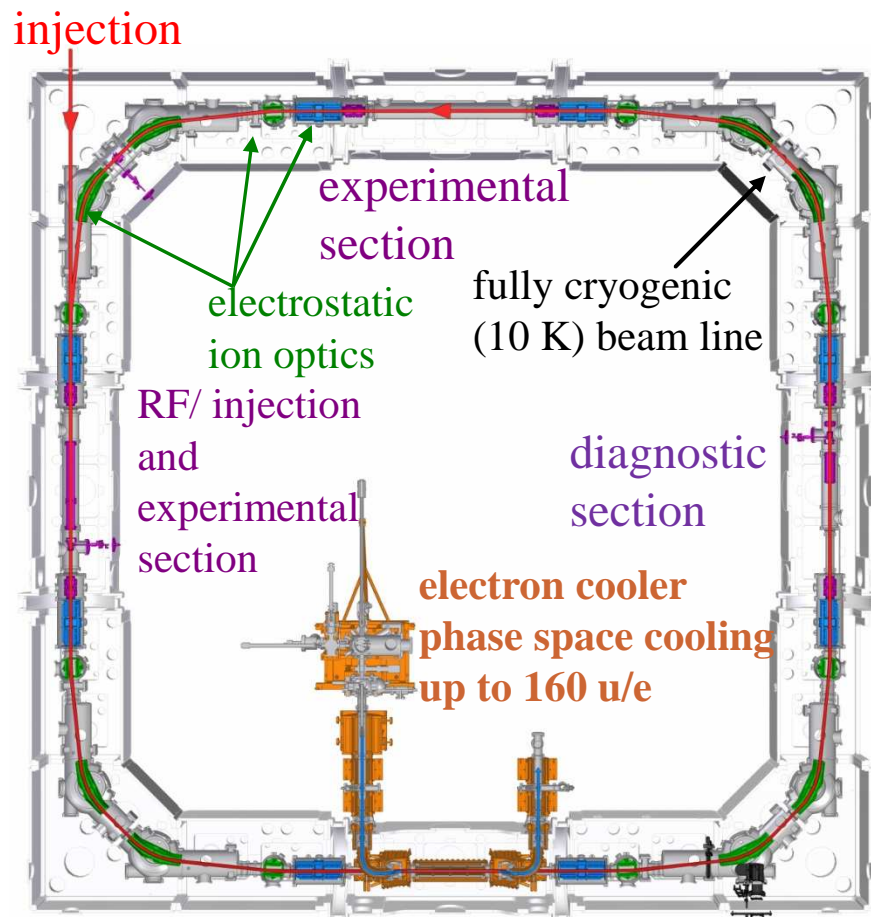


to get all molecular ions in the same molecular quantum state ($v=0, J=0$) the molecular ions have to be stored at $T < 10\text{ K}$

⇒ a new Cryogenic Storage Ring (CSR) at MPIK Heidelberg

in opposite to other storage rings it is an **electrostatic storage ring**

Overview of the CSR

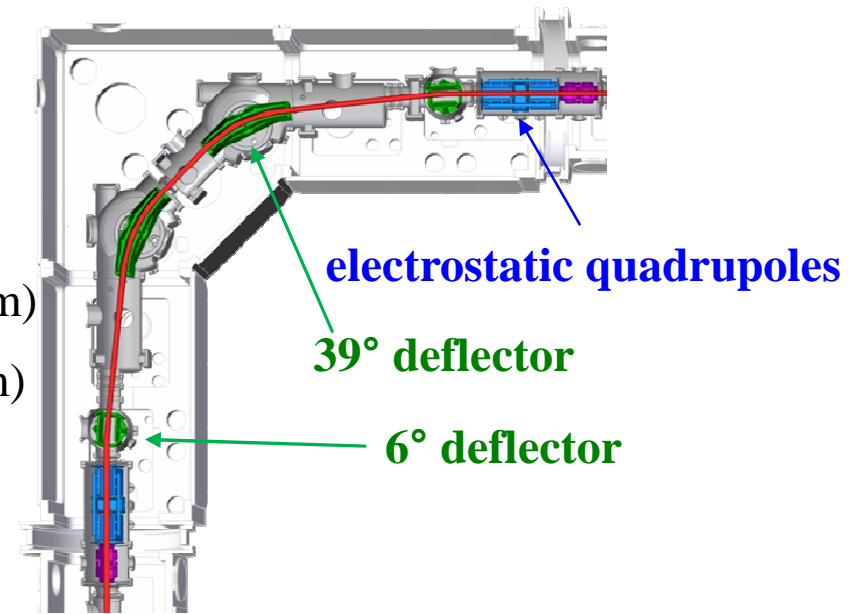


circumference: ≈ 35 m
beam energy: $(20-300) \cdot q$ keV
temperature: 10-300 K
residual gas densities:
(at $T < 10$ K): < 20 molecules/cm³

with electron cooling
m/q range: 1 -160
(at $E/Q=300$ kV)
lowest rigidity: p^+ , H^- at $E/Q=20$ kV
 $B\rho=0.02$ Tm

Electrostatic beam optics Elements

- 4-fold symmetric storage ring
all CSR corner sections identical
- 8 pairs of **quadrupoles** (± 10 kV, $\varnothing = 100$ mm)
- 8 **6°- electrostatic deflector** (± 30 kV, $g=120$ mm)
- 8 **39°-electrostatic deflector** (± 30 kV, $g=60$ mm)
- 8 vertical electrostatic deflectors



39° cylindrical deflector

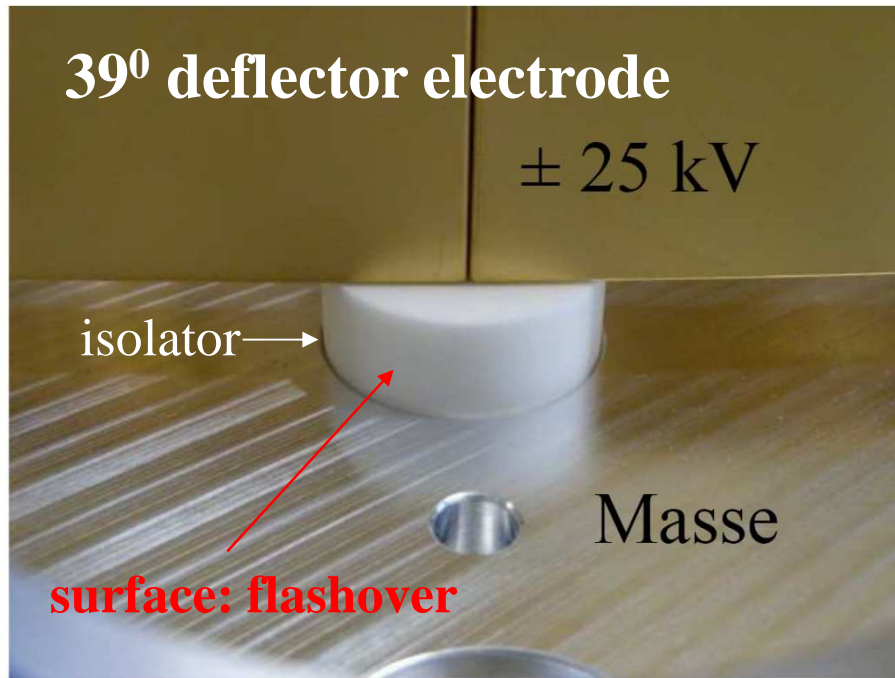


electrostatic quadrupoles with vertical steerer

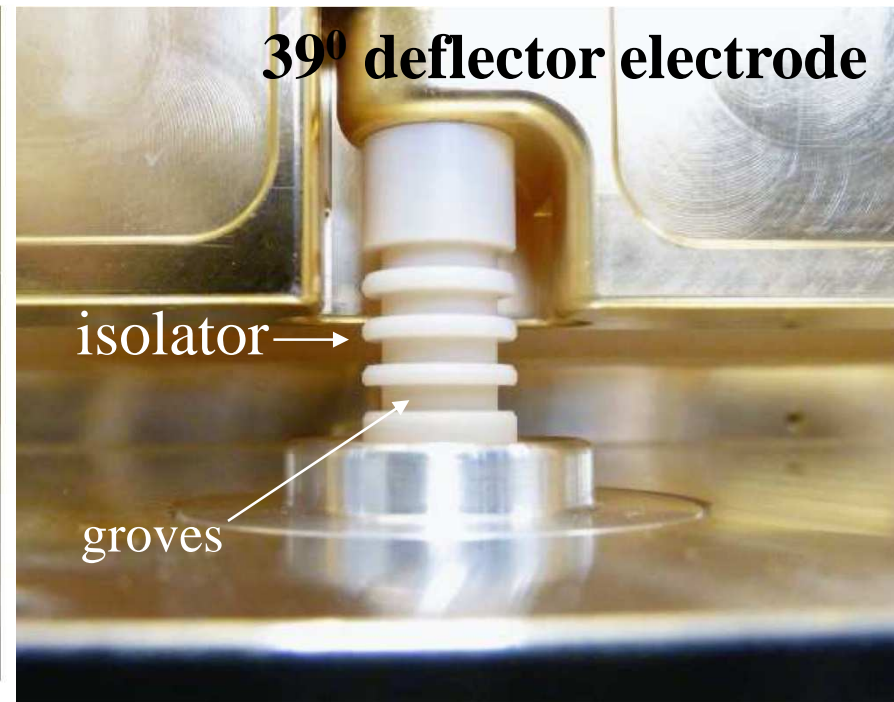


High voltage Isolators of 39° deflector electrodes

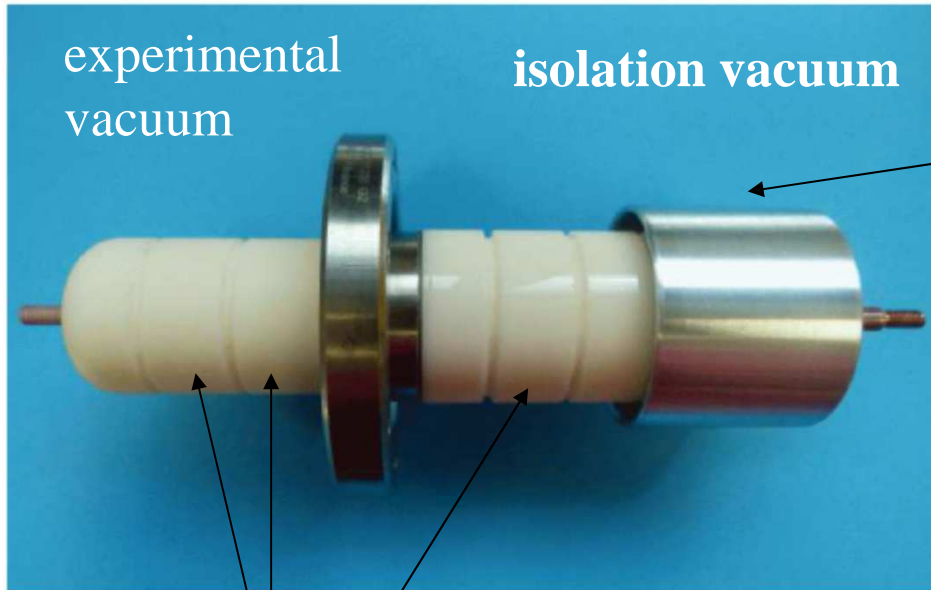
old design



new design



Prevent of flashover



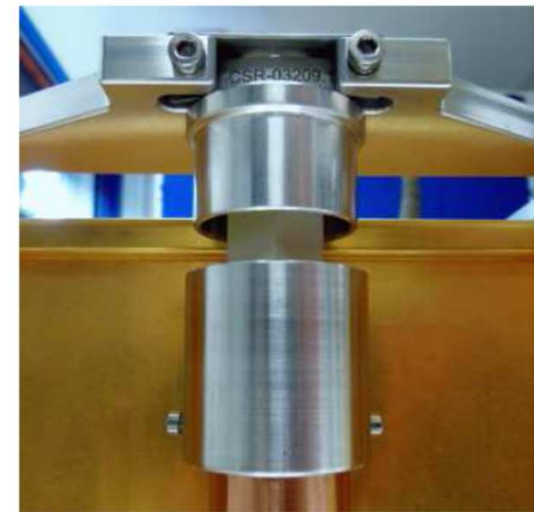
modification of the high voltage feed through

Grooves to avoid flashover

ceramic isolator of the quadrupoles

old design

new design



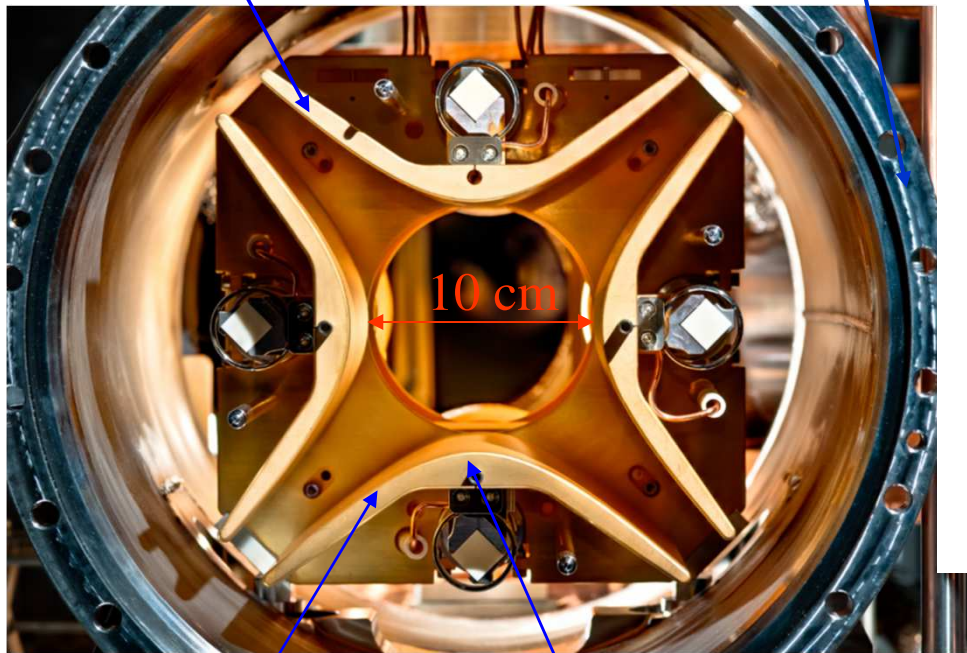
(a)

(b)

Electrostatic Quadrupole of the CSR

quadrupole
electrode

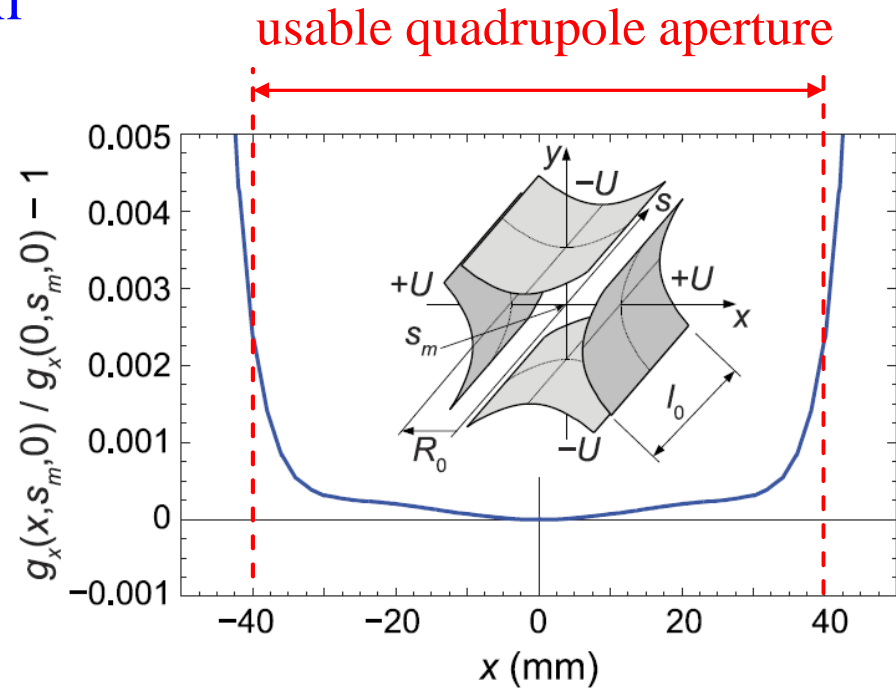
inner vacuum
chamber



quadrupole
electrode

hyperbolic
profile

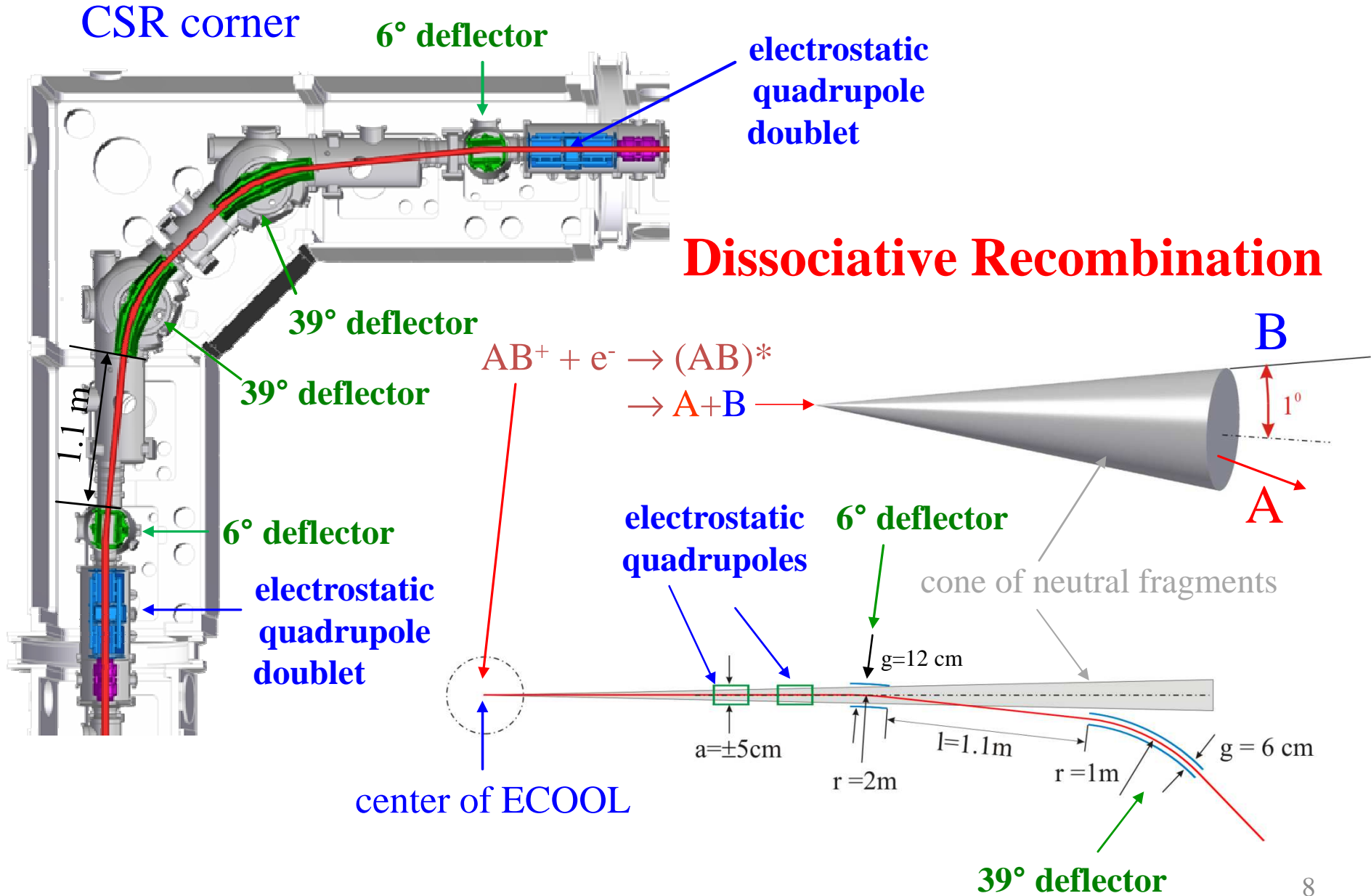
maximum electrode voltage: $U_{\max} = \pm 10 \text{ kV}$



Relative deviation of the field gradient in the CSR focusing quadrupole. The longitudinal coordinate lies in the middle of a quadrupole unit.

$l_0 = 200 \text{ mm}$

Lattice of the CSR



Lattice calculation with MAD8

MAD8 provides the opportunity to define transport matrixes by the user.

To get the 6x6 transport matrixes for the electrostatic elements the equation of motion was investigated analytical by solving the differential equation:

$$\frac{d\vec{p}(\vec{r}(t))}{dt} = Q\vec{E}(\vec{r}(t))$$

← electrical field in the electrostatic elements

with Mathematica

Cylinder deflector matrix in MAD8:

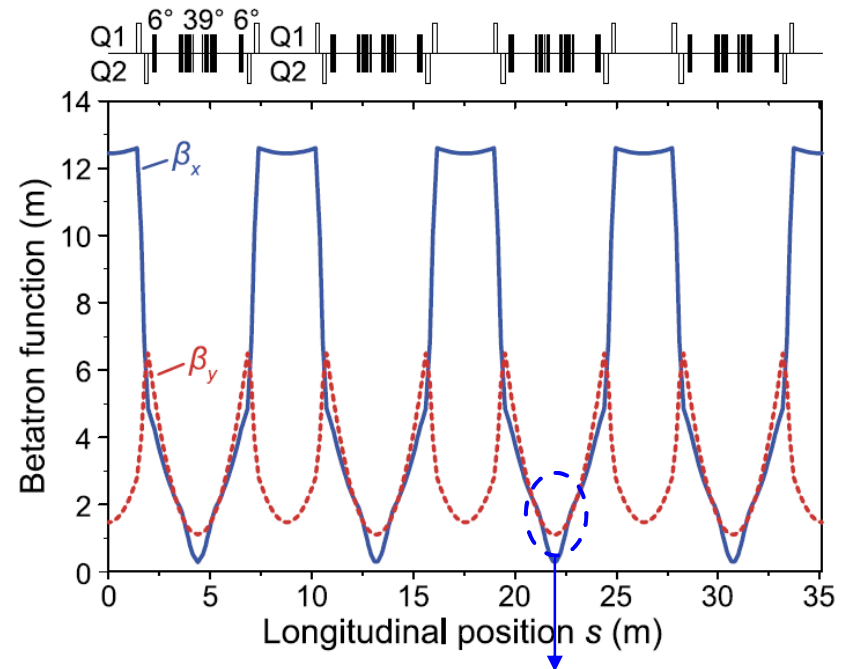
```
RK:=SQRT(2.)/RHO
DISP:=2./RHO
```

```
DEFLECTOR SEC : MATRIX, L=LD, RM(1,1)=COS(RK*LD), &
  RM(1,2)=(SIN(RK*LD))/RK, &
  RM(1,6)=(1-COS(RK*LD))*DISP/RK/RK/BETA, &
  RM(2,1)=-SIN(RK*LD)*RK, RM(2,2)=COS(RK*LD), &
  RM(2,6)=SIN(RK*LD)*DISP/RK/BETA, &
  RM(3,3)=1, RM(3,4)=LD, &
  RM(4,3)=0, RM(4,4)=1, &
  RM(5,1)=-SIN(RK*LD)*DISP/RK/BETA, &
  RM(5,2)=- (1-COS(RK*LD))*DISP/RK/RK/BETA, &
  RM(5,5)=1.0, &
  RM(5,6)=(- (LD-SIN(RK*LD)/RK)*DISP*DISP/RK/RK+ &
  LD/GAMMA/GAMMA)/BETA/BETA, &
  RM(6,6)=1.0
```

transit time effects: η, f_s ..

```
a: vkicker
DEFLECTOR: line(a,10*(DEFLECTOR_SEC,a))
```

Example of MAD8 calculation



small horizontal beam size in the deflectors

Horizontal and vertical betatron functions

β_x and β_y calculated by the MAD8 code for the standard settings of the CSR ($Q_x=Q_y=2.59$)

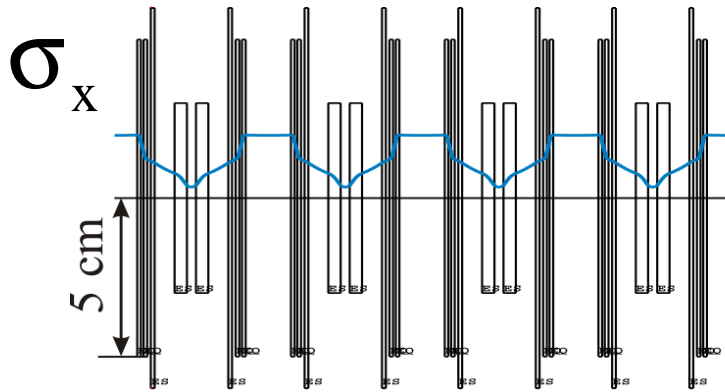
coupling of the horizontal and vertical motion.

Coupling effects were been investigated experimentally and by simulation (later in the talk)

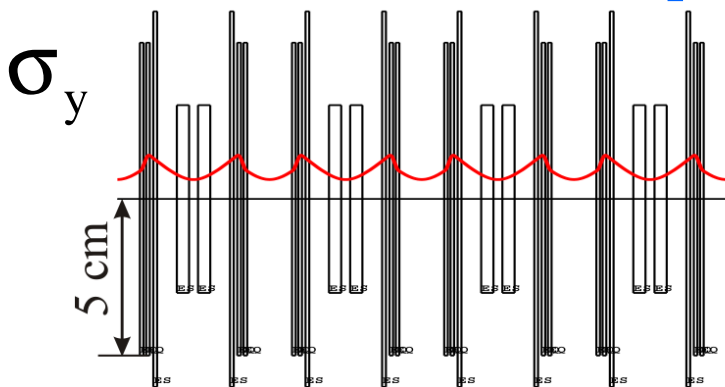
β function and envelopes (standard mode)

COSY infinity calculation

horizontal beam envelope



vertical beam envelope



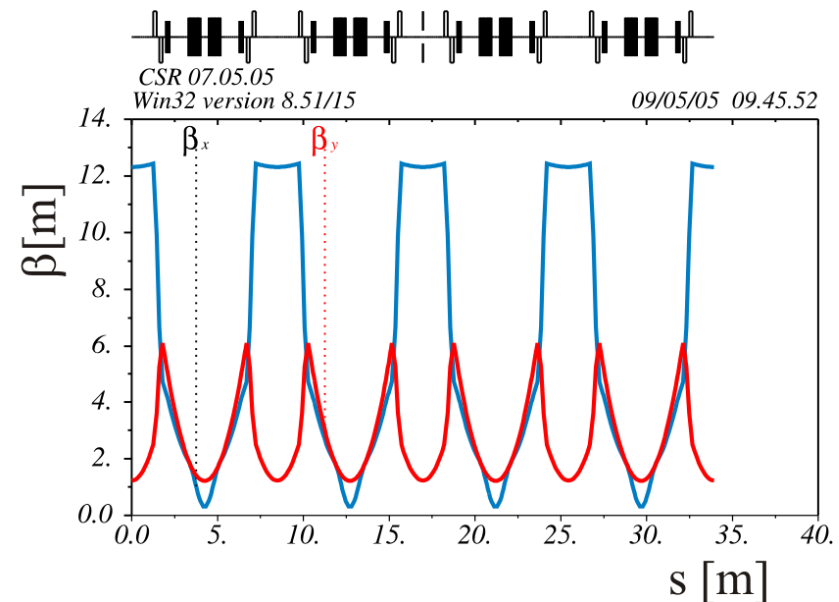
quadrupole settings:

$$Q_1: k = 5.58 \text{ 1/m}^2 \Leftrightarrow 4.19 \text{ kV (E/Q=300 kV)}$$

$$Q_2: k = -7.04 \text{ 1/m}^2 \Leftrightarrow -5.28 \text{ kV (E/Q=300 kV)}$$

MAD8 calculation

horizontal and vertical β function



envelopes calculation for

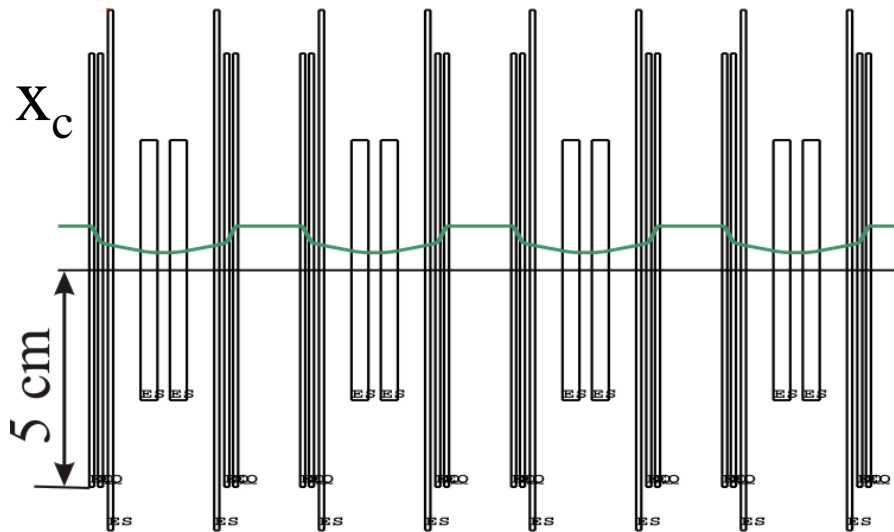
$$\varepsilon_x = 100 \text{ mm} \cdot \text{mrad} \quad \varepsilon_y = 100 \text{ mm} \cdot \text{mrad}$$

$$\varepsilon_x = \frac{(2 \cdot \sigma_x)^2}{\beta_x} \quad \varepsilon_y = \frac{(2 \cdot \sigma_y)^2}{\beta_y}$$

Dispersion (standard mode)

COSY infinity calculation

closed orbit x_c for $\Delta E/E=0.01$

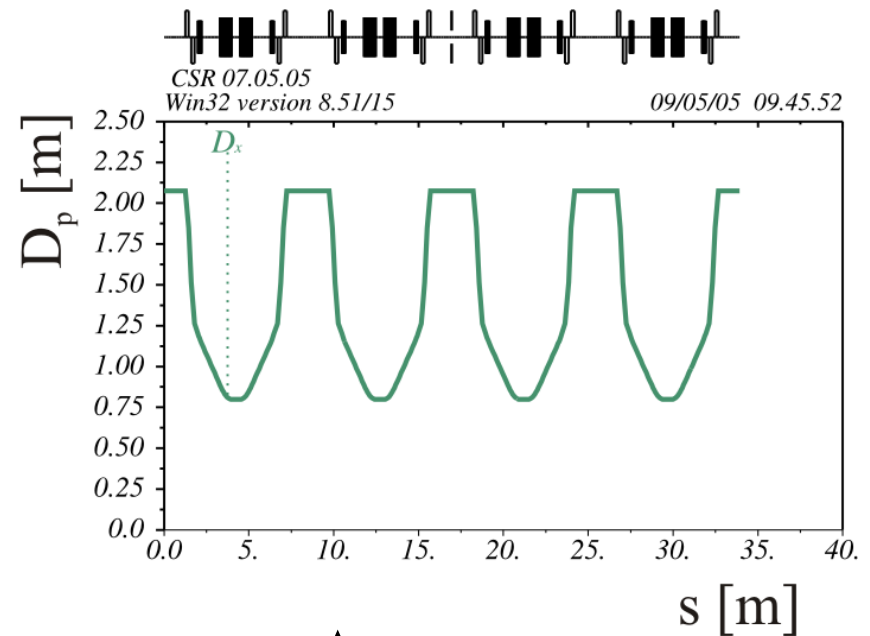


$$x_c = D_E \cdot \frac{\Delta E}{E} \Rightarrow D_{E,\max} = 1.04 \text{ m}$$

$$\Leftrightarrow D_{p,\max} = 2.08 \text{ m}$$

quadrupole settings:

MAD8 calculation



$$x_c = D_p \cdot \frac{\Delta p}{p}$$

$$D_{p,\max} = 2.08 \text{ m}$$

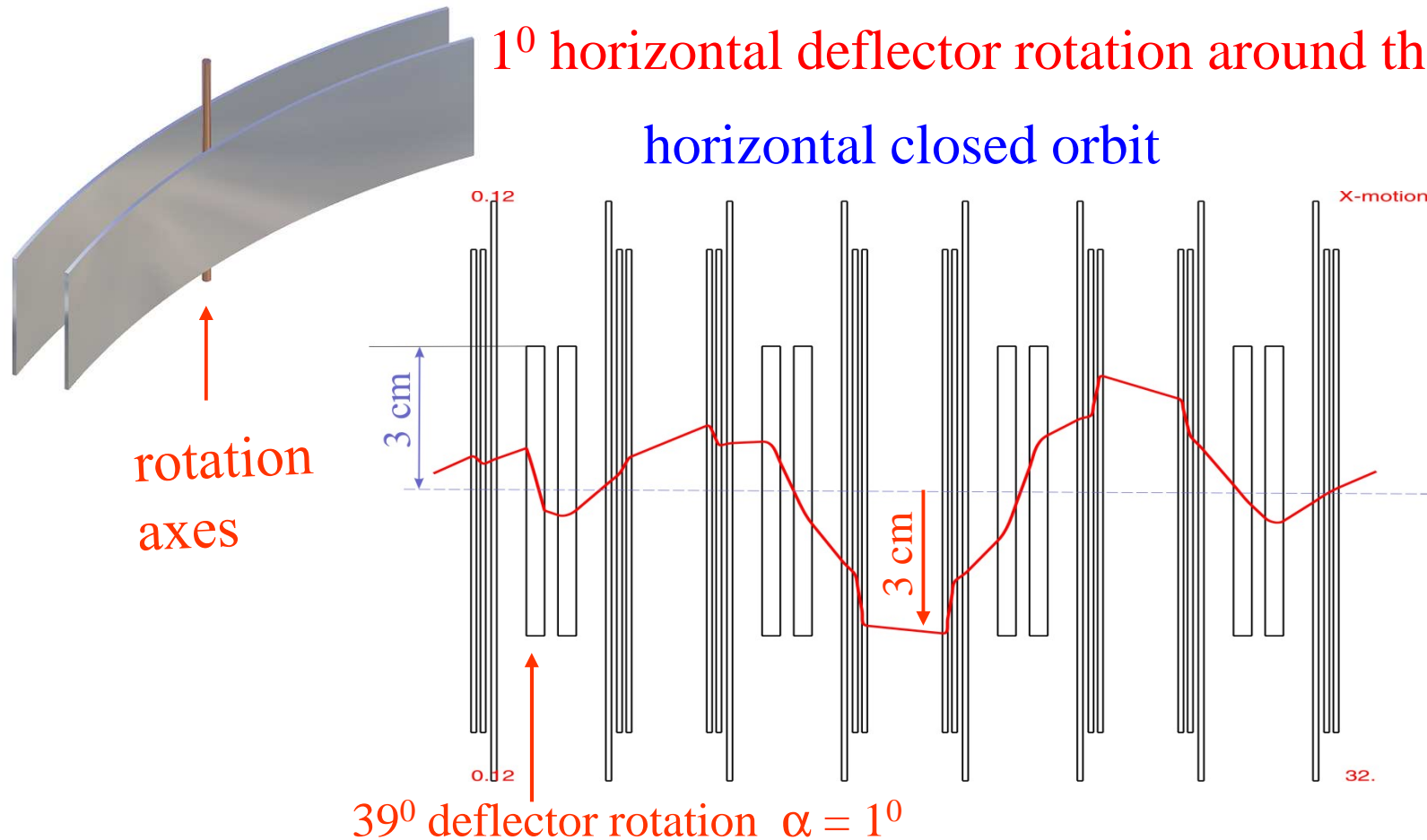
Q_1 : $k = 5.58 \text{ 1/m}^2 \Leftrightarrow 4.19 \text{ kV (E/Q=300 kV)}$

Q_2 : $k = -7.04 \text{ 1/m}^2 \Leftrightarrow -5.28 \text{ kV (E/Q=300 kV)}$

Determination of misalignment effects with COSY Infinity

Misalignment of the 39⁰ deflector

1⁰ horizontal deflector rotation around the y-axes



maximum closed orbit distortion should be less than 1 mm

⇒ alignment error $\alpha \leq \pm 0.03^{\circ}$

Alignment precision

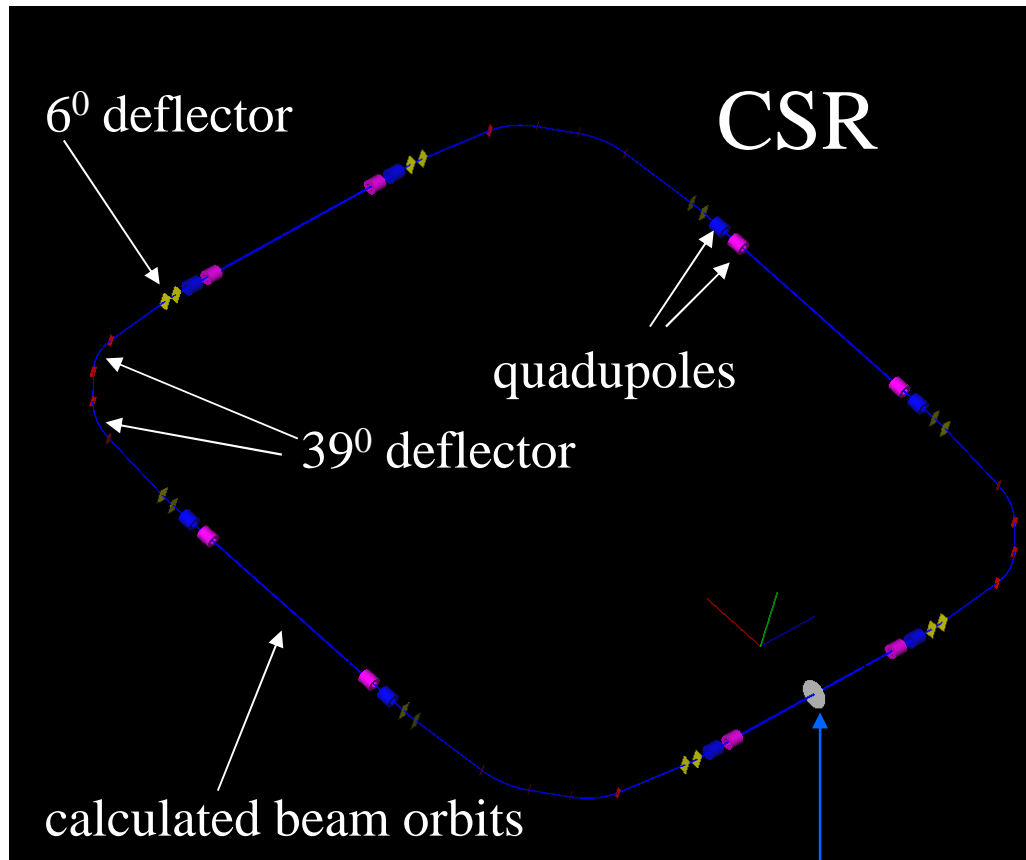
Calculated for a maximum closed orbit shift of 1 mm

element	degree of freedom	nominal value	measurements*
6°-Deflektor	Rot. horiz.	$\leq 0,15^\circ$	$0,095^\circ \pm 0,058^\circ$
6°-Deflektor	Rot. vert.	$\leq 0,15^\circ$	$0,022^\circ \pm 0,001^\circ$
6°-Deflektor	Transl. horiz.	$\leq 1,0 \text{ mm}$	$0,40 \text{ mm} \pm 0,05 \text{ mm}$
39°-Deflektor	Rot. horiz.	$\leq 0,03^\circ$	$0,000^\circ \pm 0,004^\circ$
39°-Deflektor	Rot. vert.	$\leq 0,06^\circ$	$0,016^\circ \pm 0,004^\circ$
39°-Deflektor	Transl. horiz.	$\leq 0,5 \text{ mm}$	$0,20 \text{ mm} \pm 0,03 \text{ mm}$
Quadrupoldublett	Rot. horiz.	$\leq 0,015^\circ$	$0,000^\circ \pm 0,010^\circ$
Quadrupoldublett	Rot. vert.	$\leq 0,03^\circ$	$0,040^\circ \pm 0,016^\circ$
Quadrupoldublett	Transl. horiz.	$\leq 0,50 \text{ mm}$	$0,30 \text{ mm} \pm 0,05 \text{ mm}$
Quadrupoldublett	Transl. vert.	$\leq 0,40 \text{ mm}$	$0,16 \text{ mm} \pm 0,05 \text{ mm}$

*Alignment change measurements of the ion optical elements during the cool down process from room temperatures below T=40 K

Tracking through real electrostatic fields with G4beamline

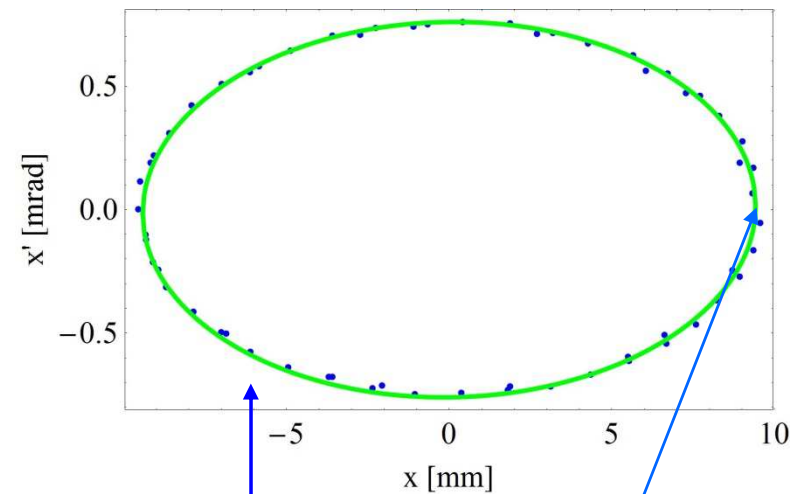
G4beamline screen output



each element is described by the field table obtained with TOSCA

start and observation point of the **phase space coordinates**

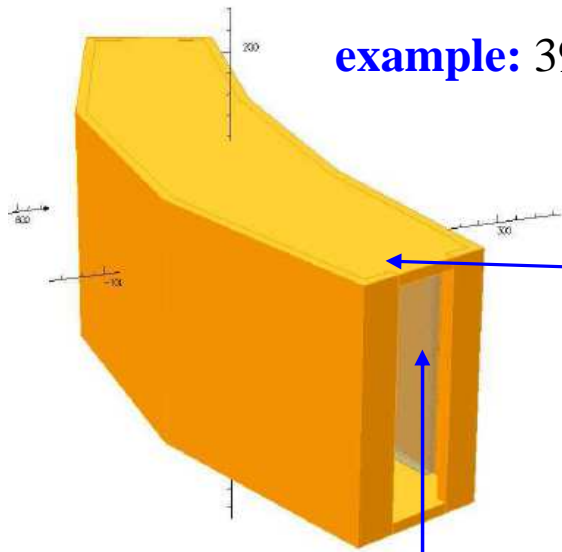
horizontal phase space coordinates of a single particle at observation point obtained for several turns



start coordinate $x=10$ mm

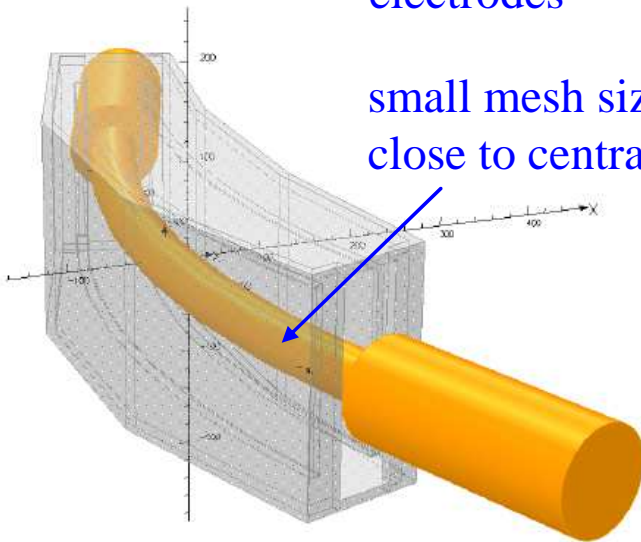
Calculation of the field maps with TOSCA

example: 39° deflector



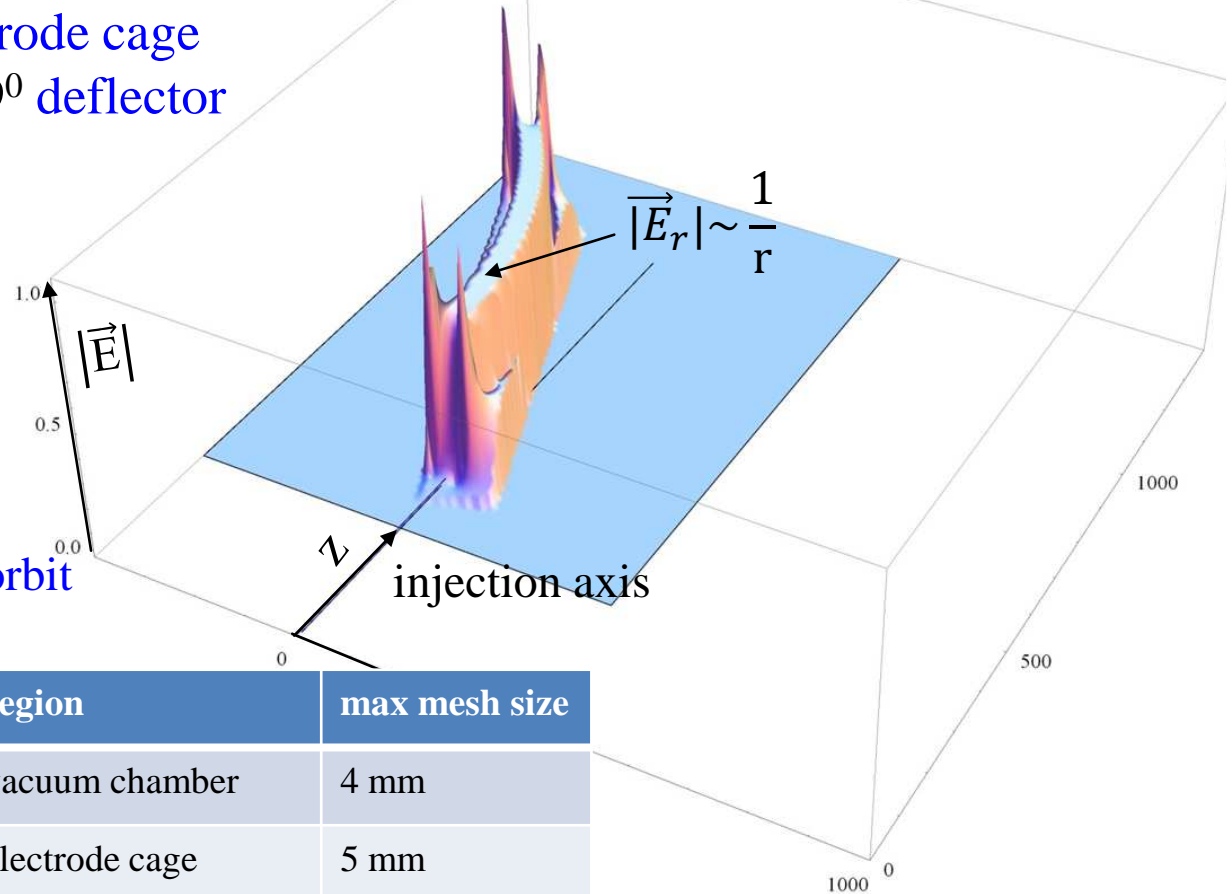
electrode cage
of 39° deflector

electrodes



small mesh size
close to central orbit

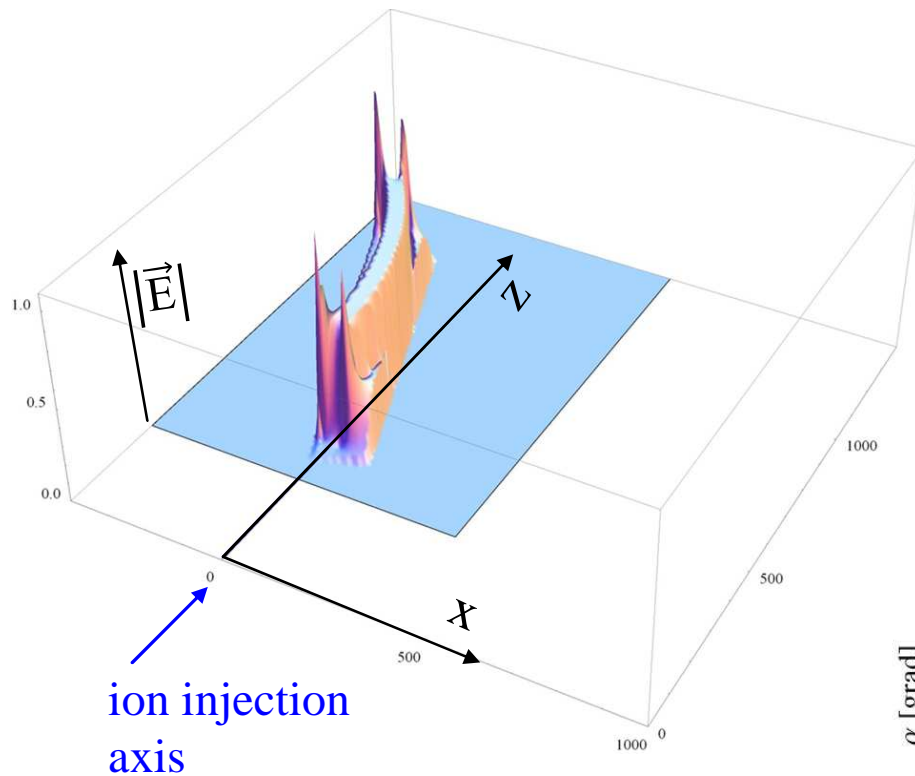
absolute value of electric field in the
plane of the central orbit



region	max mesh size
vacuum chamber	4 mm
electrode cage	5 mm
electrodes	4 mm
around central orbit	2 mm

Determine of the deflection angle of the 39° deflector

Length of the electrodes changed in two 2-3 iterations until a total deflection angle of 39° in tracking calculations with a protons were realized.

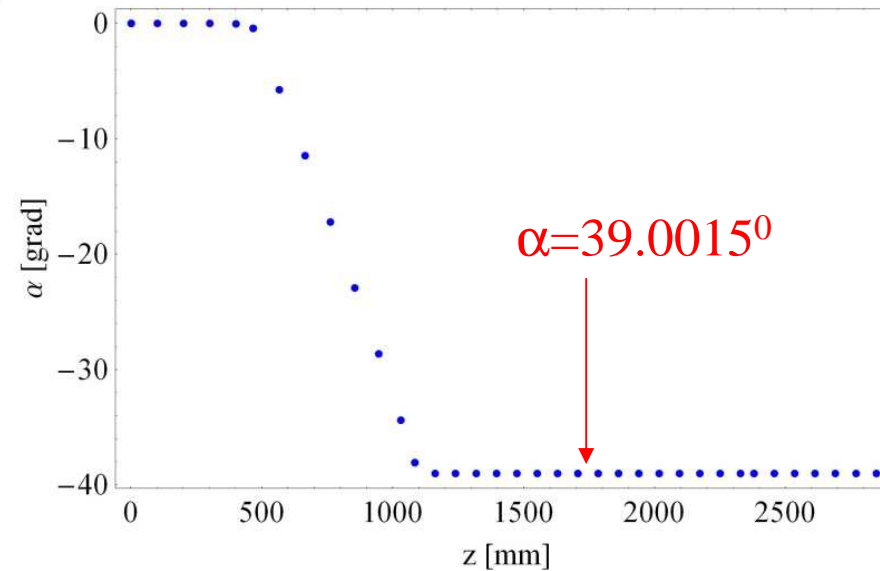


deflection angle

$$\alpha = \left| \arctan \left(\frac{v_x}{v_z} \right) \right|$$

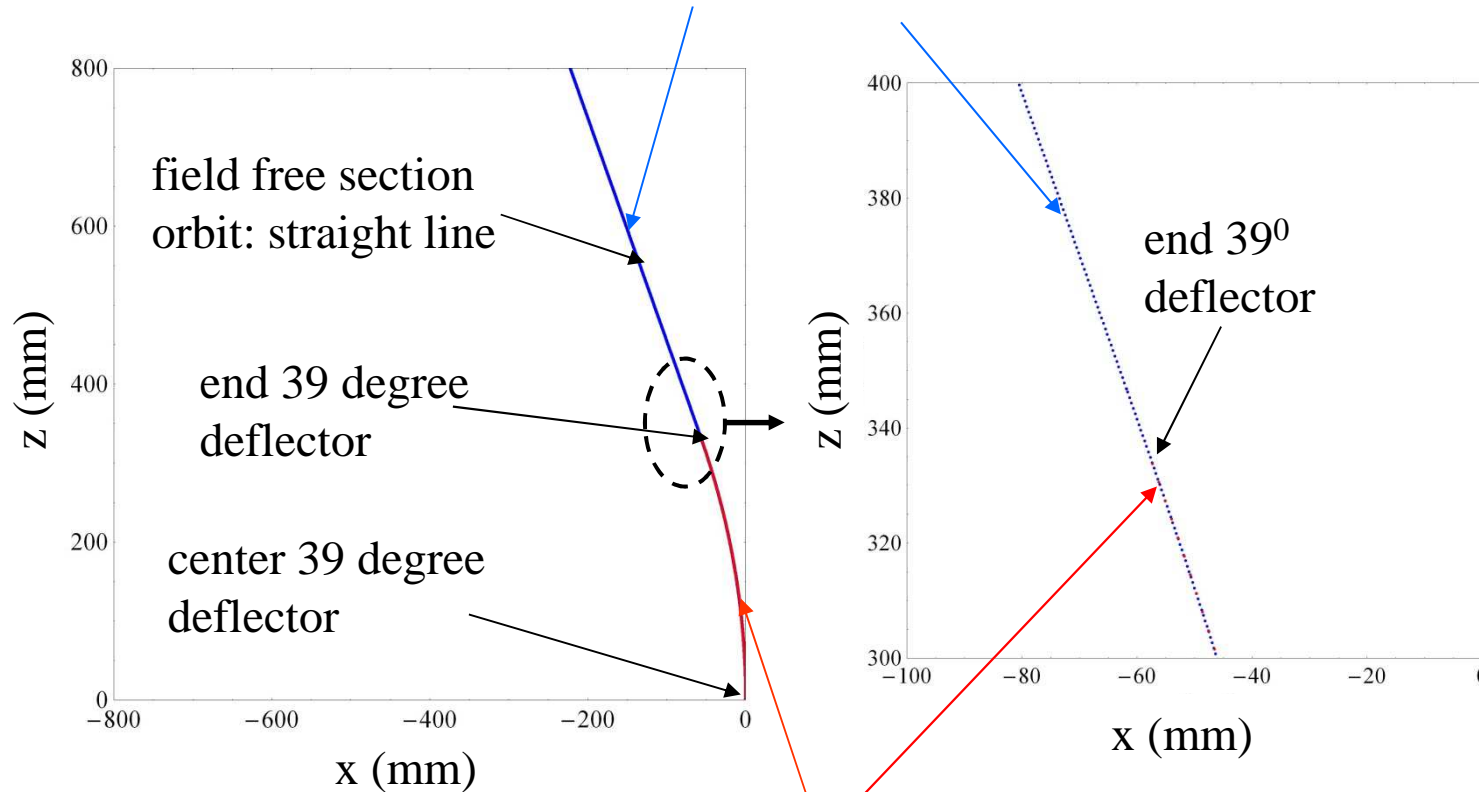
v_x – x coordinate of the velocity
 v_z – z coordinate of the velocity

deflection angle was calculated from v_x, v_y determined with G4beamline in a single ion tracking calculation



Nominal and actual orbit calculated with g4beamline

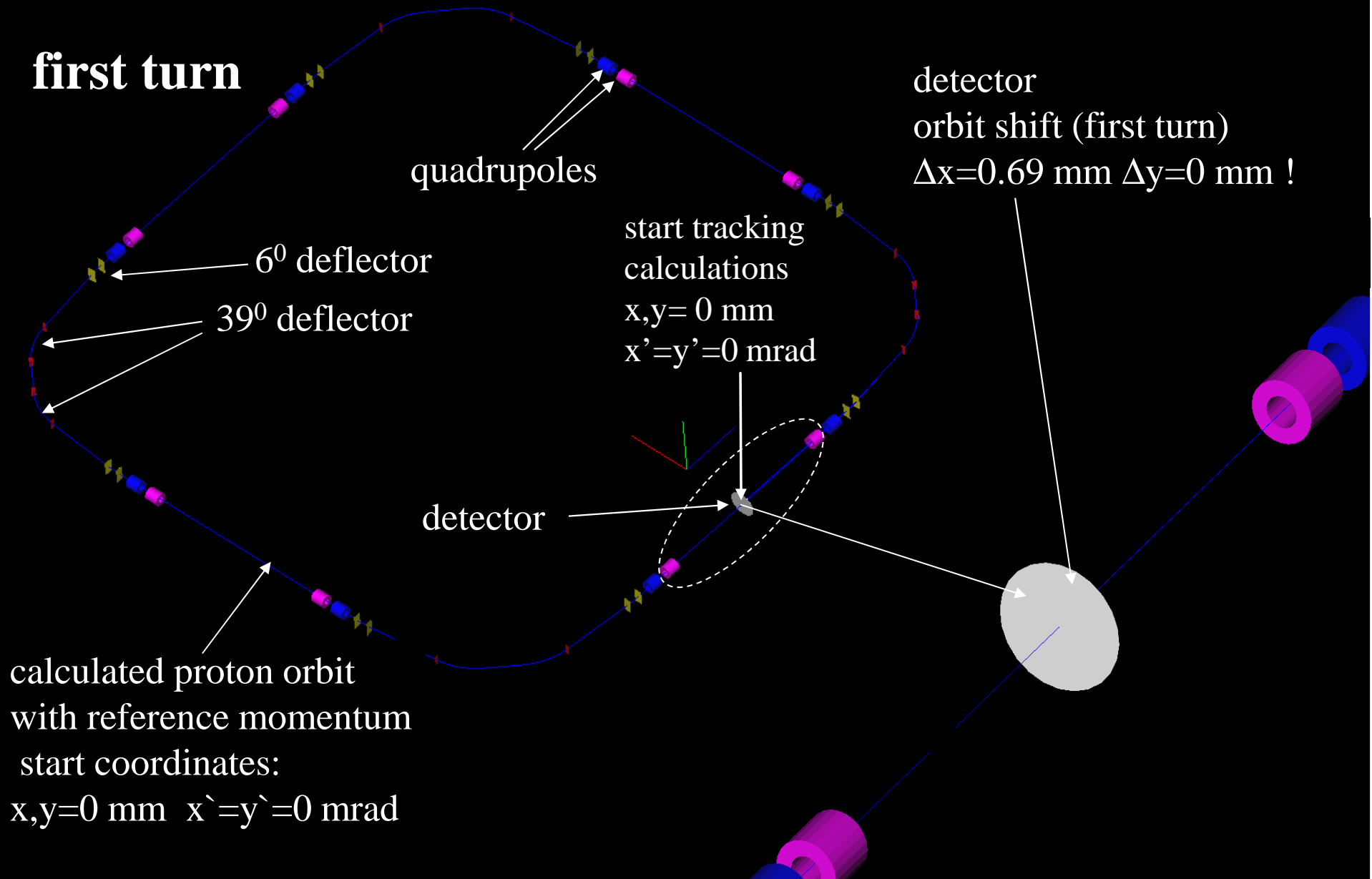
proton orbit with reference momentum,
tracked through the 39° deflector



nominal orbit (central orbit): circle with $r=1000$ mm

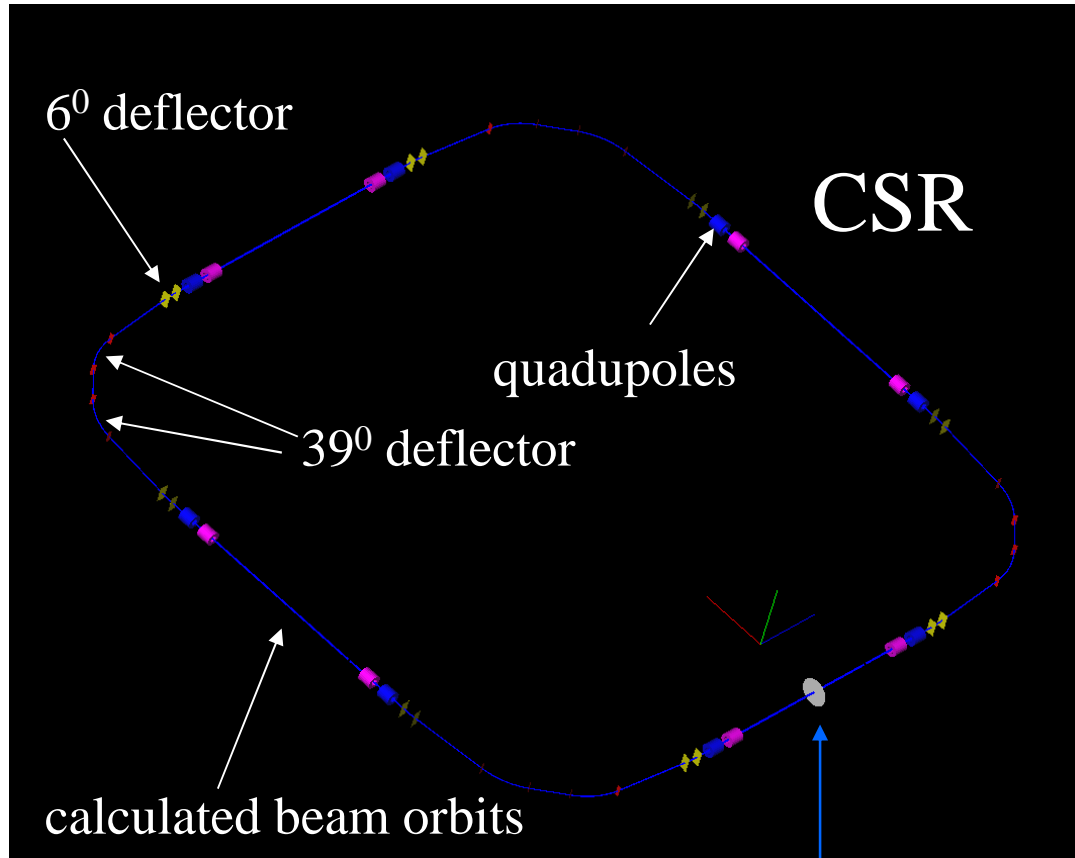
tracked reference particle is exactly on the nominal (central orbit)

Construction of CSR ring in G4beamline

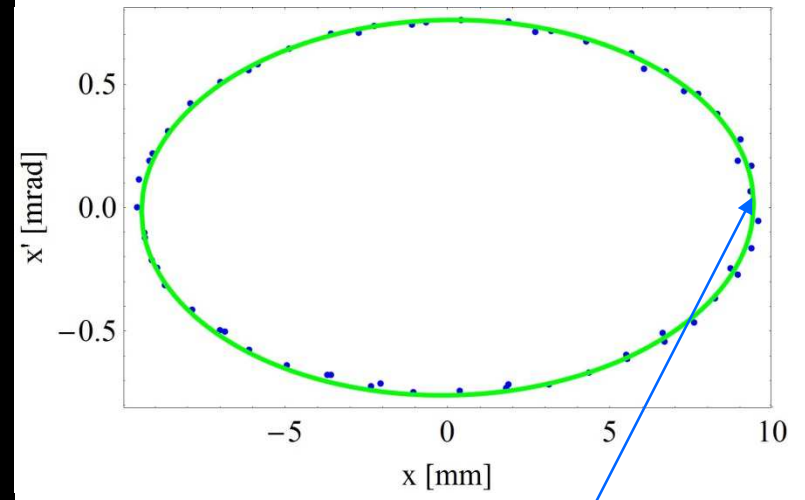


Determination of the closed orbit shift

G4beamline screen output



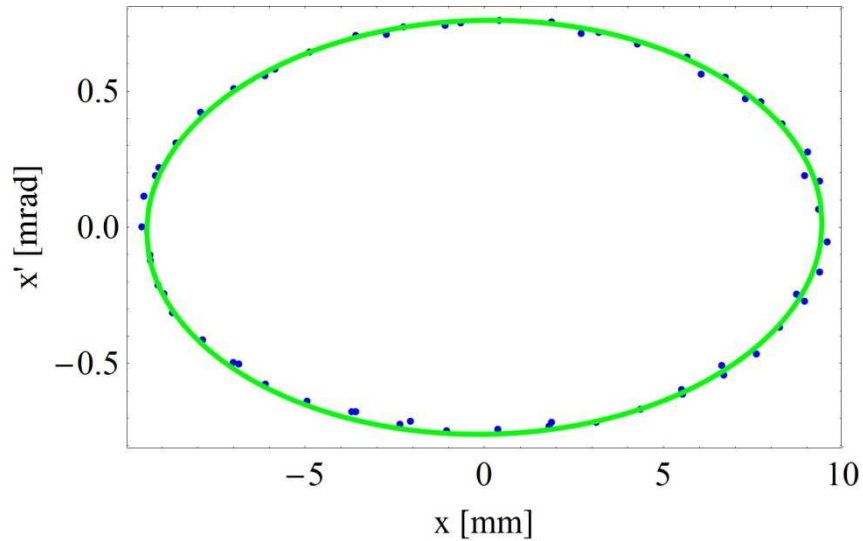
horizontal phase space coordinates of a single particle at observation point with reference momentum



$$\Delta x = 0.405 \text{ mm}$$
$$\Delta x' = -0.047 \text{ mrad}$$

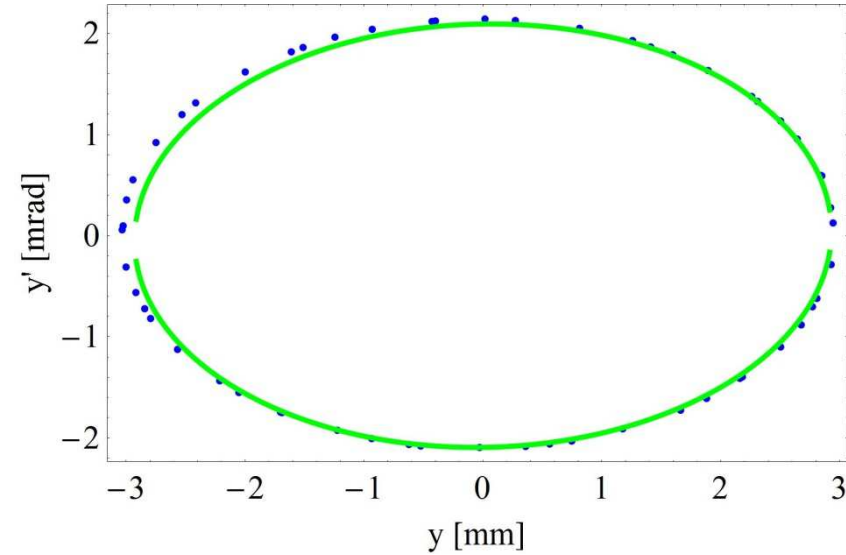
Twiss parameter at the center of a straight section

horizontal



$\alpha = -0.01856$
 $\beta = 12.41 \text{ m}$
 $\gamma = 0.08061$
 $\varepsilon = 7.15 \text{ mm} \cdot \text{mrad}$

vertical



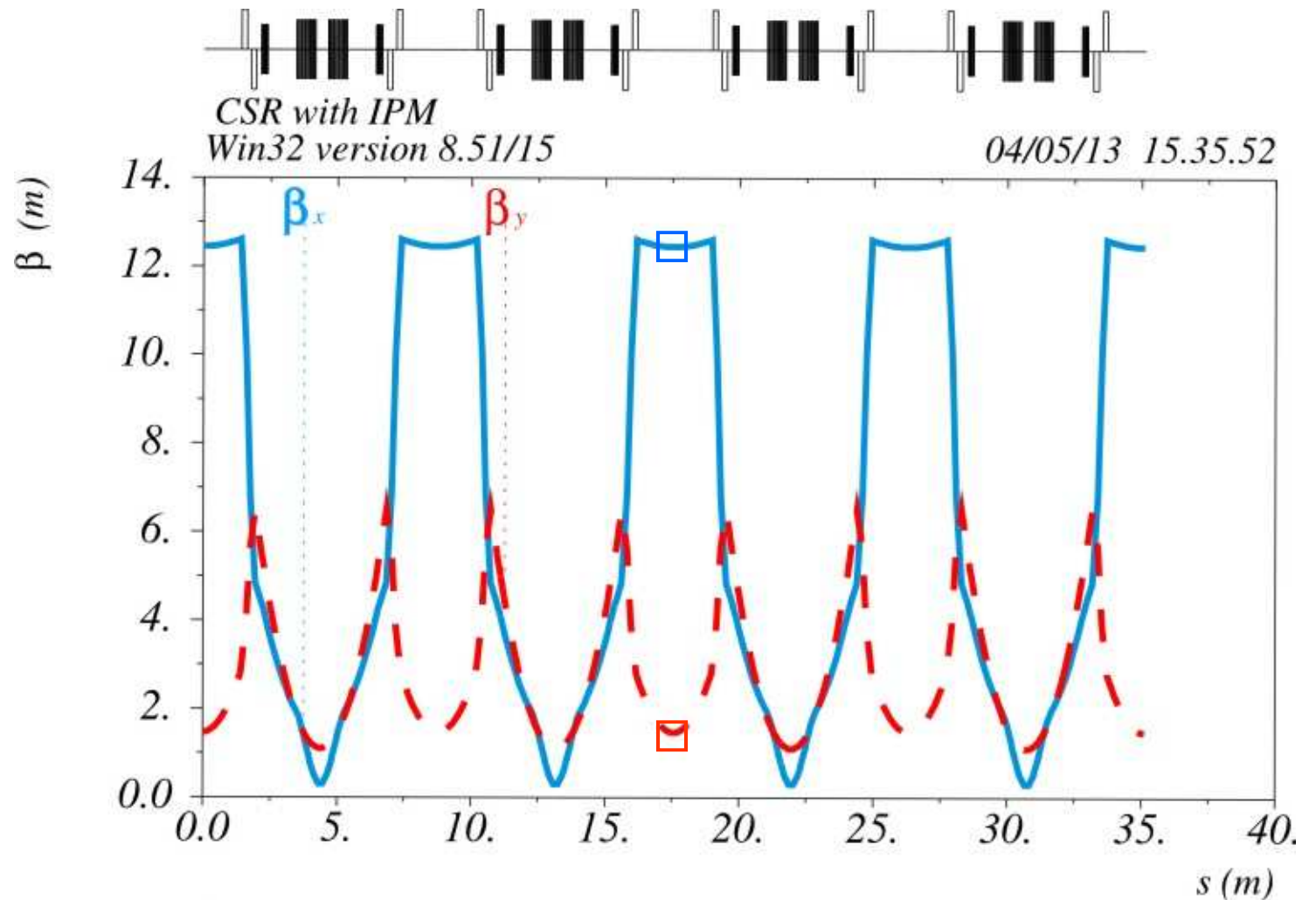
$\alpha = -0.0217$
 $\beta = 1.40 \text{ m}$
 $\gamma = 0.7143$
 $\varepsilon = 6.13 \text{ mm} \cdot \text{mrad}$

quadrupole setting for 300 keV protons:

family1: $U = 4.015 \text{ kV}$

family2: $U = -5.030 \text{ kV}$

Calculated β functions with MAD8



$\delta_E / p_0 c = 0.$

MAD8

G4beamline (G4bl)

Table name = TWISS

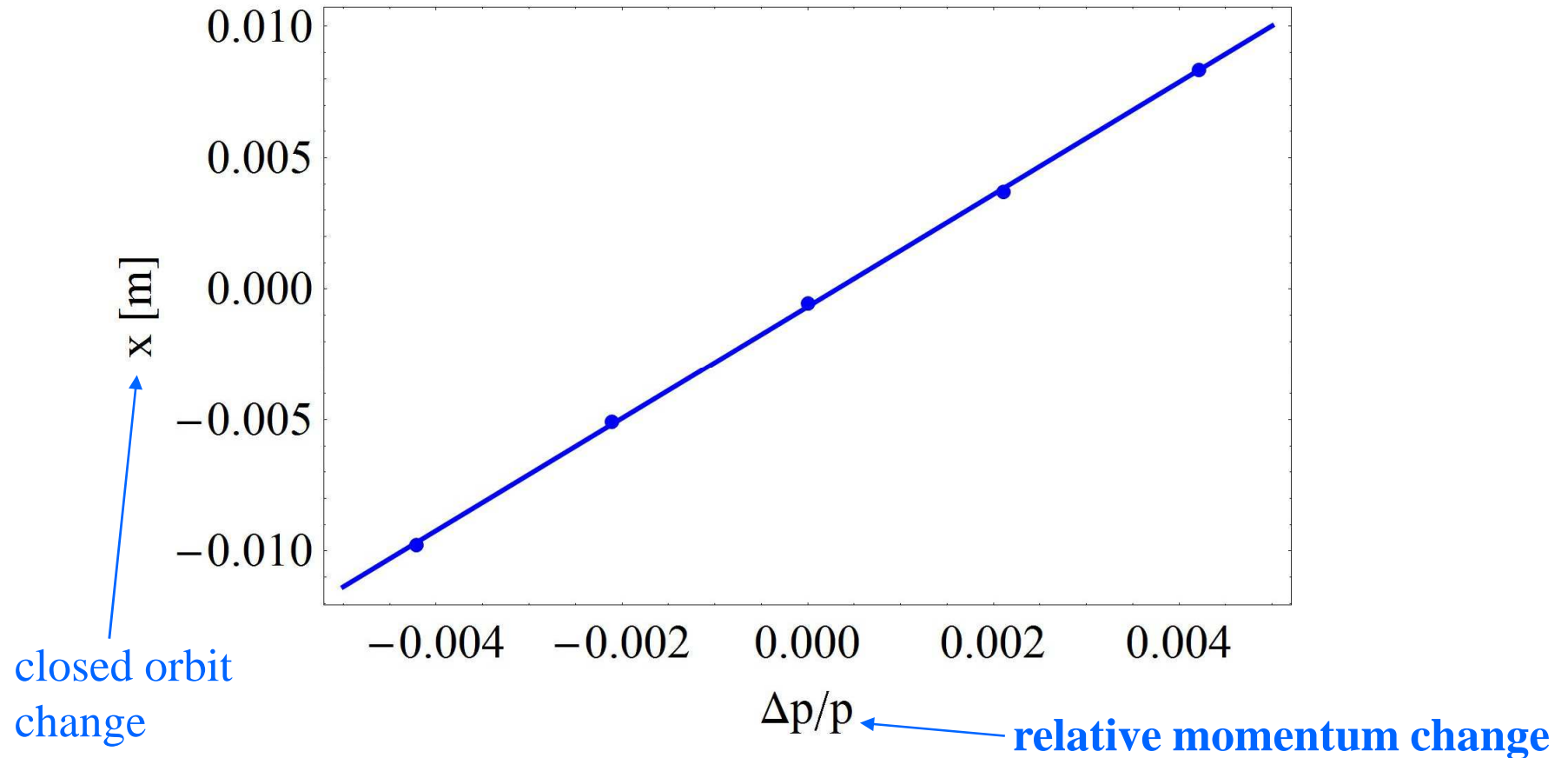
$\beta_x = 12.44$ m

$\beta_x = 12.41$ m

$\beta_y = 1.47$ m

$\beta_y = 1.40$ m

Dispersion comparison between G4bl and MAD8

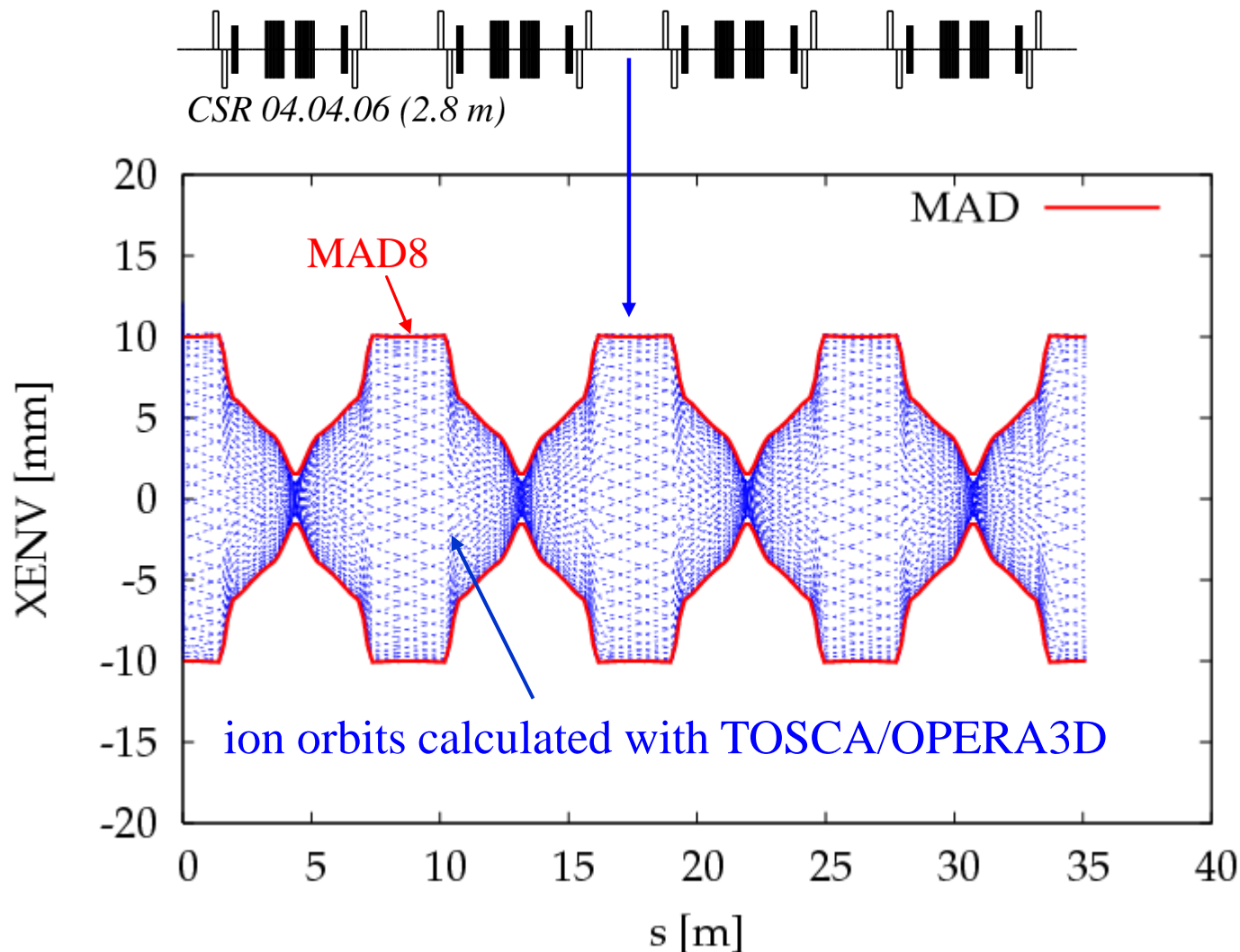


⇒ dispersion $D_x=2.1$ m (G4beamline)

MAD8: $D_x=2.06$ m center straight section

Horizontal envelope in the CSR

Comparison TOSCA and MAD8



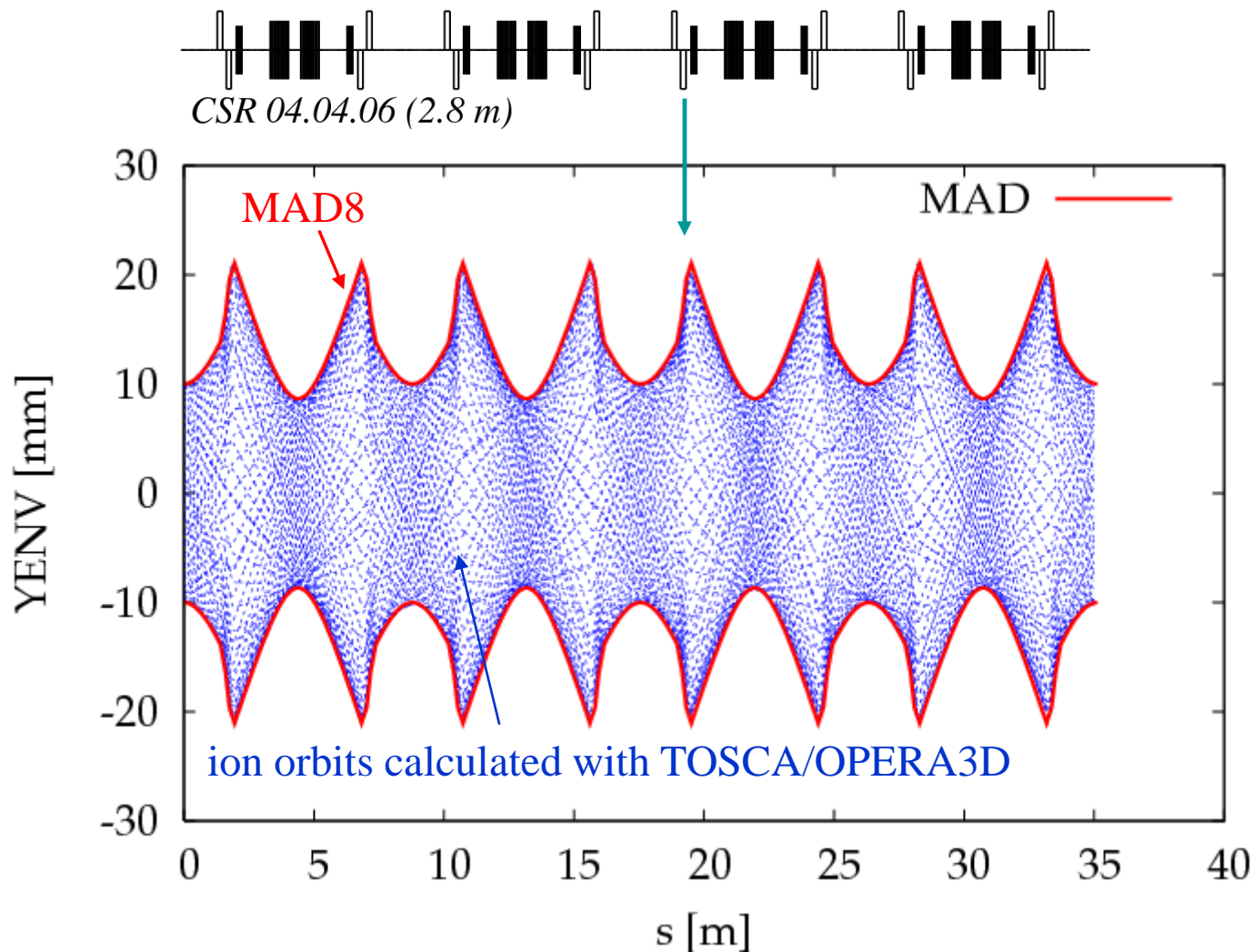
Opera 3D calculations

start coordinate:
lying on ellipse with
 $\epsilon_x = 8 \text{ mm} \cdot \text{mrad}$
 $\beta_x = 12.1 \text{ m}$
 $\alpha_x = 0$

ion: 20 keV proton

Vertical envelope in the CSR

Comparison TOSCA and MAD8



Opera 3D calculations

start coordinate:
lying on ellipse with
 $\epsilon_y = 68.1 \text{ mm} \cdot \text{mrad}$
 $\beta_y = 1.3 \text{ m}$
 $\alpha_y = 0$

ion: 20 keV proton

Comparison of MAD8, g4beamline and Tosca simulations

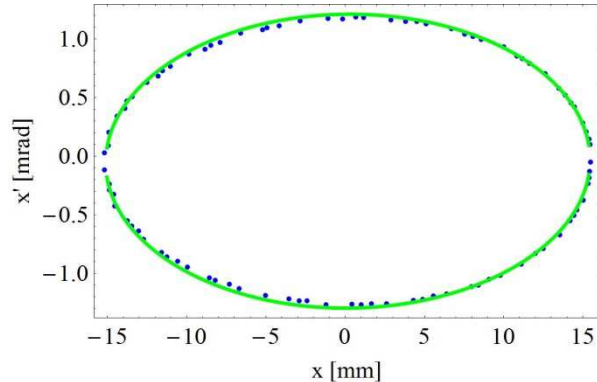
TABLE I. Betatron functions (β_x, β_y) and dispersion (D_x) in the center of the CSR straight sections, together with betatron tunes Q_x, Q_y of the CSR. Results from matrix calculations (MAD8²⁹) are compared to those from all-ring tracking calculations using TOSCA³² and G4beamline.³³ The tracking calculations also yield the approximate ring acceptances A_x, A_y , which are given for zero-emittance ion beams.

Parameter	MAD8	TOSCA	G4beamline	Unit
β_x	12.44	12.1	12.41	m
β_y	1.47	1.3	1.4	m
D_x	2.06	2.1	2.1	m
Q_x	2.59	2.60	2.60	
Q_y	2.59	2.61	2.62	
A_x		120	120	mm mrad
A_y		180	170	mm mrad

A_x - horizontal acceptance for $\epsilon_y \rightarrow 0$ (without consideration of magnetic field of the earth)
 A_y - vertical acceptance for $\epsilon_x \rightarrow 0$

Influence of the magnetic field of the earth

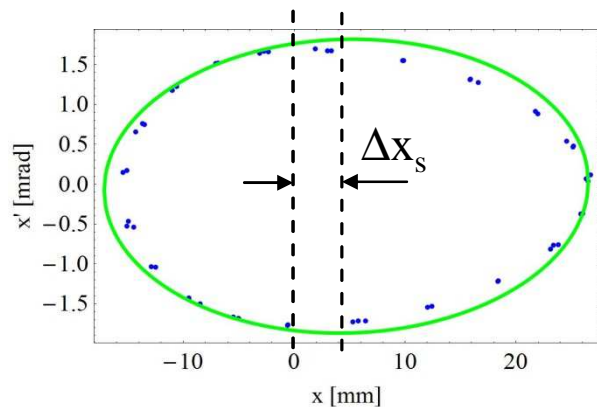
Horizontal phase space at the center of the injection straight section
calculated for **protons** and $x_{\text{start}} = -15$ mm



without earth magnetic field

E=300 keV

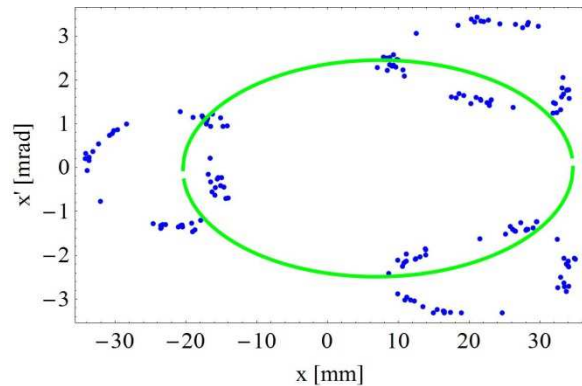
$\Delta x_s = 0.172$ mm $\Delta x_s' = -0.04$ mrad



with earth magnetic field

E= 300 keV

$\Delta x_s = 4.69$ mm $\Delta x_s' = -0.025$ mrad



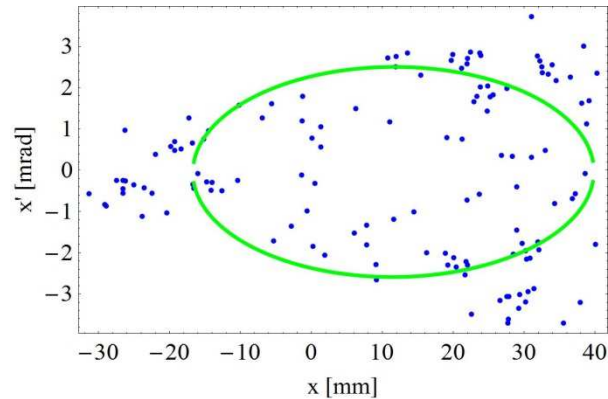
with earth magnetic field

E= 100 keV

$\Delta x_s = 7.11$ mm $\Delta x_s' = -0.019$ mrad

Influence of the magnetic field of the earth II

Horizontal phase space at the center of the injection straight section
Calculated for proton and $x_{\text{start}} = -15$ mm



with earth magnetic field

$E = 50$ keV

$\Delta x_s = 11.55$ mm $\Delta x_s' = -0.158$ mrad

beam lost !

with earth magnetic field

and proton energy of $E = 20$ keV

for small proton energies ($E < 300$ keV) proton motion are not linear
at the CSR.

Effect of the magnetic field of the earth is more or less negligible
if the proton energy $E_p \geq 0.5$ MeV

Minimum Energy where earth magnet field is neglect able

ion deflection in magnetic field of the earth $\delta = \frac{\int_a^b \overset{\substack{\text{transverse magnetic field} \\ \text{of the earth}}}{B_{\perp}} ds}{B\rho}$ ← beam rigidity

$B\rho = \frac{p}{Q}$ ← ion momentum
← ion charge

Magnetic field of the earth is negligible if: $B\rho > B\rho_{lim}$

⇒ ion energy E where magnetic field of the earth is negligible:

$$E > E_p \frac{q^2}{A}$$

E_p -minimum proton energy where earth magnetic field is negligible at the CSR:

$E_p \approx 0.5 \text{ MeV}$ (determined with G4beamline tracking calculations)

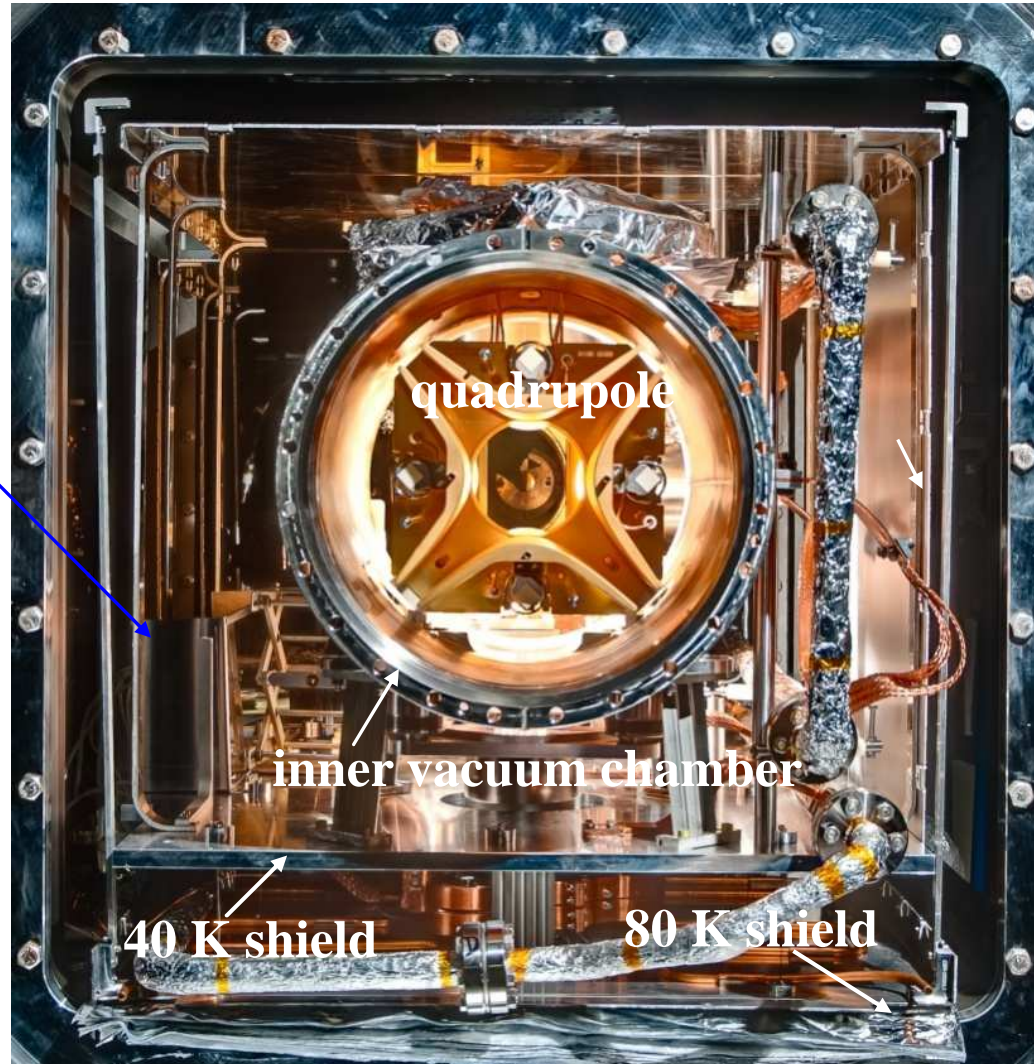
A-ion mass

q- ion charge in units of e

For example $^{40}\text{Ar}^+$ with $E=50 \text{ keV}$ is well above the limit and chosen for the first CSR beam times carried out in the year **2014**

Cryostat of the CSR

isolation vacuum
ca. 10^{-6} mbar



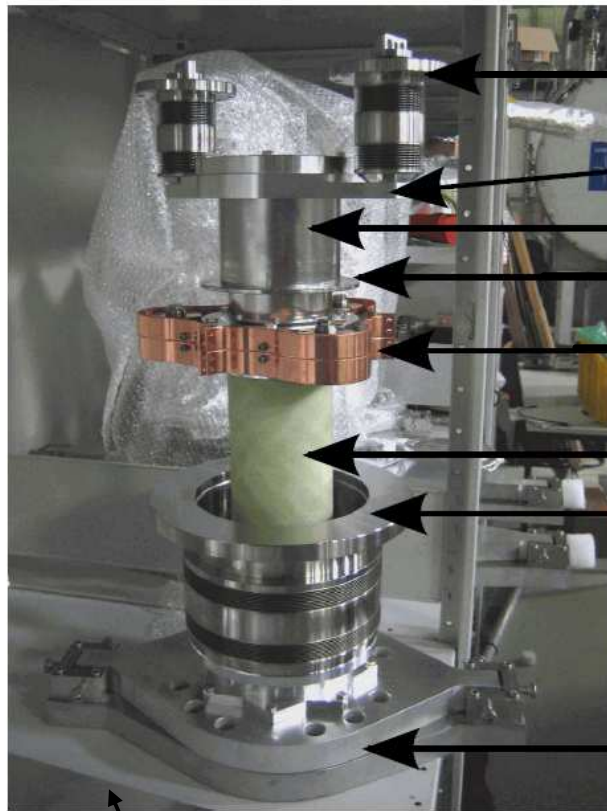
isolation
vacuum chamber

inner vacuum chamber

40 K shield

80 K shield

The support of the optical elements



concrete block

experimental vacuum chamber

thermal anchor at 10 K

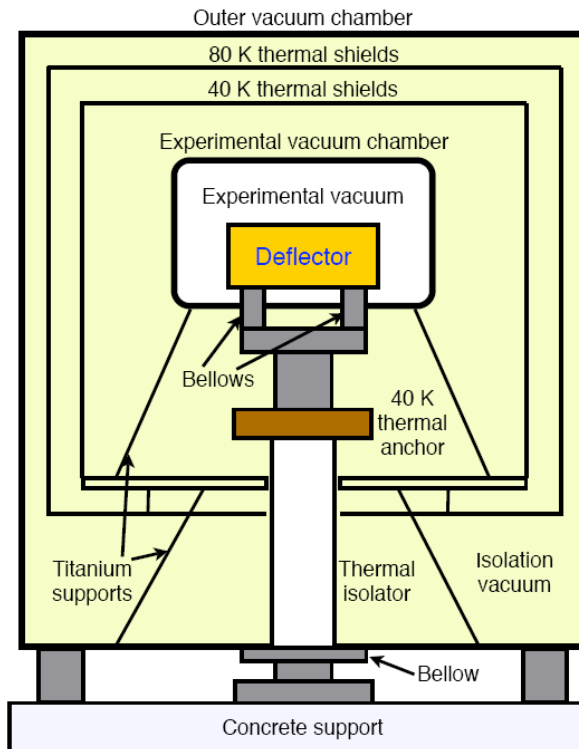
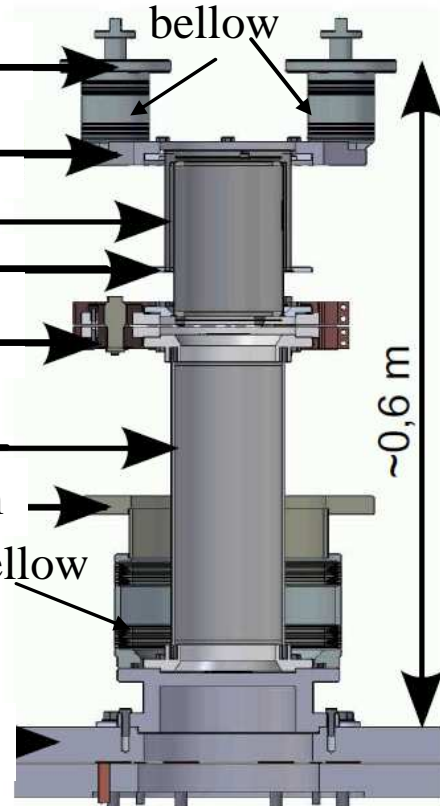
stainless steel meander

thermal anchor at 40 K

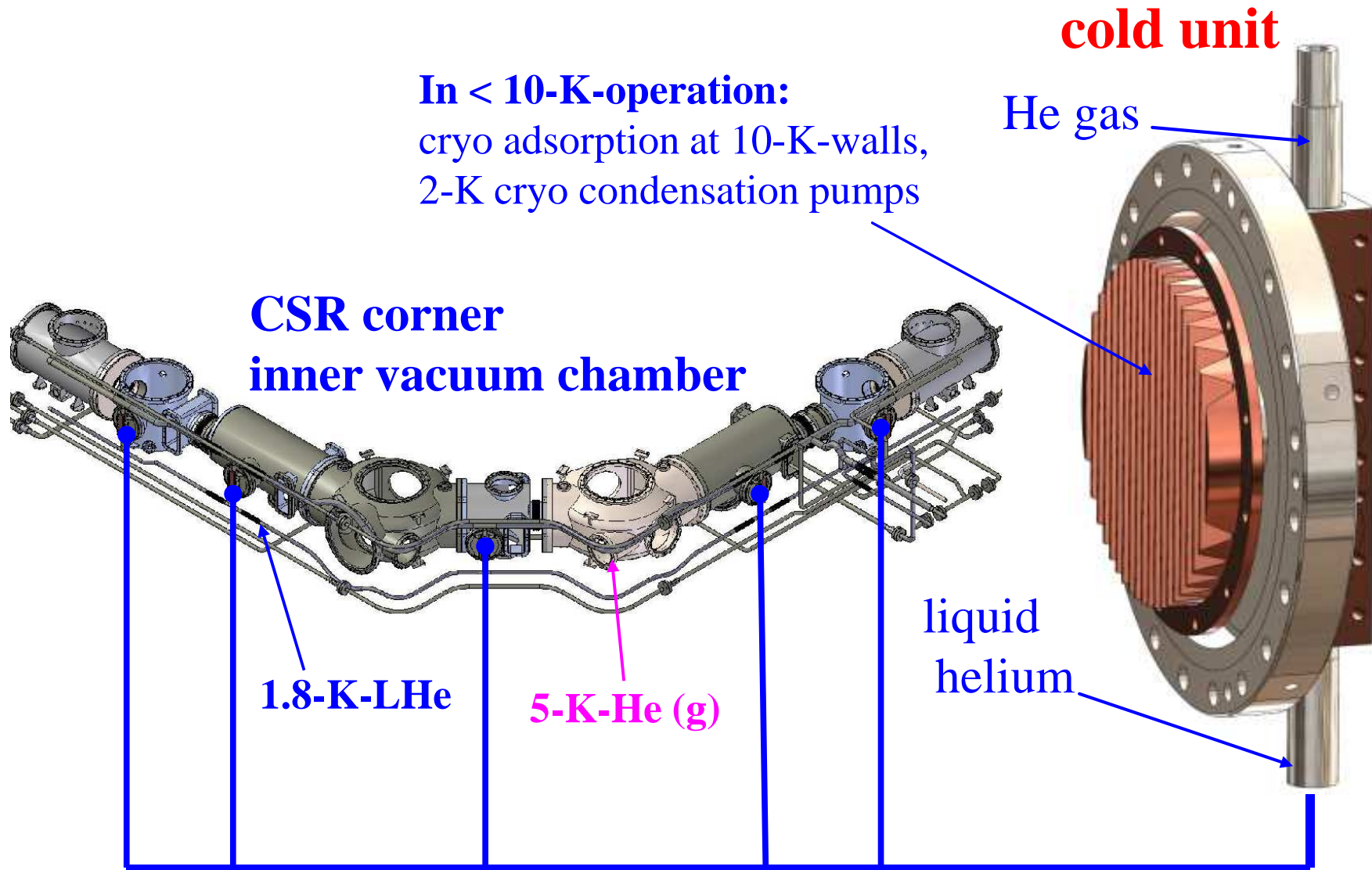
thermal anchor at 80 K

GFK tube

beginning of isolation vacuum



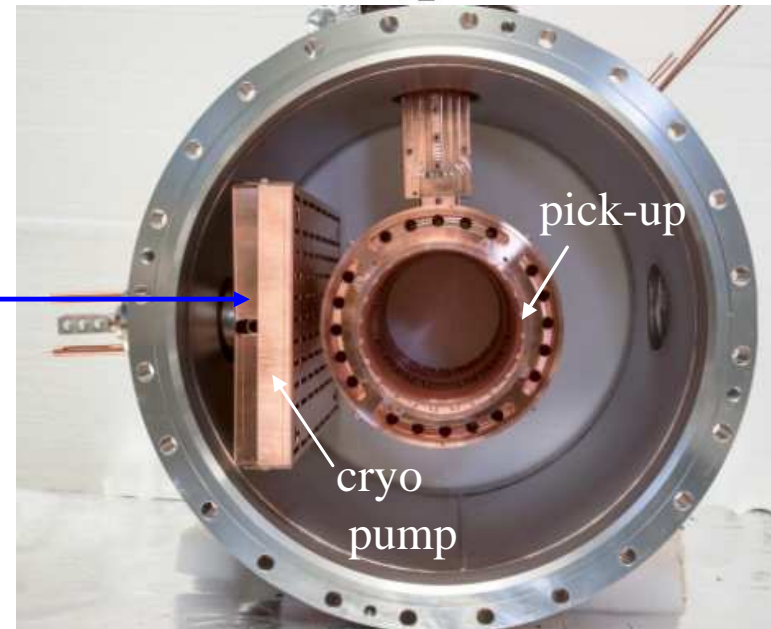
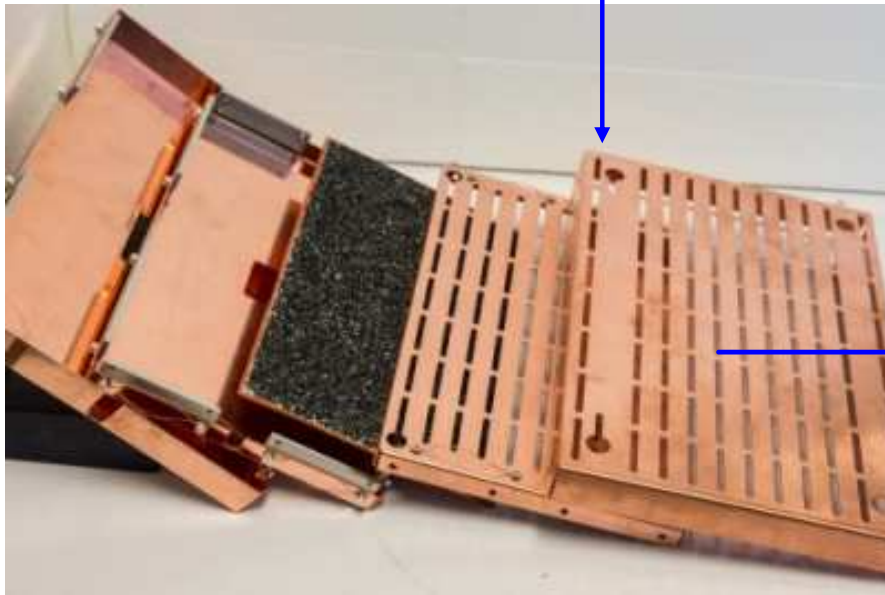
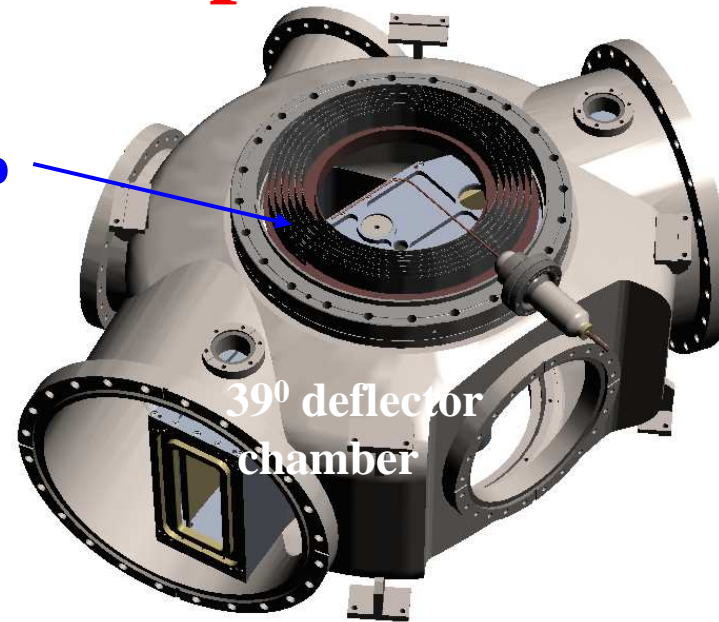
Pumping at cryogenic temperatures



Pumping in the 300 K operation

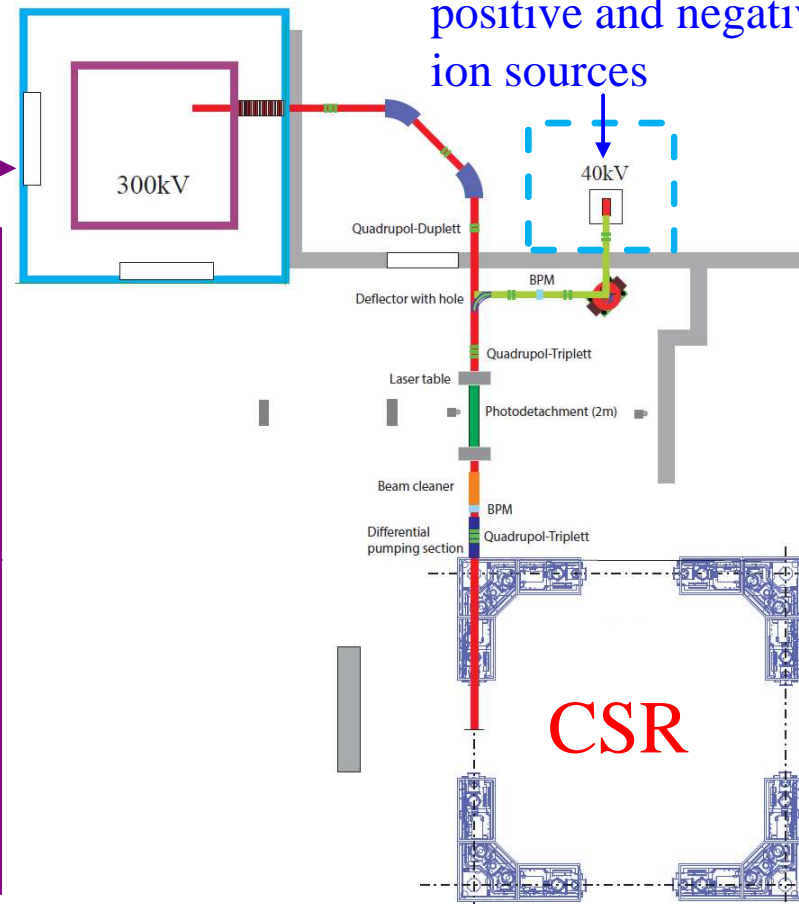
In 300-K-operation:
250°C bake-out,
Ion-getter pumps,
NEG pump (strips),
bake-able charcoal **cryo-pumps**

NEG pump



High Voltage platforms

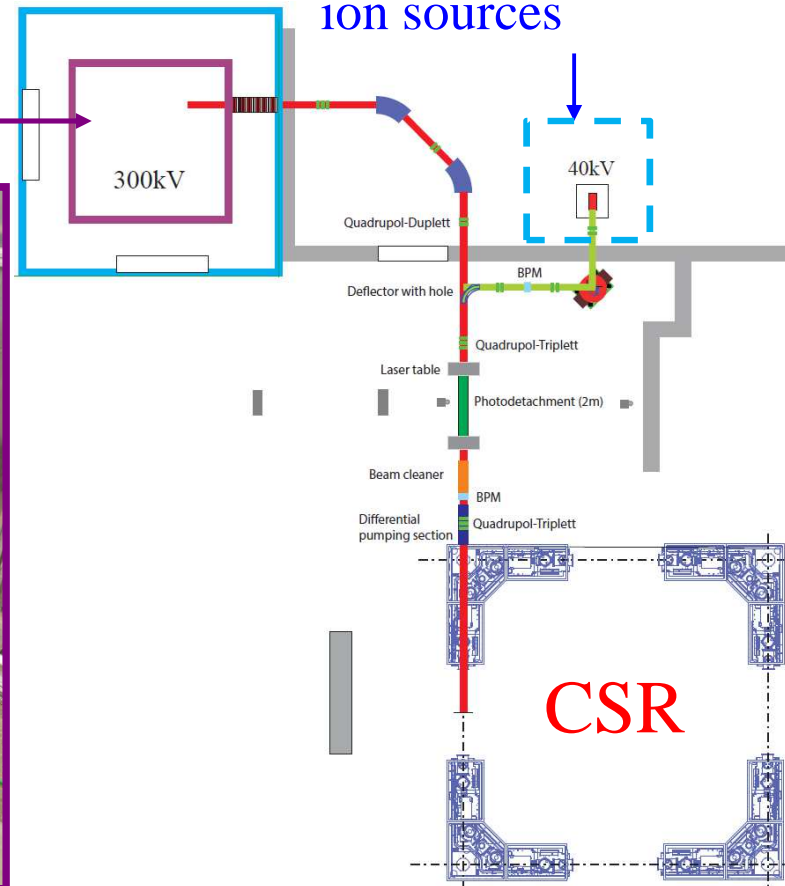
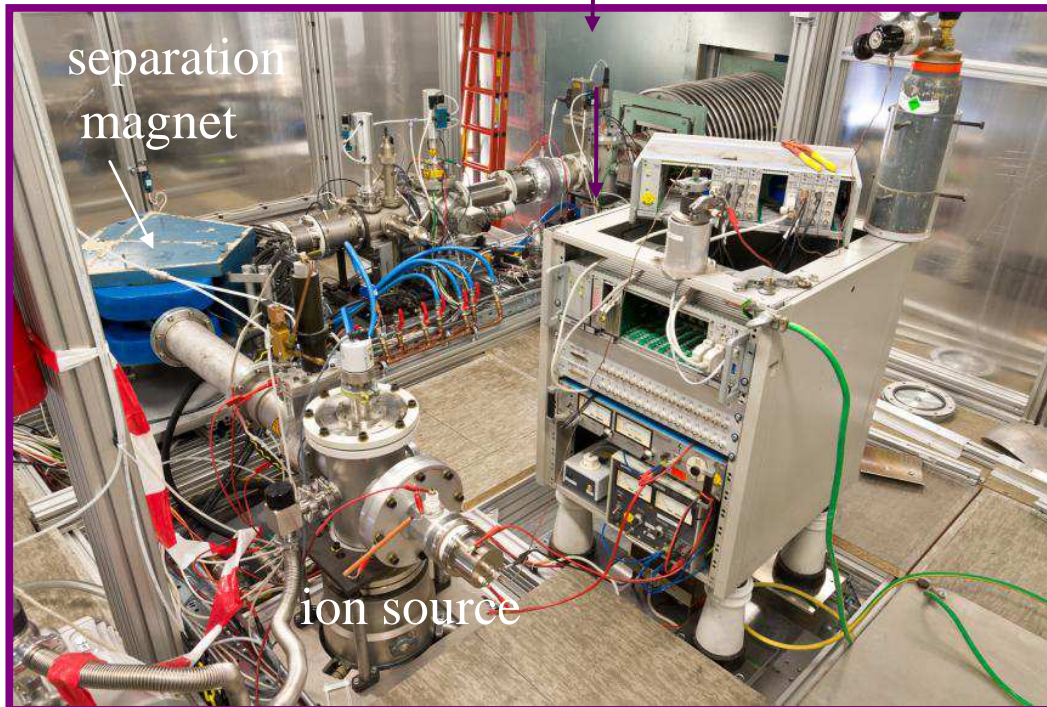
CSR main injector:
ion sources on a high
voltage platform of ± 300 kV



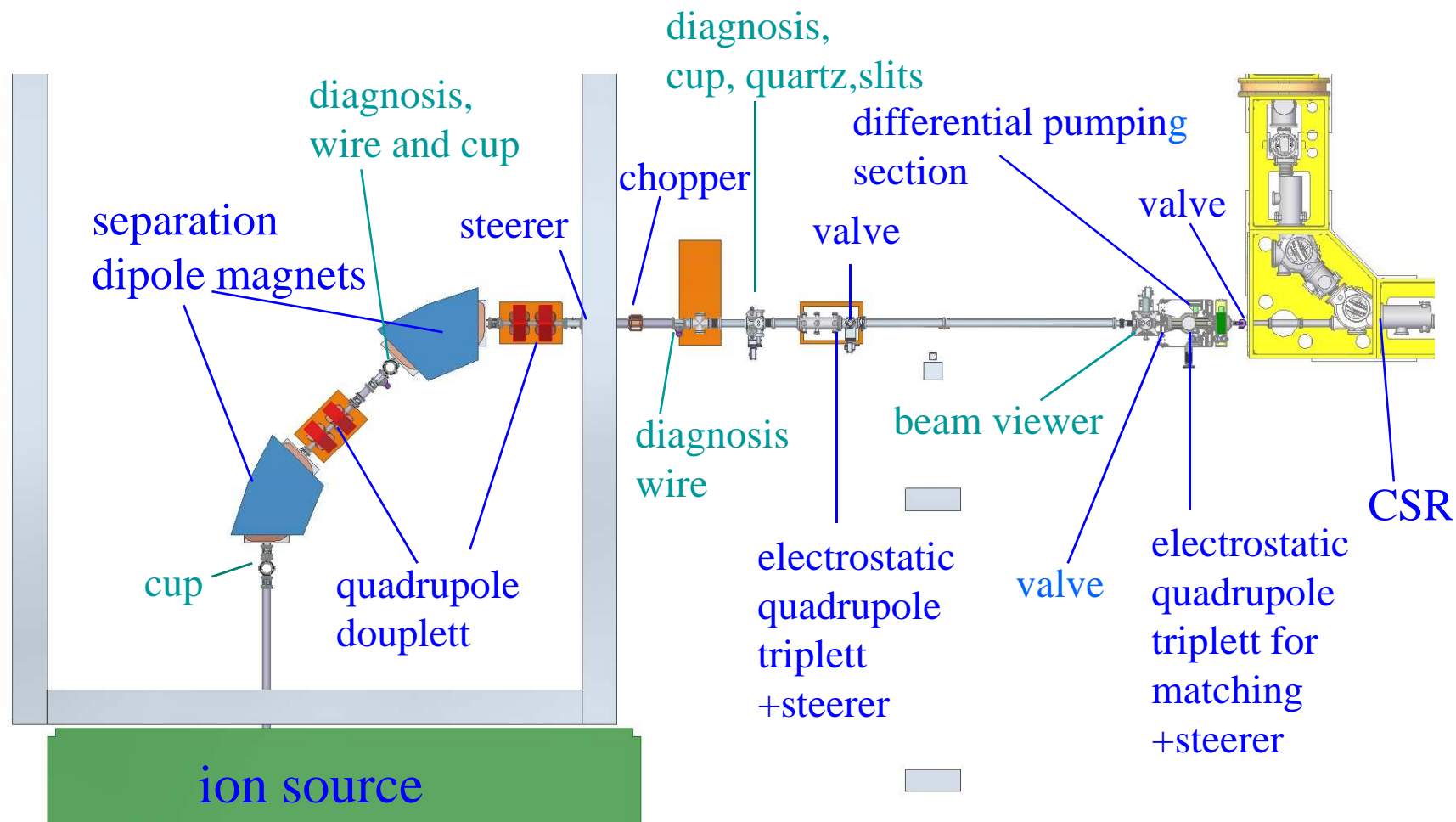
Ion sources

± 40 keV platform with positive and negative ion sources

CSR main injector: ± 300 kV

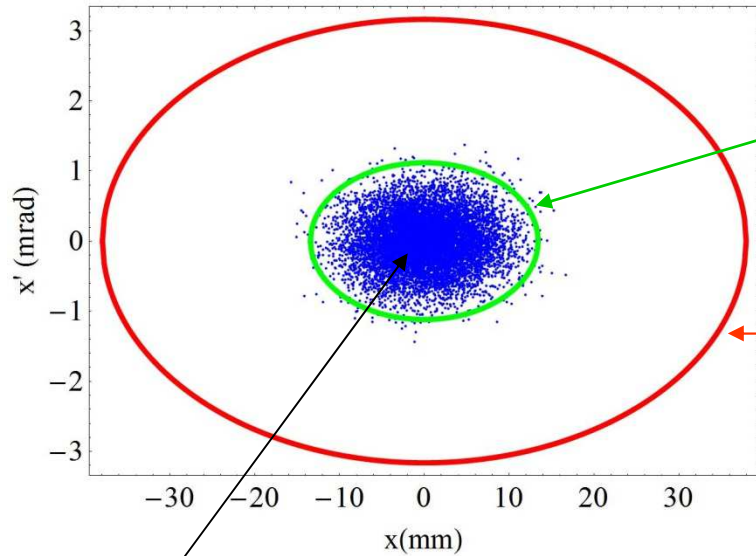


Transferline between ion source and CSR



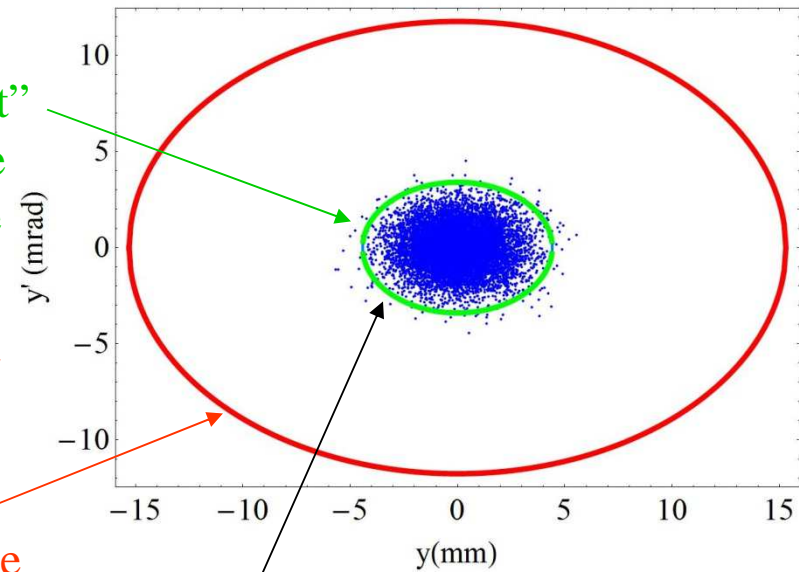
Matching

matched horizontal phase space
at center injection straight section



horizontal phase space of injector beam
 $\epsilon_x = 15 \text{ mm} \cdot \text{mrad}$

matched vertical phase space
at center injection straight section



vertical phase space of injector beam
 $\epsilon_y = 15 \text{ mm} \cdot \text{mrad}$

“closed orbit”
in transverse
phase space

horizontal
acceptance
 $A_x (\epsilon_y \rightarrow 0)$

vertical
acceptance
 $A_y (\epsilon_x \rightarrow 0)$

matching condition:

$$\alpha_{x,i} = \alpha_{x,CSR}$$

$$\alpha_{y,i} = \alpha_{y,CSR}$$

injector beam →

$$\beta_{x,i} = \beta_{x,CSR}$$

$$\beta_{y,i} = \beta_{y,CSR}$$

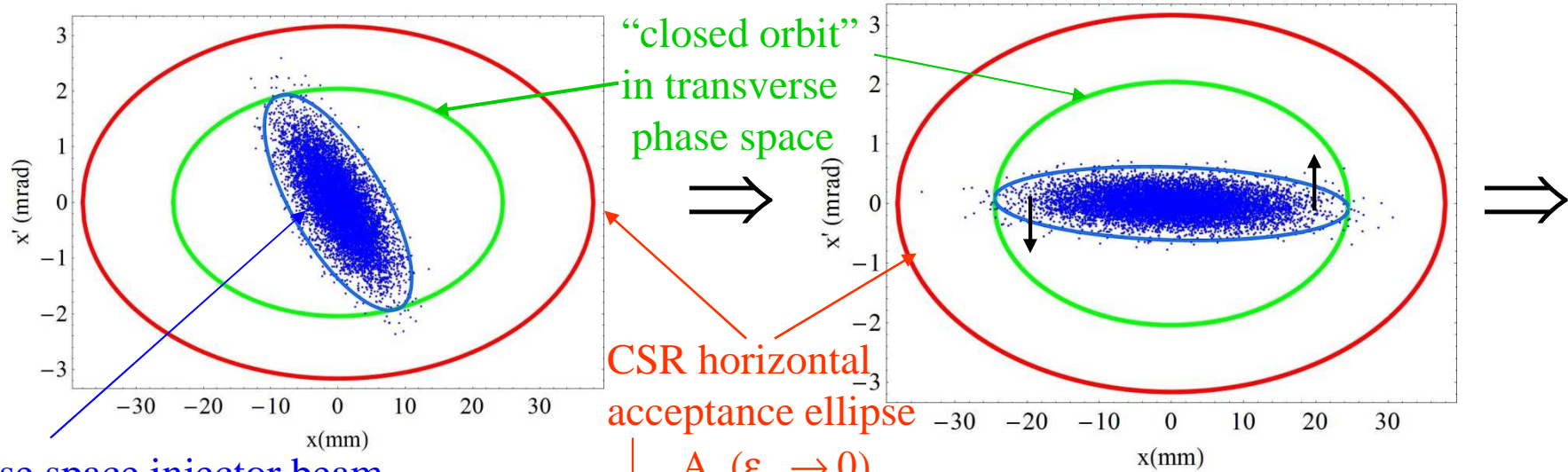
← CSR TWISS parameter
at the center of straight section
for injection

remark: no dispersion matching is done

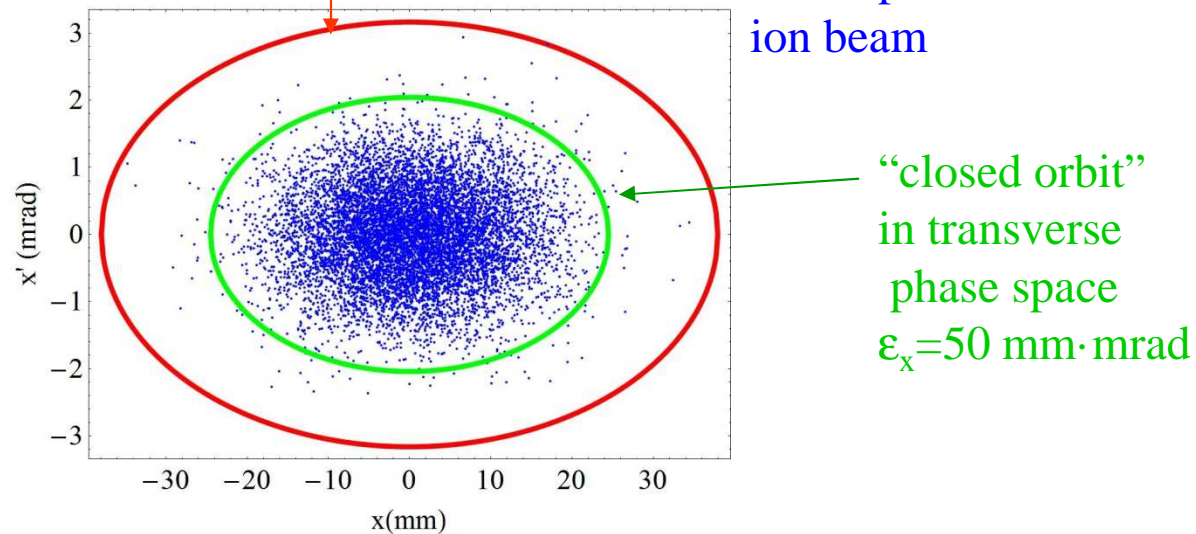
Mismatching

horizontal phase space direct after injection
at center of injection straight section

phase space of the injected particle starts
to rotate with double betatron frequency

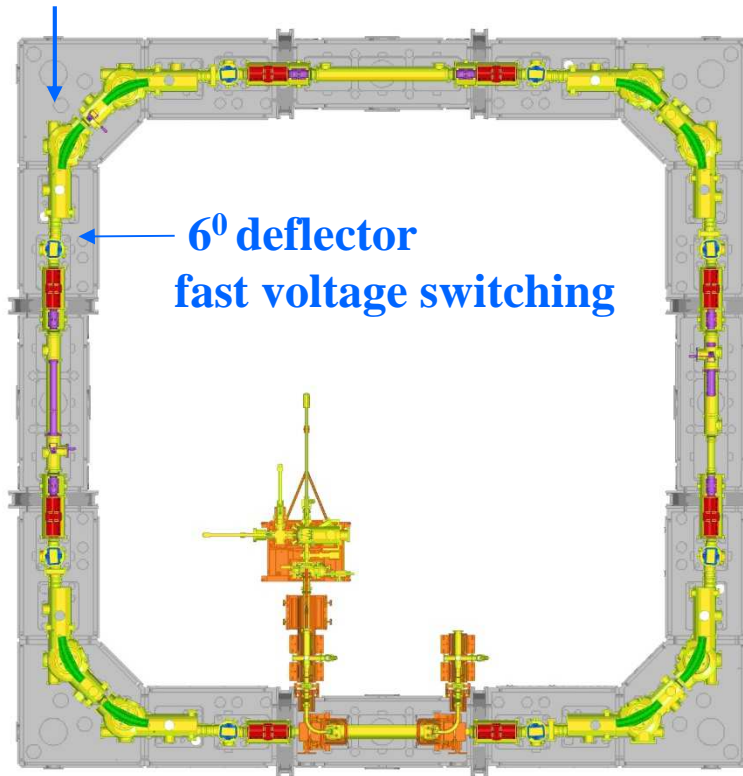


due to non linearity's
horizontal phase space
blow up



Single Turn injection

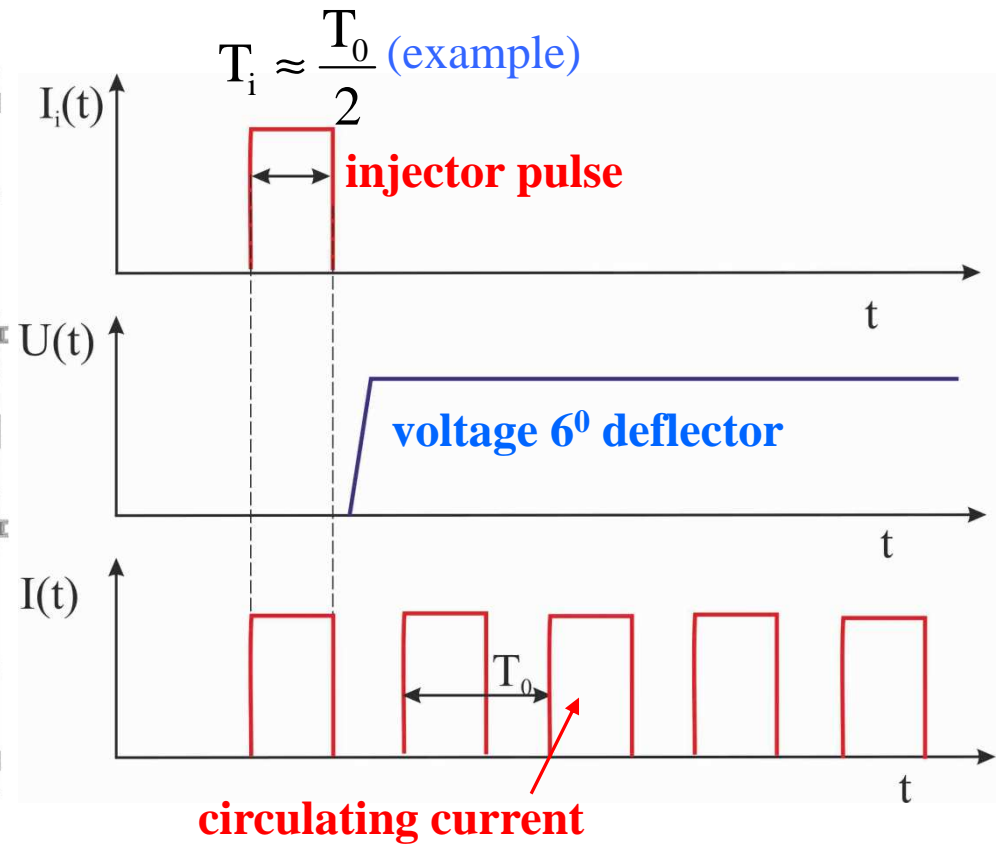
injector beam



6° deflector
fast voltage switching

T_0 -revolution time

T_i -injector beam pulse length



Space charge limit of a stored ion beam

incoherent tune shift:

$$N = \frac{A}{q^2} \frac{2\pi}{r_p} \cdot B \cdot \beta^2 \cdot \gamma^3 \cdot \epsilon_{2\sigma} \cdot (-\Delta Q)$$

maximum possible emittance

pessimistic

$$\epsilon_{2\sigma} \approx \left(\frac{2}{3}\right)^2 A_c(\epsilon_x = \epsilon_y) \quad A_c(\epsilon_x = \epsilon_y) \approx A_x(\epsilon_y \rightarrow 0) / 2$$

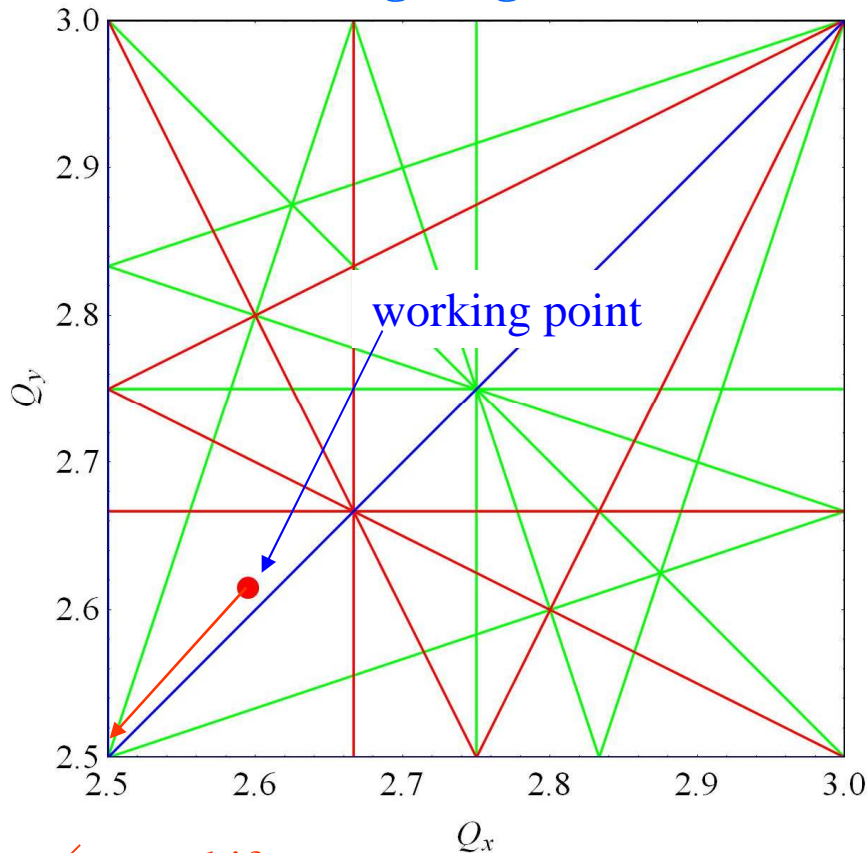
$$A_x(\epsilon_x = \epsilon_y) \leq A_x(\epsilon_y \rightarrow 0)$$

2σ emittance

ΔQ- maximum possible tune shift

acceptance with:

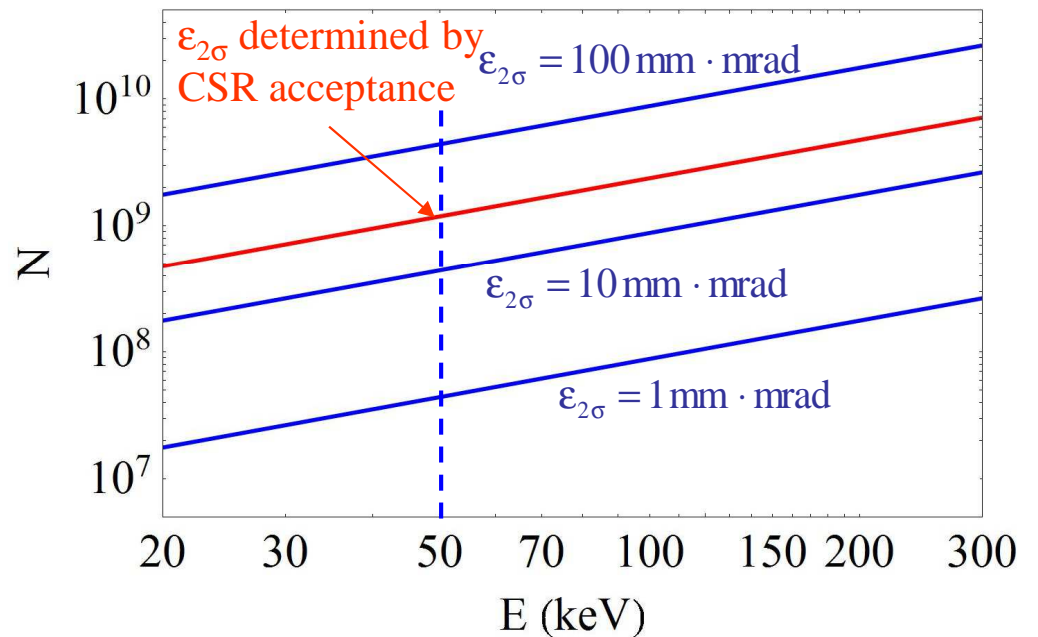
working diagram (S=1)



tune shift

calculated for $q=1$, $B=1$ and $\Delta Q = -0.1$

maximum possible particle number N

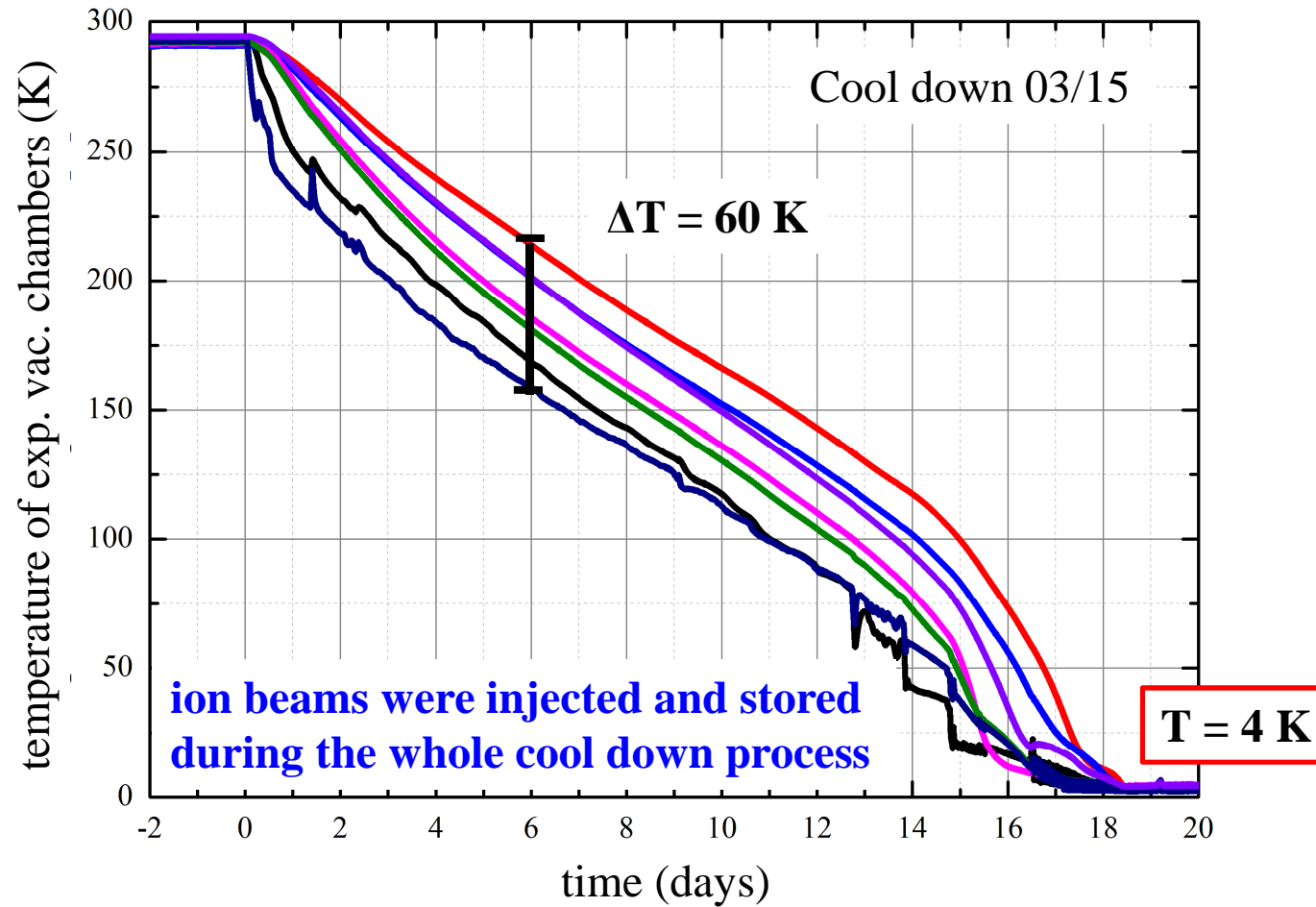


remark: $N \sim A \cdot \beta^2 \sim E$ ($\gamma=1$) particle number N valid for all single charged ions !

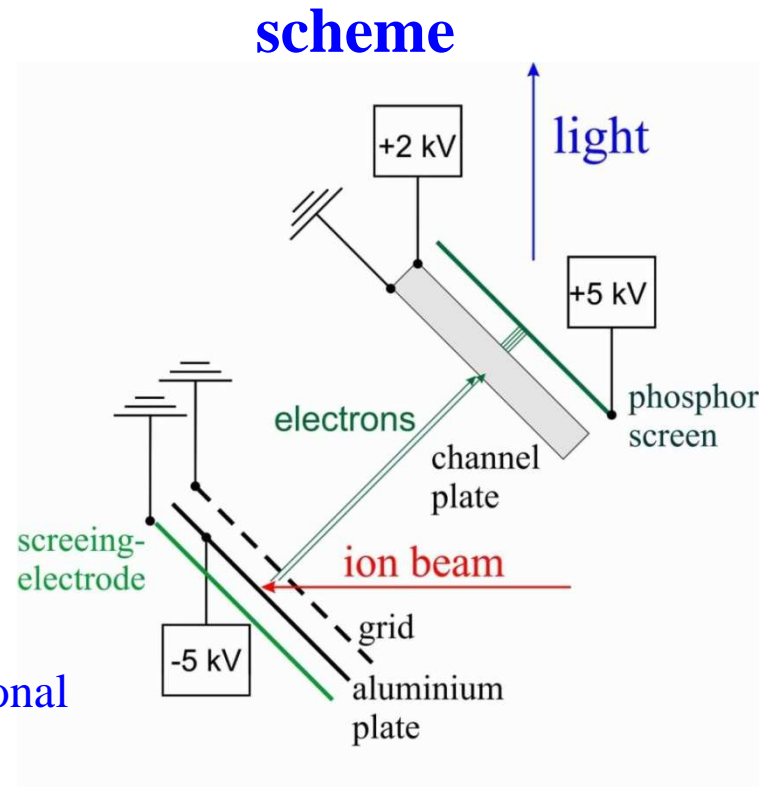
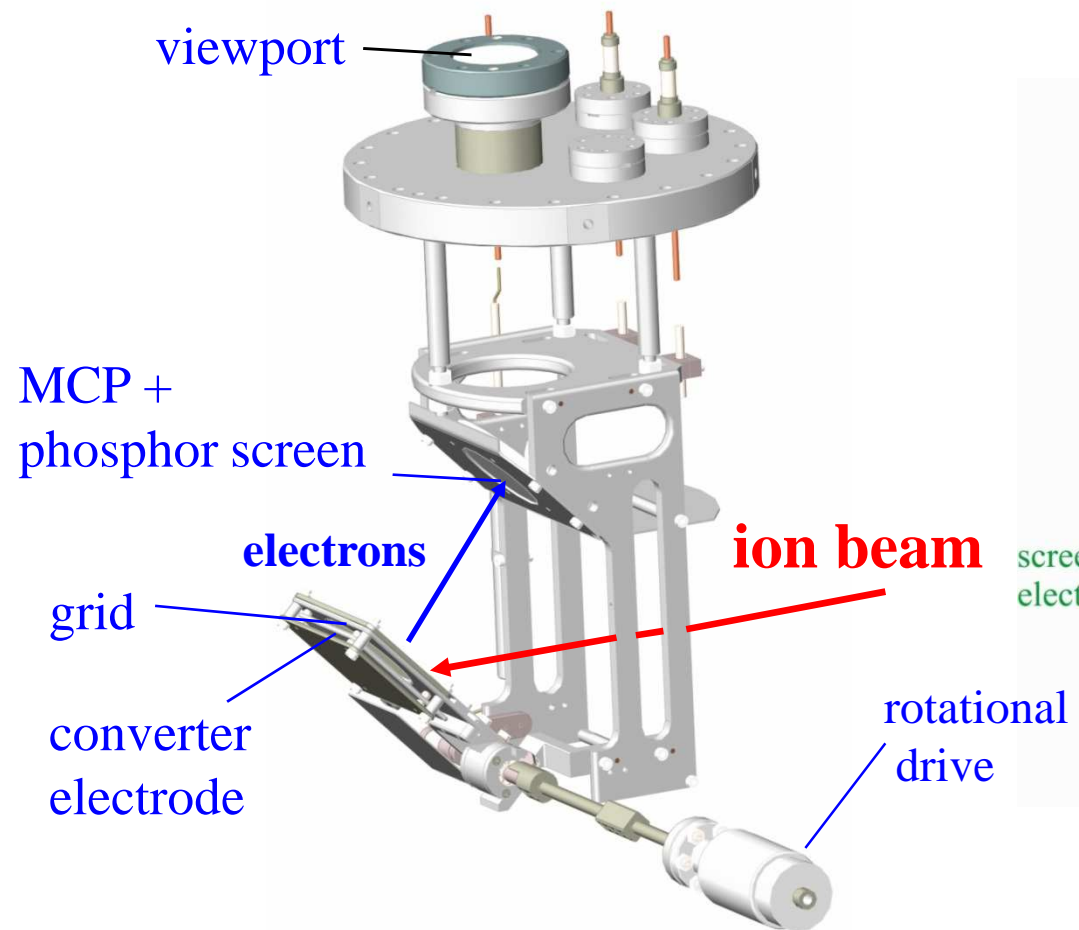
First Cryogenic operation



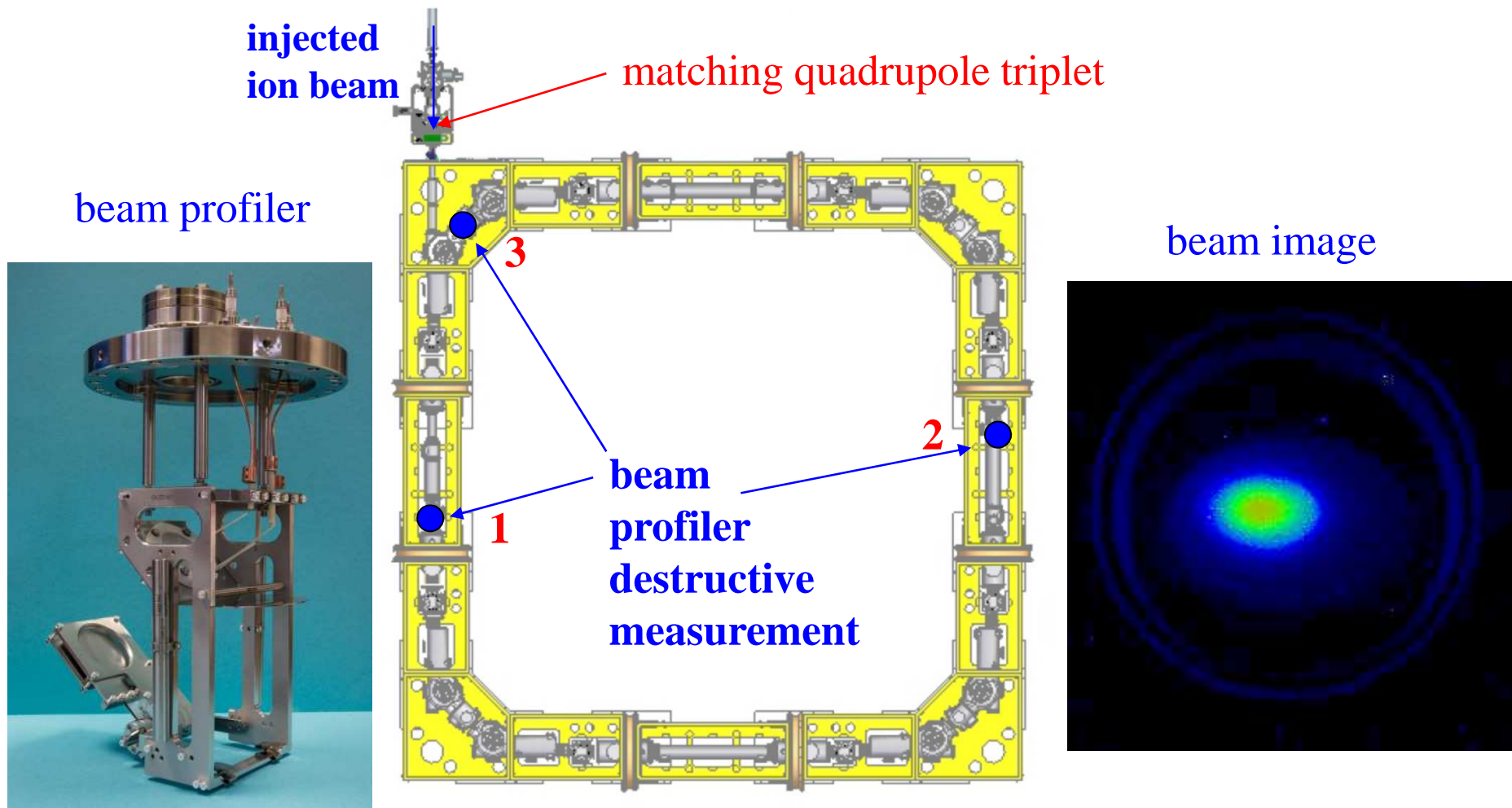
Cool down of the CSR



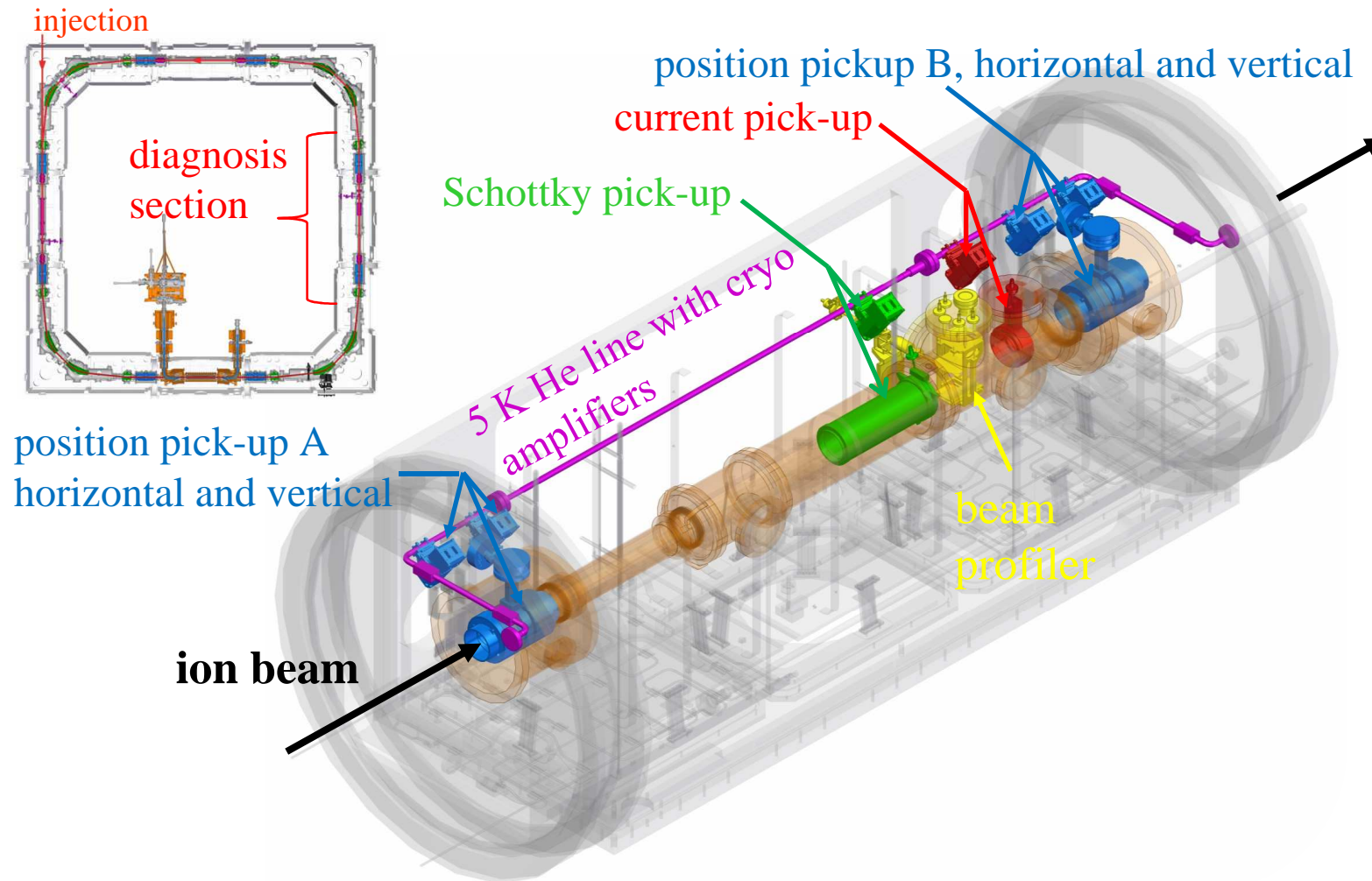
Beam profiler for first turn diagnosis



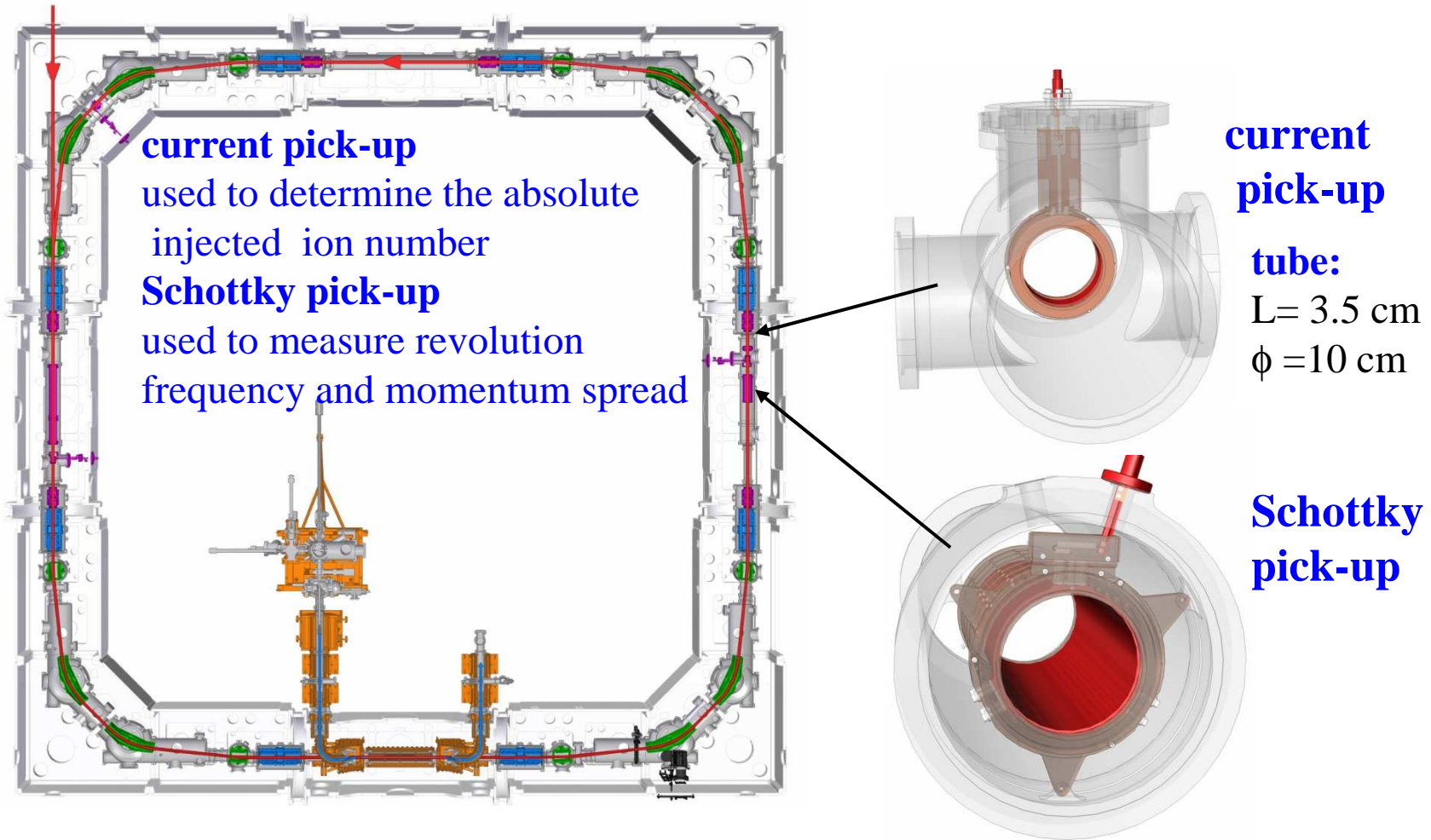
Diagnosics for ion beam injection



The diagnosis section

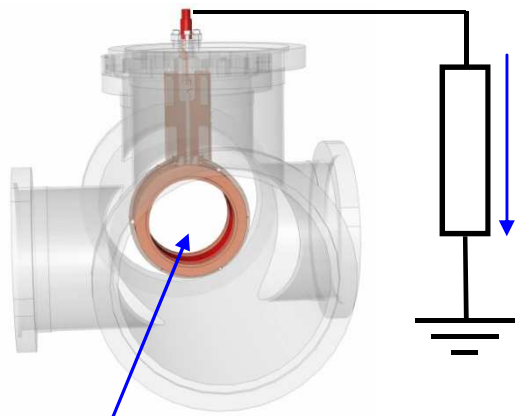


The current and Schottky pick-up



Current pick-up

- used to measure the **absolute number** of the injected ion number (pulsed beam)
- sensitivity 10^6 singly charged ions



$$U(t) = \frac{X_u}{C} \frac{L}{v} I(t)$$

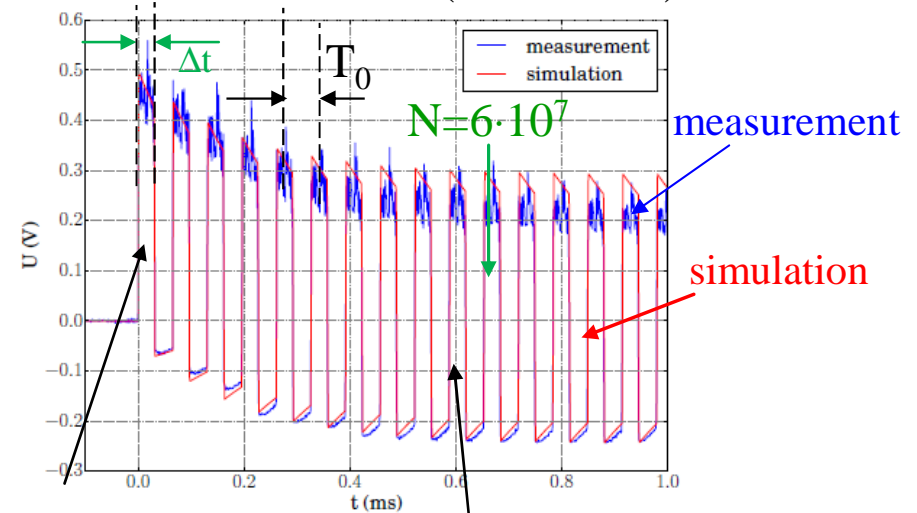
X_u - signal amplification
 L - pick-up length
 v -velocity
 C - capacity

tube: $\phi = 10$ cm, $L = 3.5$ cm

integration over one pulse

$$N = \frac{1}{qe} \int_{t_1}^{t_2} I(t) dt = \frac{1}{qe} \frac{Cv}{L} \int_{t_1}^{t_2} \frac{U(t)}{X_u} dt$$

measured current signal of an $^{40}\text{Ar}^+$ ions ($E = 60$ keV)



injected ion pulse

stored ion pulse

T_0 - revolution time

pulse length Δt is set up with an chopper located in the transfer line to the CSR

Schottky noise spectrum



Schottky pick-up

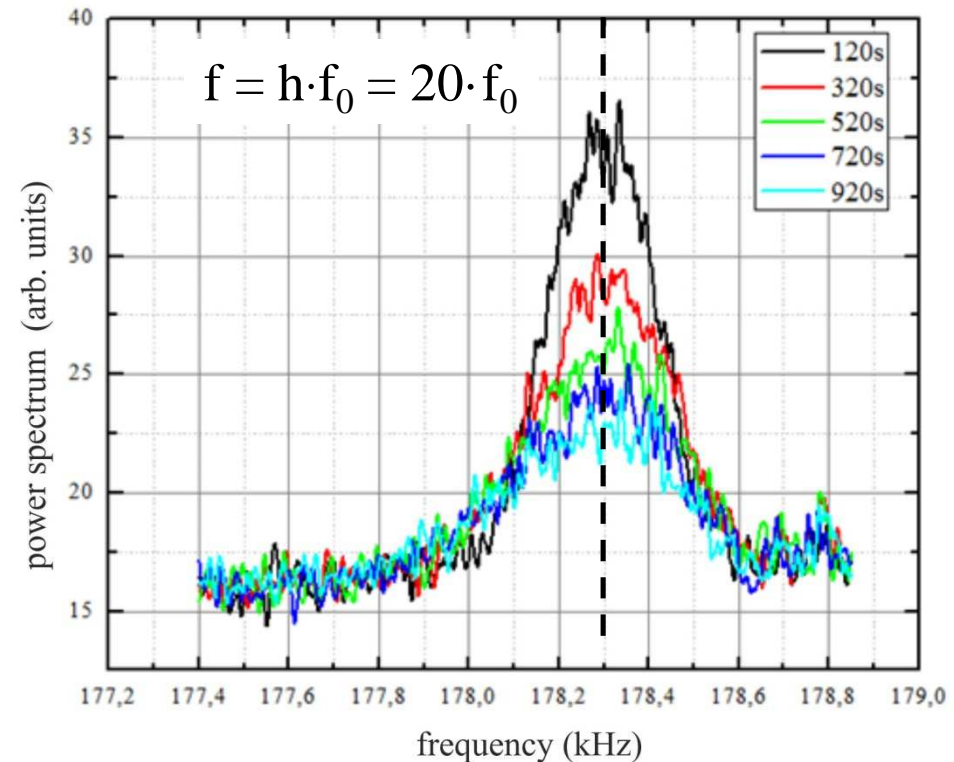
slip factor

$$\eta = \frac{\Delta f / f}{\Delta p / p}$$

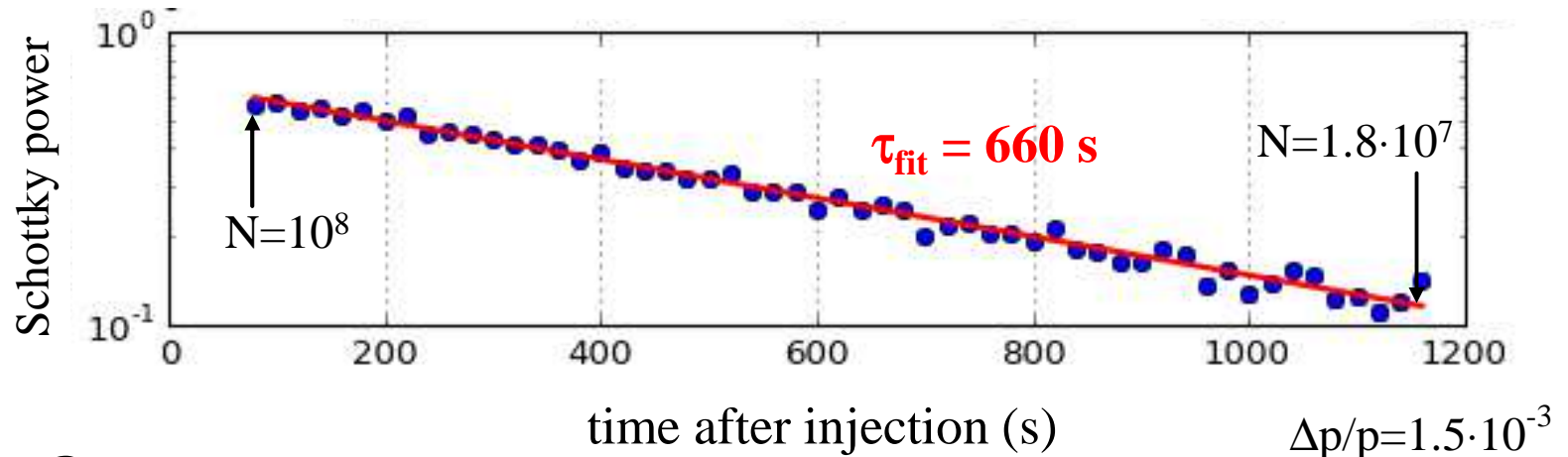
$$= 1 - \frac{1}{\gamma_{th}^2} = 0.7 \quad (\text{non relativistic approach})$$

standard mode

Time development of the Schottky noise spectrum (60 keV CO₂⁻ ions)

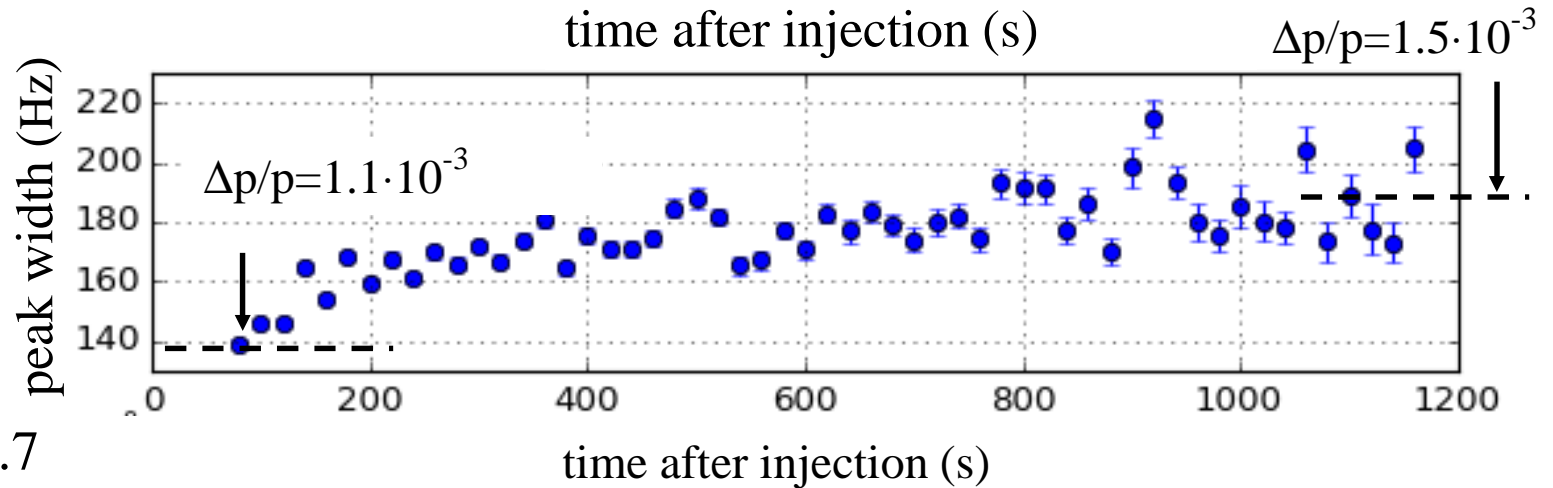


Lifetime Measurements of a stored Co_2^- beam with Schottky noise analysis



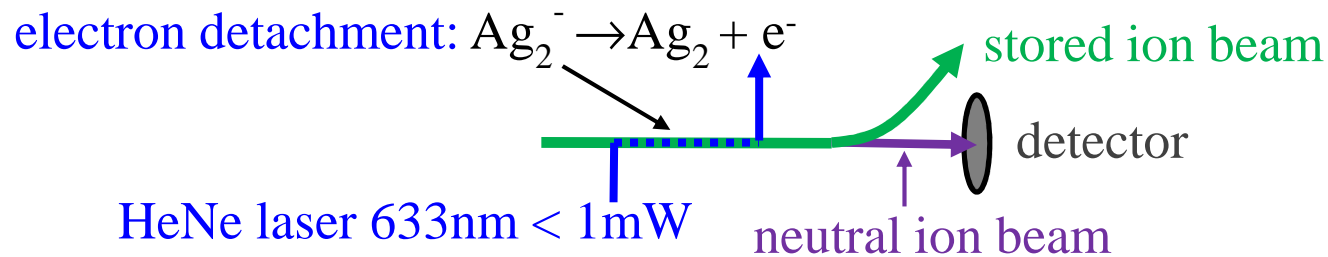
due to noise on the electrodes increasing of $\Delta p/p$

$$\eta = \frac{\Delta f / f}{\Delta p / p} = 1 - \frac{1}{\gamma_{\text{th}}^2} = 0.7$$

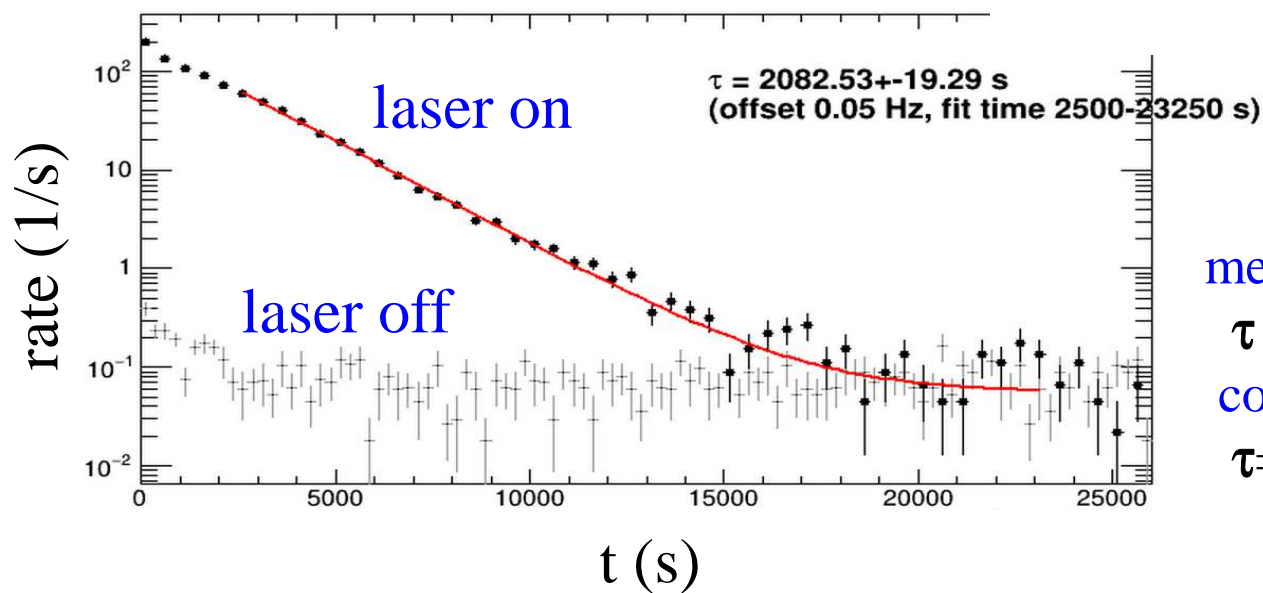


observation frequency: $f = h \cdot f_0 = 20 \cdot f_0$

Lifetime Measurement of stored Ag_2^- ions ($E=60$ keV)



neutral rate on the detector



measured life time:

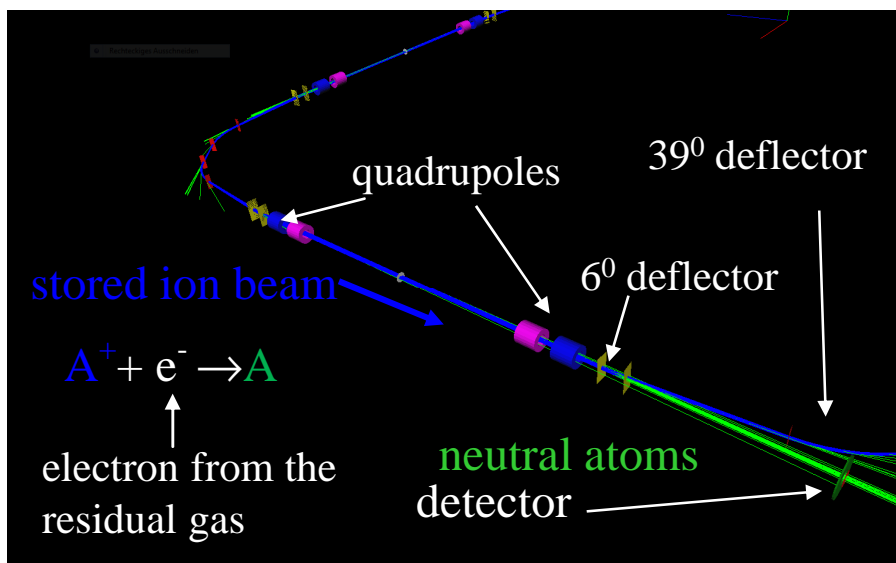
$$\tau = 2082 \text{ s}$$

corrected for laser depletion:

$$\tau = 2500 \text{ s}$$

Measurement of the residual gas density

simulation of the neutralization process **with g4beamline**



simulation results

fraction of ions η_f hitting the detector

$\epsilon_{x,90\%}$ (mm mrad)	η_f
0.5	0.126
9.1	0.119
23.0	0.118

average value $\eta_f = 0.121$

σ - cross section for neutralization

singly charged 50-60 keV ions (for H_2):

Ar^+ : $\sigma = 5.3 \cdot 10^{-16} \text{ cm}^2$ O^- : $\sigma = 3.4 \cdot 10^{-16} \text{ cm}^2$

v - velocity

n - residual rest gas density

$R(t)$ - detector rate

$N(t)$ - number of stored particles

$$R(t) = \eta_f \cdot \frac{N(t)}{\tau_c} \quad \tau_c = \frac{1}{n \cdot v \cdot \sigma}$$

measurement:

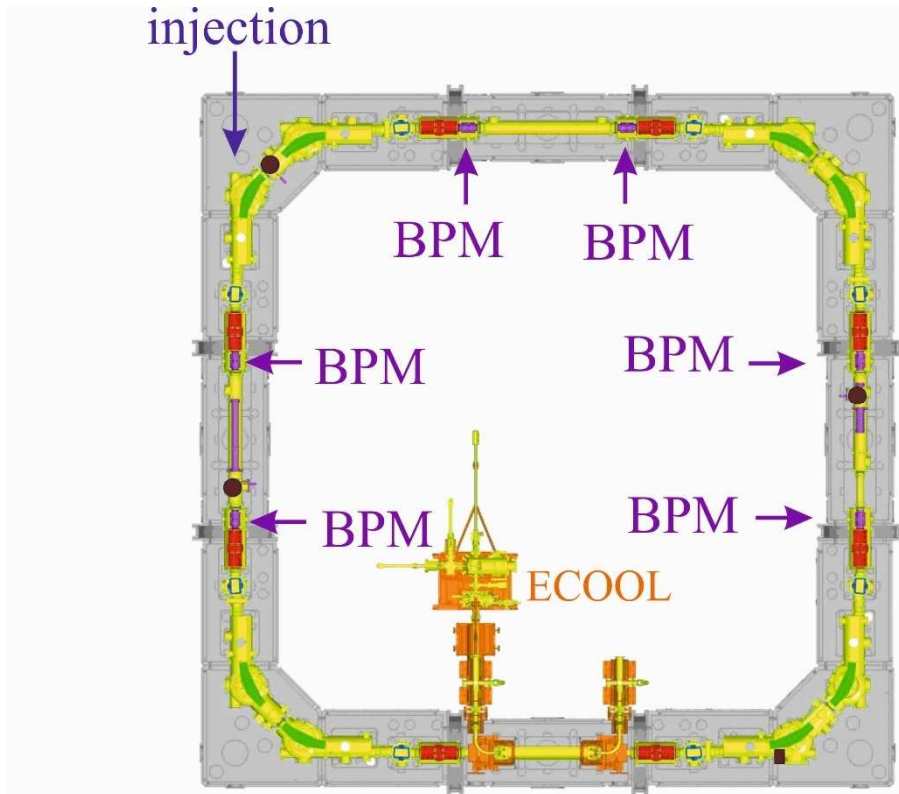
$^{40}Ar^+$ ($E=60 \text{ keV}$) and $N=2 \cdot 10^8$:

$R < 10 \text{ 1/s} \Rightarrow n < 20 \text{ H}_2 \text{ molecules/cm}^3 \text{ !!!}$

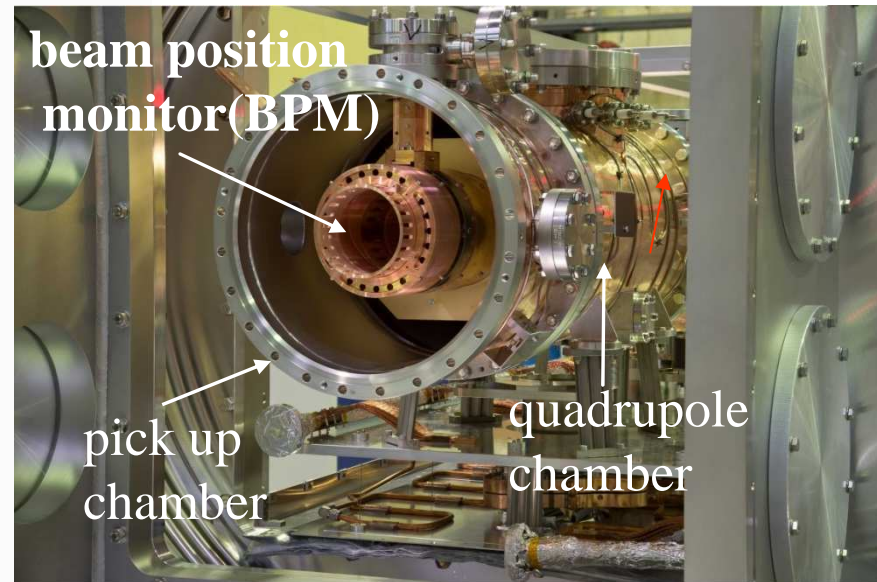
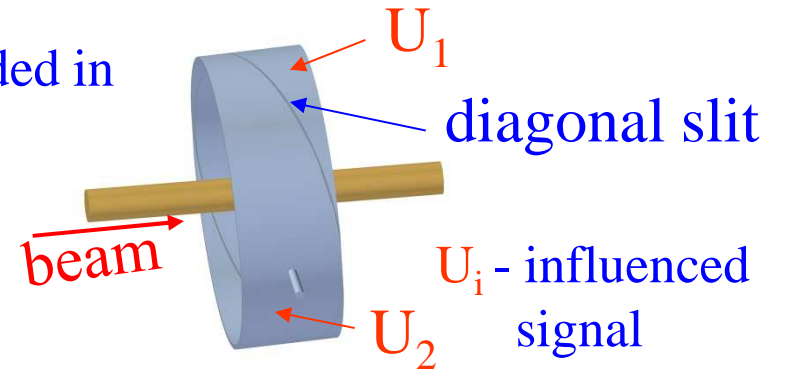
\Rightarrow vacuum life time: $\tau_v > 10^6 \text{ s} \approx 280 \text{ h} \Rightarrow$ lifetime is not residual gas dependent !!!

Beam Position Monitor (BPM)

CSR has 6 horizontal and 6 vertical position pick ups (BPM)



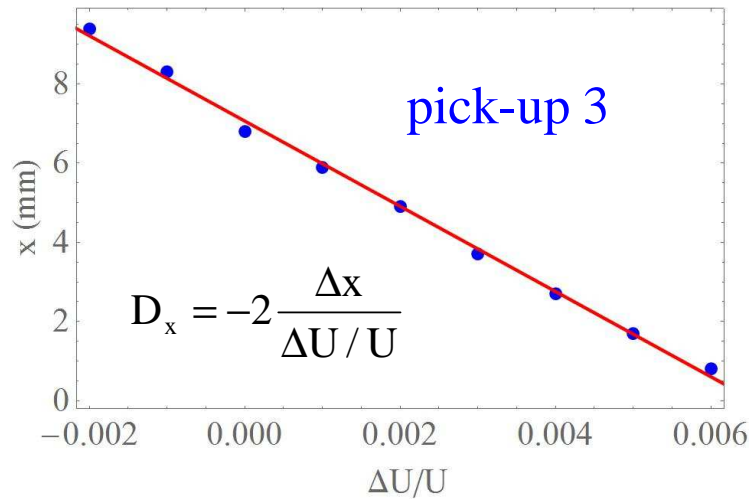
tube divided in two parts



Dispersion in the straight section

pick-up measurements

closed orbit change x via variation of all potentials by $\Delta U/U$



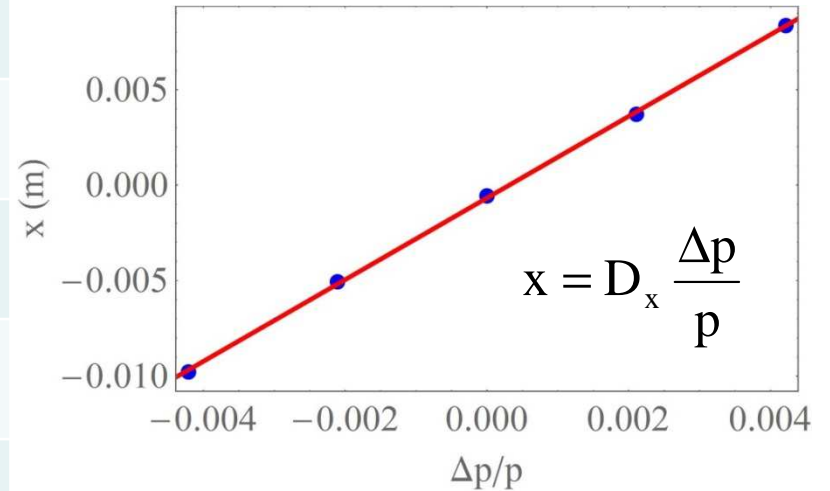
average value

$$\bar{D}_x = 2.17 \text{ m}$$

pick-up	D_x (m)
1	2.19
2	2.23
3	2.15
4	2.17
5	2.16
6	2.09

g4beamline simulation

tracking of particles with different momenta and plotting the closed orbit position x as a function of $\Delta p/p$

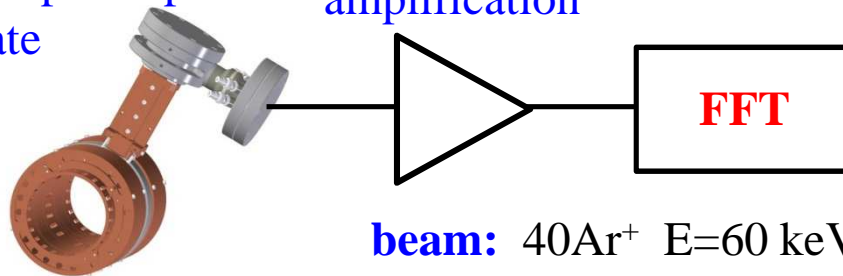


$$D_x = 2.14 \text{ m}$$

Application of pick-up measurements

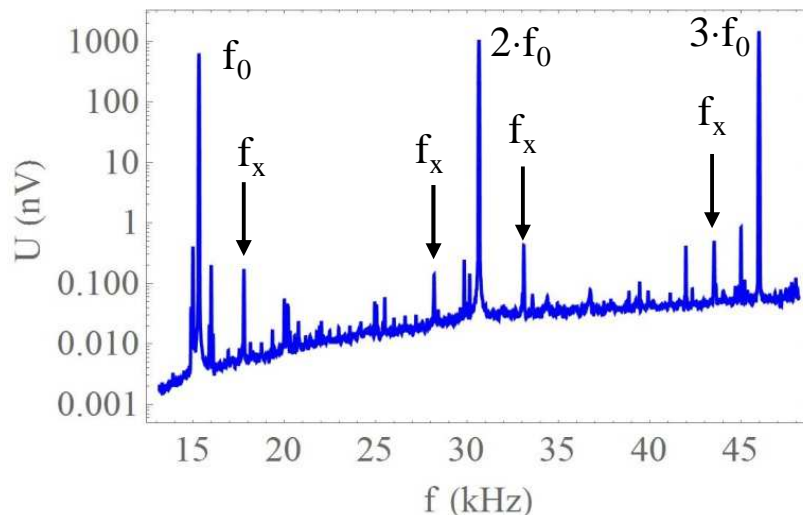
determination of the horizontal and vertical tune

one pick-up
plate



excitation of the betatron oscillation by off axis injection of the beam

spectrum of a pick-up signal induced on a horizontal plate



f_0 - revolution frequency

f_x - betatron side band

$$f_x = f_0 (n \pm q_x)$$

n- integer number

q_x - non integer part of the tune

effective quadrupole length

The effective quadrupole length are determine by matching the measured tunes with the calculated tunes.

result:

calculated with **TOSCA**: $l_{\text{eff}}=0.211$ m

measurement:

quadrupole family 1: $l_{\text{eff}}=0.208$ m

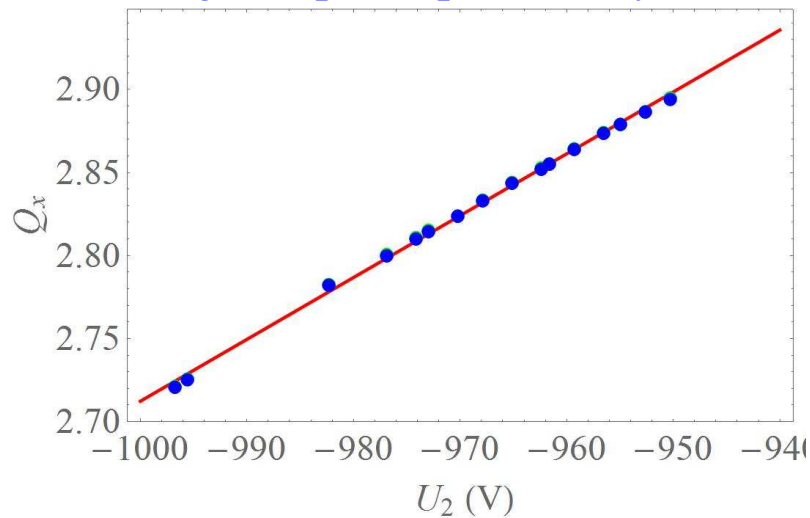
quadrupole family 2: $l_{\text{eff}}=0.209$ m

Determination of horizontal β_x and vertical β_y functions

$$\Delta Q_x = \frac{1}{4\pi} \int \beta_x(s) \cdot \Delta K(s) ds$$

$$\Rightarrow \bar{\beta}_x = \frac{\pi U}{2 K} \frac{\Delta Q_x}{\Delta U} \frac{1}{L_m}$$

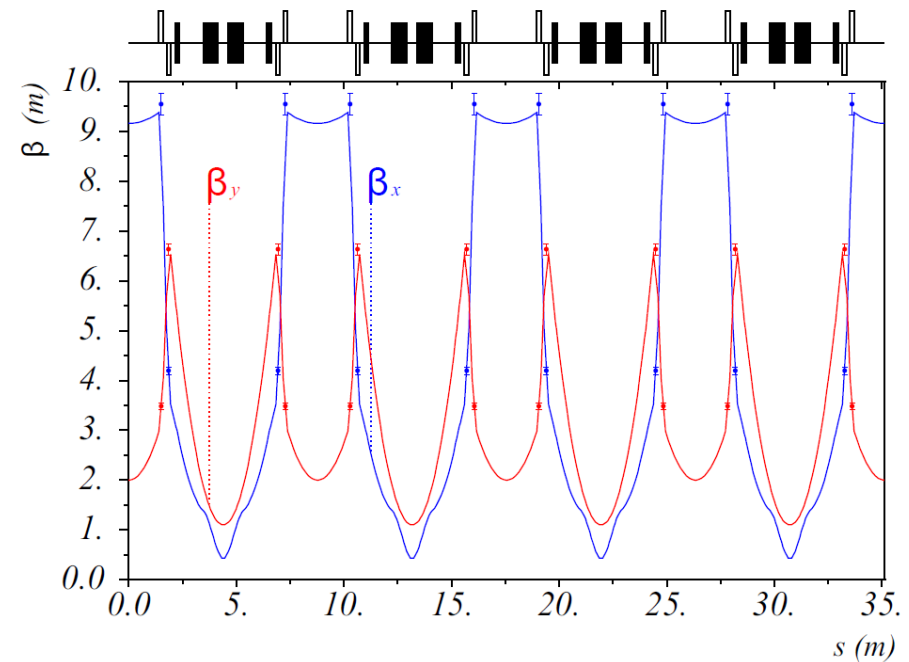
horizontal tune as a function of voltage of quadrupole family 2



Q_x - horizontal tune

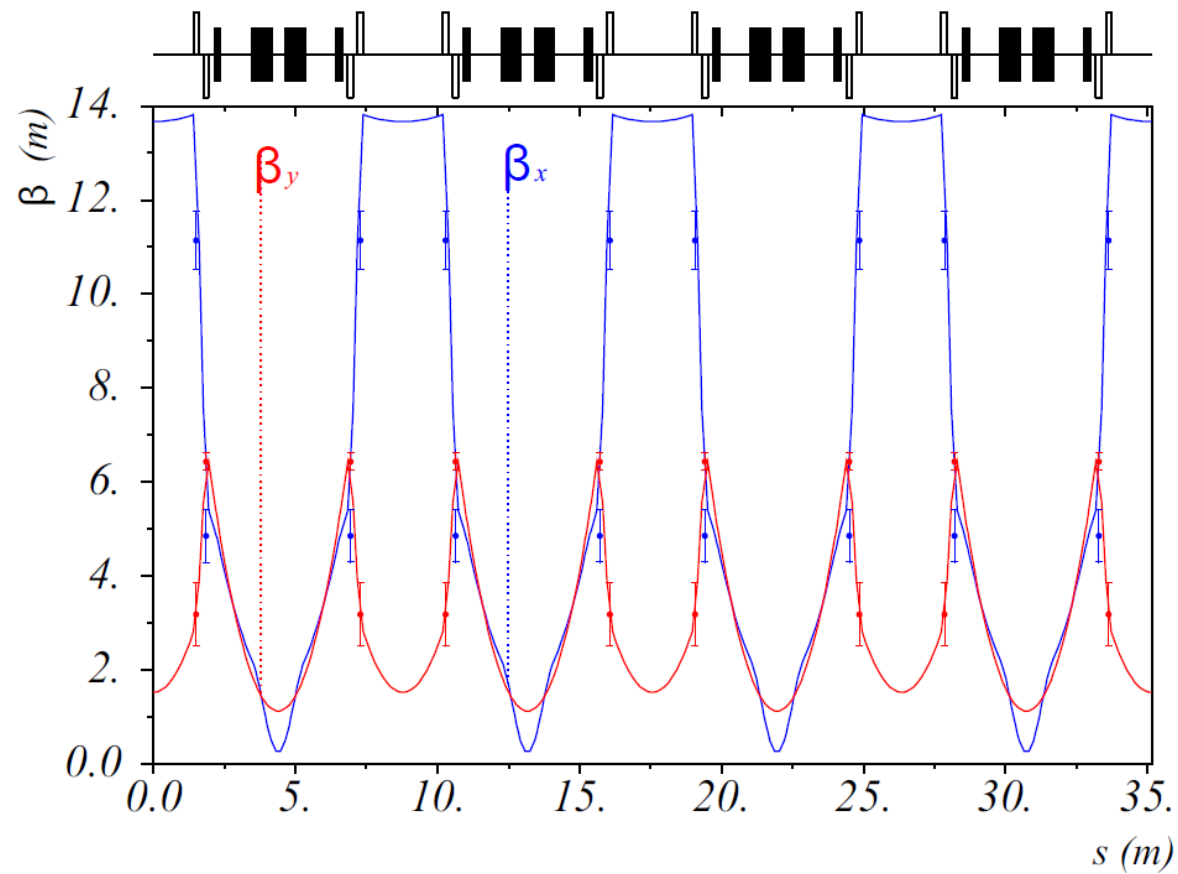
U₂ - voltage of quadrupole family 2

MAD calculation of horizontal and vertical β function (standard mode)



- measured vertical β_x function
- measured vertical β_y function

Comparison of measured and calculated β function for working point II



- measured vertical β_x function
- measured vertical β_y function

The slip factor η and momentum compaction α_p

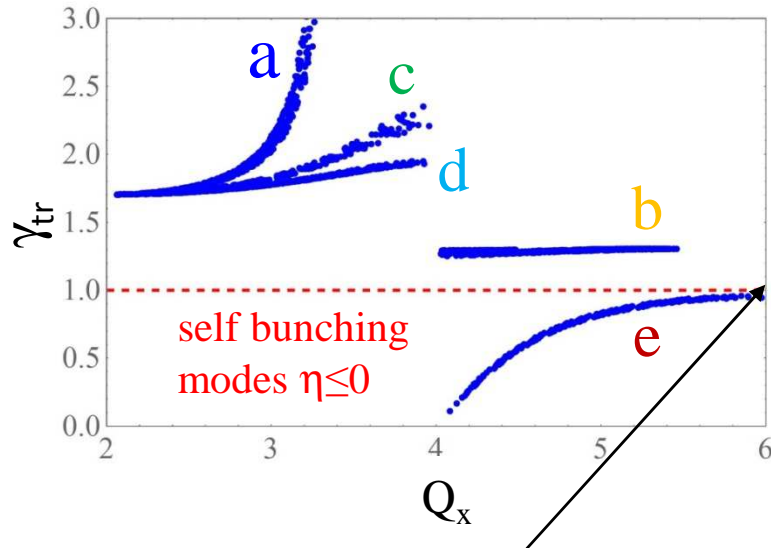
slip factor η in the non relativistic approach ($\gamma \rightarrow 1$)

different to magnetic storage ring

$$\eta = \frac{\Delta f / f}{\Delta p / p} = 1 - 2\alpha_p = 1 - \frac{1}{\gamma_{tr}^2}$$

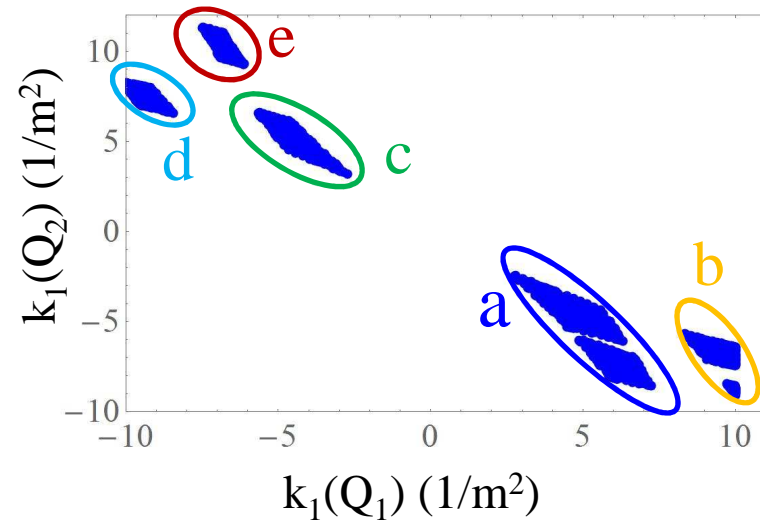
γ_{tr} - gamma transition parameter
 α_p - momentum compaction $\alpha_p = \frac{\Delta C / C}{\Delta p / p}$
 f- revolution frequency
 p- momentum
 C- circumference

γ_{tr} as a function as a horizontal tune Q_x



isochronous mode with $\eta=0$
 unfortunately: $Q_x=6$
 strong resonance !

Stability diagram of CSR



$k_1(Q_1)$ and $k_1(Q_2)$ are the quadrupole strength of quadrupole family 1 and quadrupole family 2

Measurement of the slip factor η at the CSR

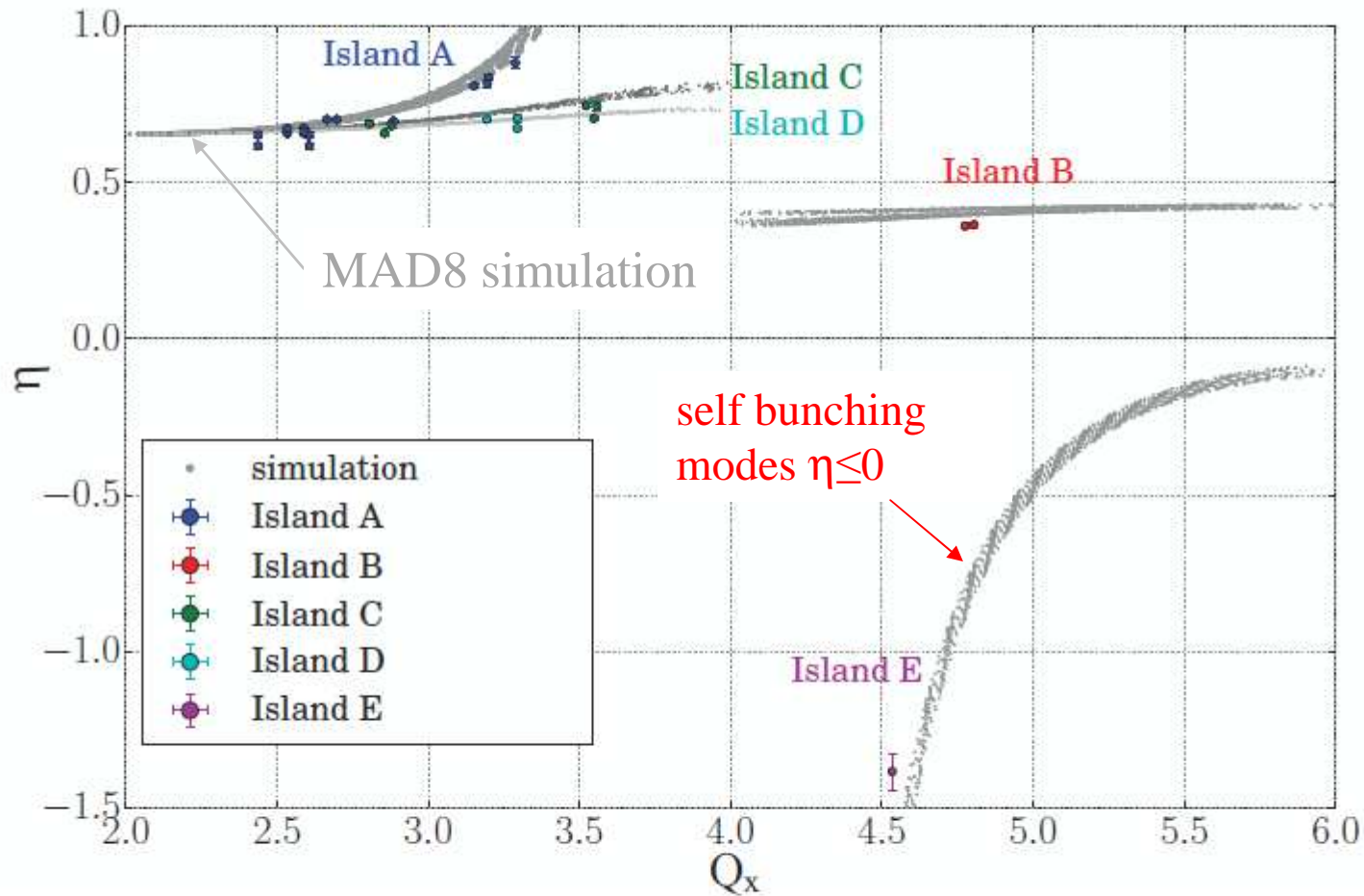
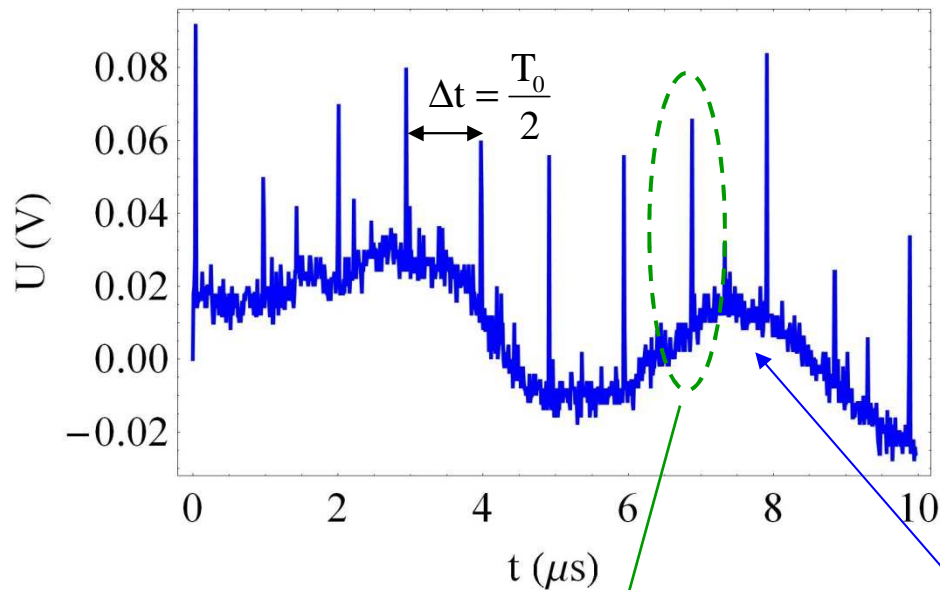


Figure 3. The measured (markers with error bars) and simulated (gray markers) phase slip factors for the cryogenic storage ring CSR as a function of the measured and simulated horizontal tune Q_x , respectively.

Self Bunching at $\eta < 0$ observed at the TSR

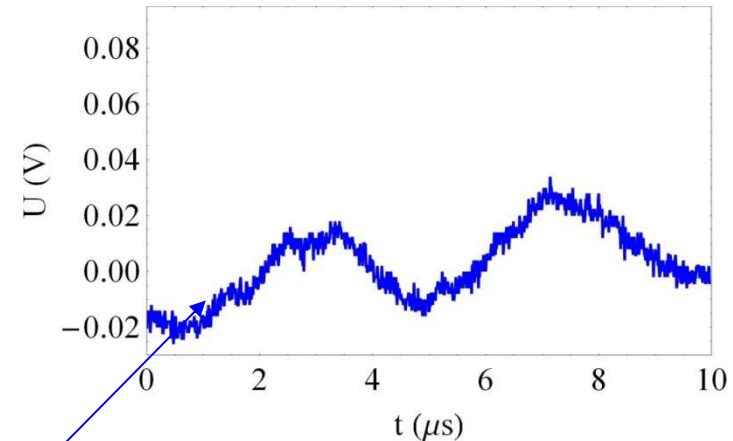
pick-up voltage

with beam, without rf $U_0=0$, ECOOL on



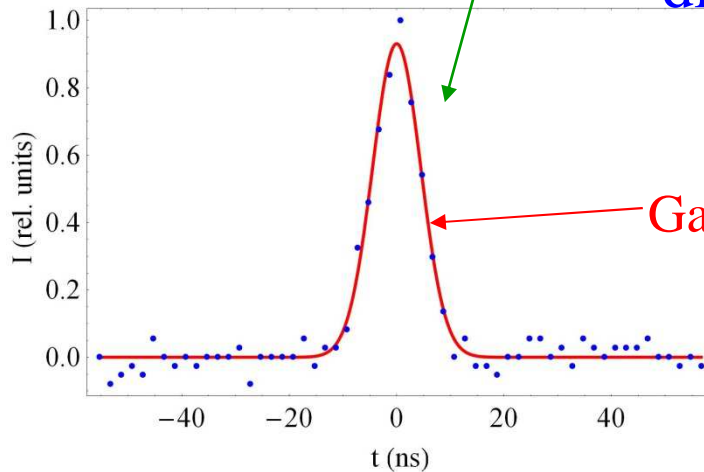
pick-up voltage

without beam, without rf, ECOOL on

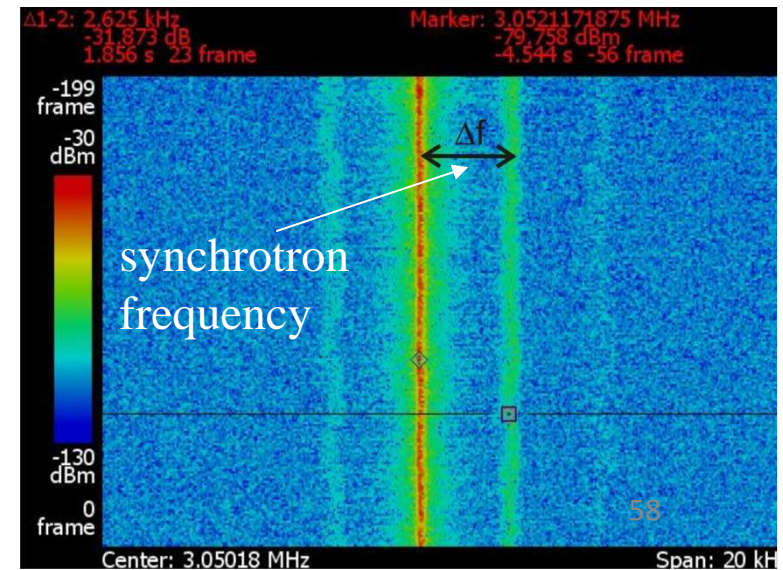


synchrotron side band caused by self bunching

disturbance

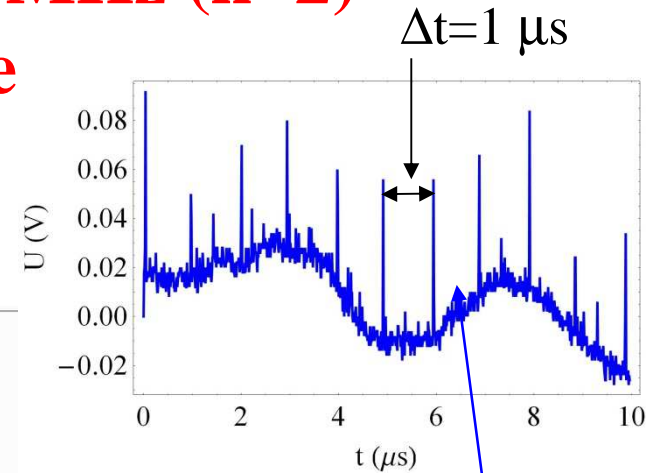
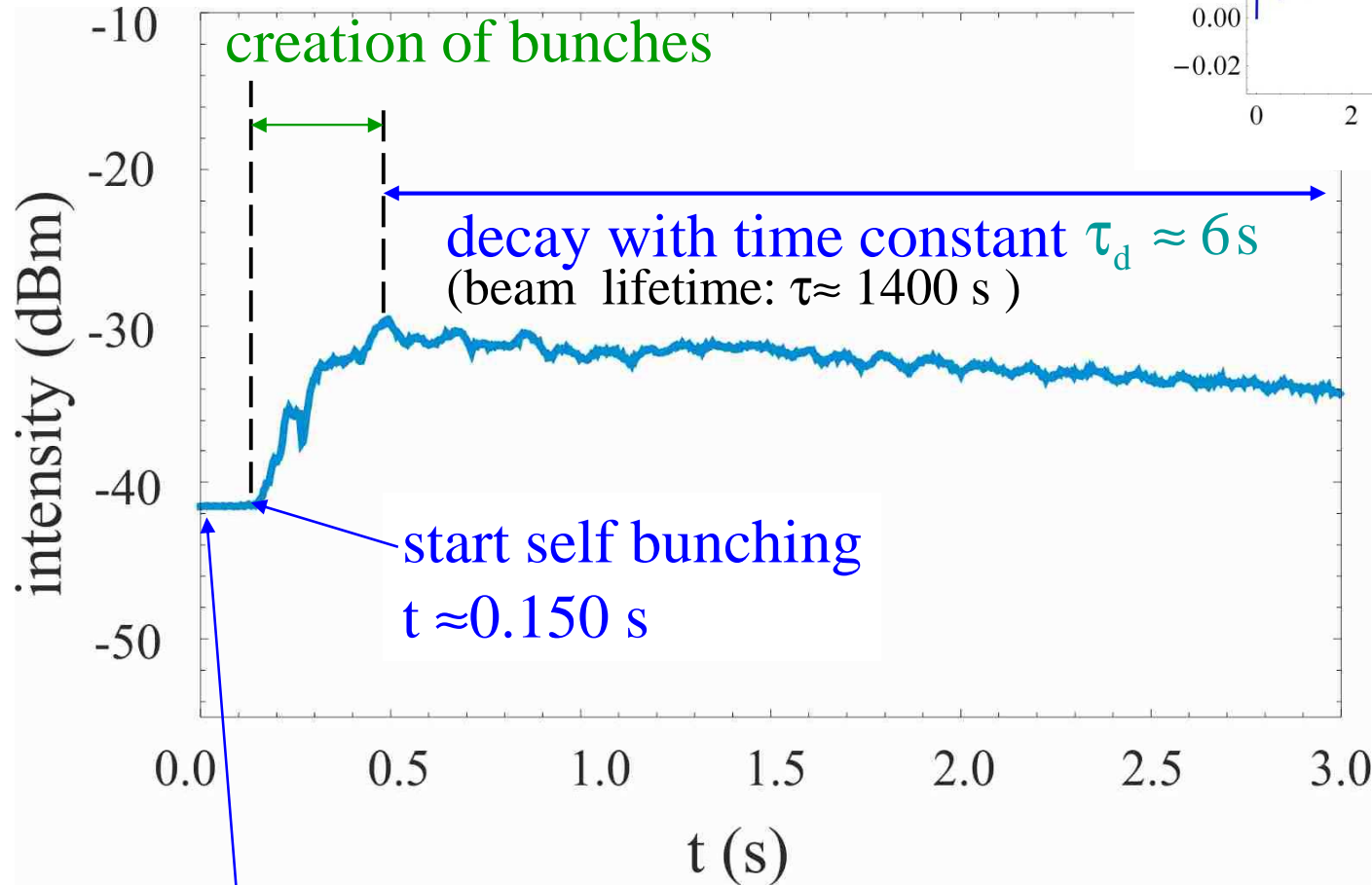


$I \approx 2 \mu\text{A}$
 $\sigma = 4.5 \text{ ns}$
 beam: $^{12}\text{C}^{6+}$
 $E = 50 \text{ MeV}$



Pick-up signal measured at $f=1$ MHz ($h=2$) as a function of time

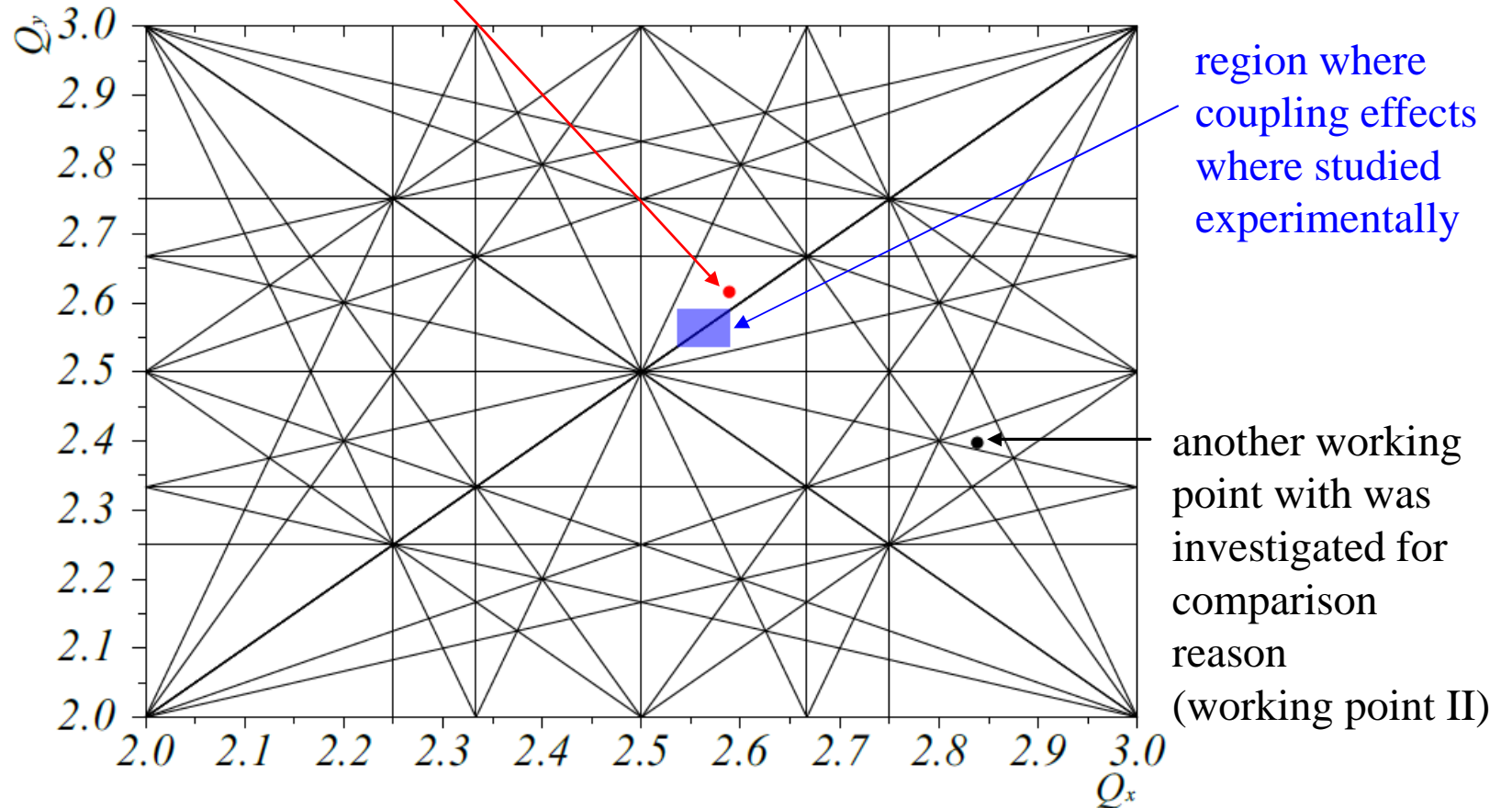
observation frequency $f = 1.0$ MHz



injection at $t=0$ s and start electron cooling

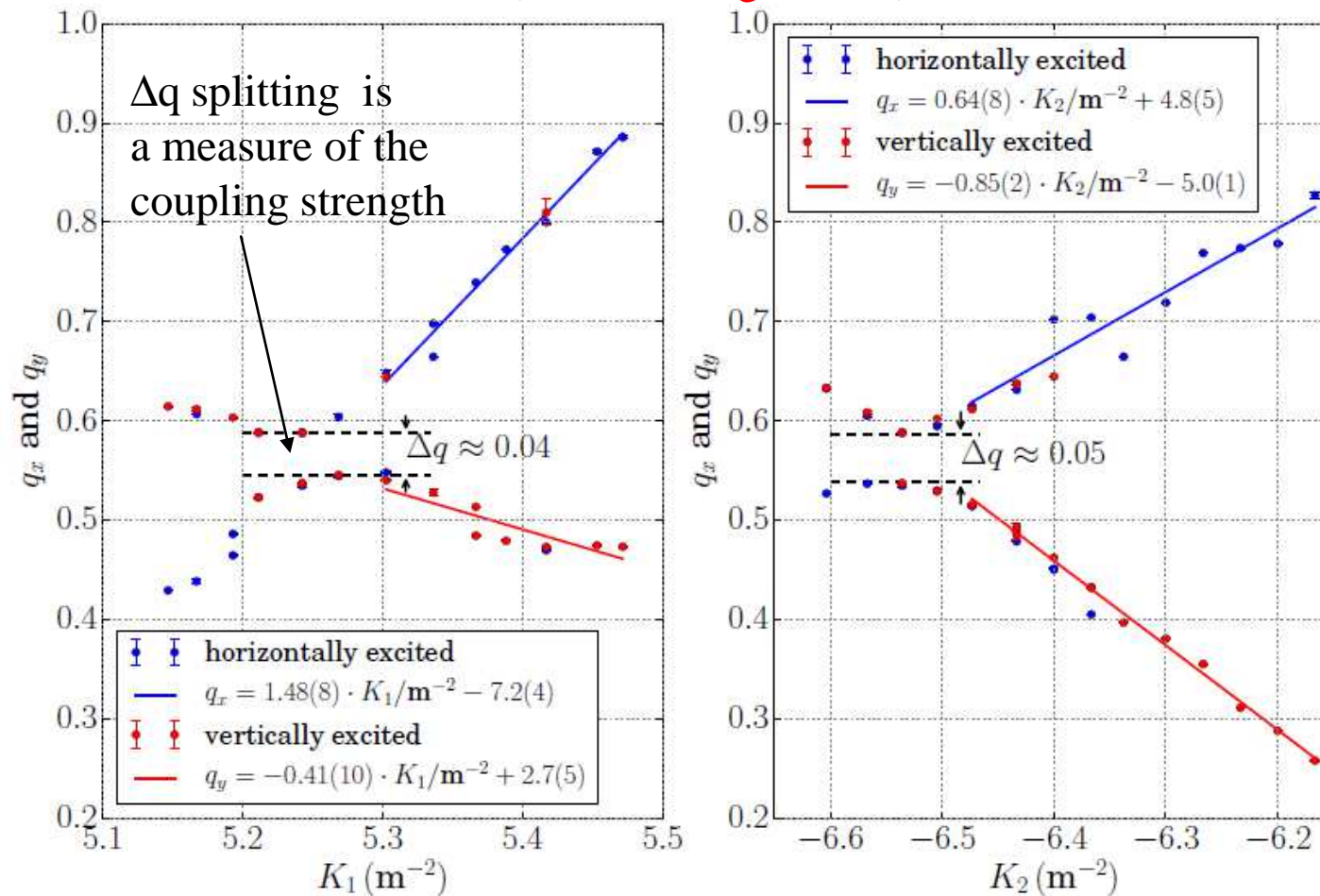
CSR working point

working point for electron cooling to enable a large incoherent tune shift



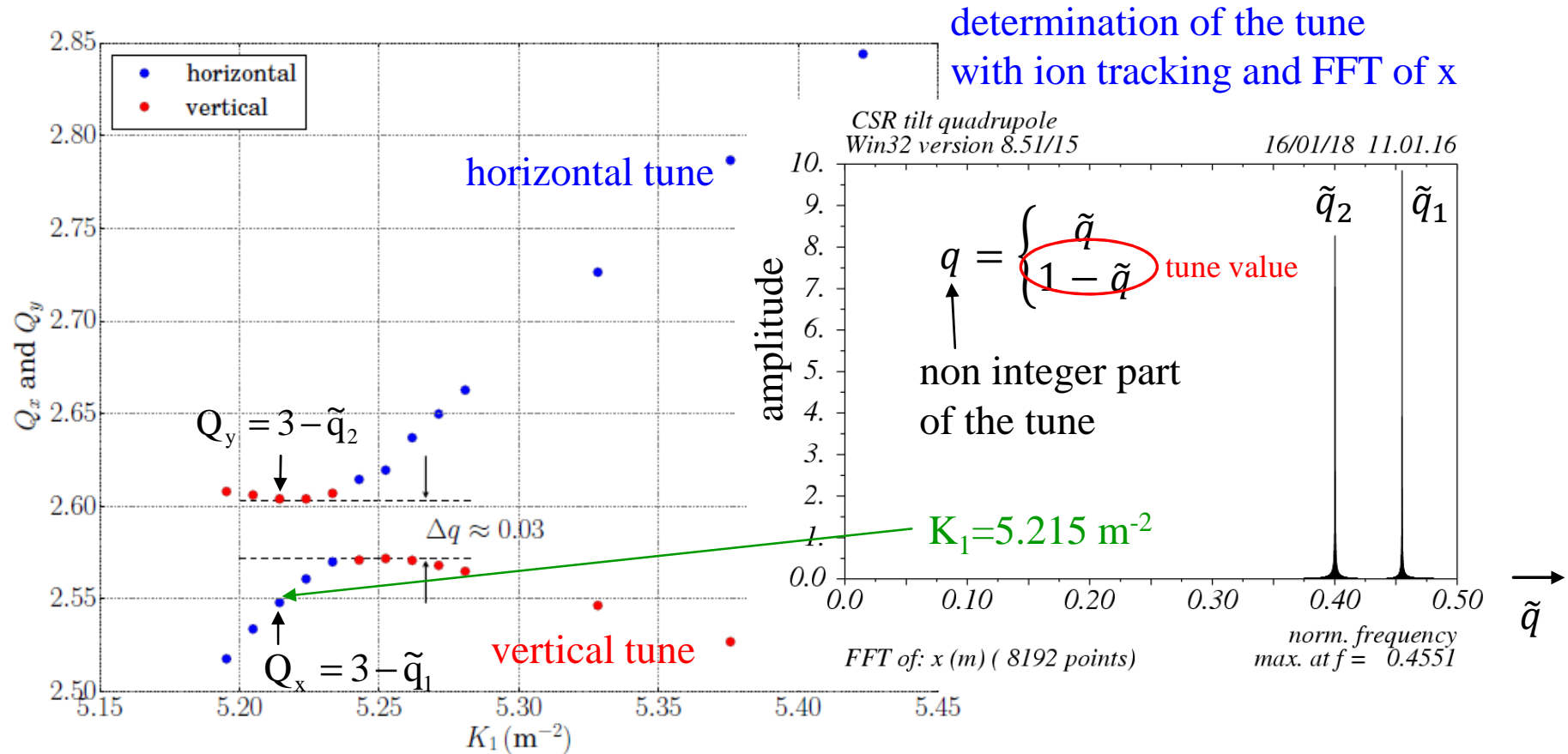
Operation of the CSR close to the coupling resonance

(ECOOOL magnets off)



Measured fractional tune values q_x and q_y as a function of the quadrupole strengths of family 1 and 2 close to the coupling resonance. In the left plot $k_2 = -6.54 \text{ m}^{-2}$ and in the right plot $k_1 = 5.24 \text{ m}^{-2}$

Explanation of the coupling effect

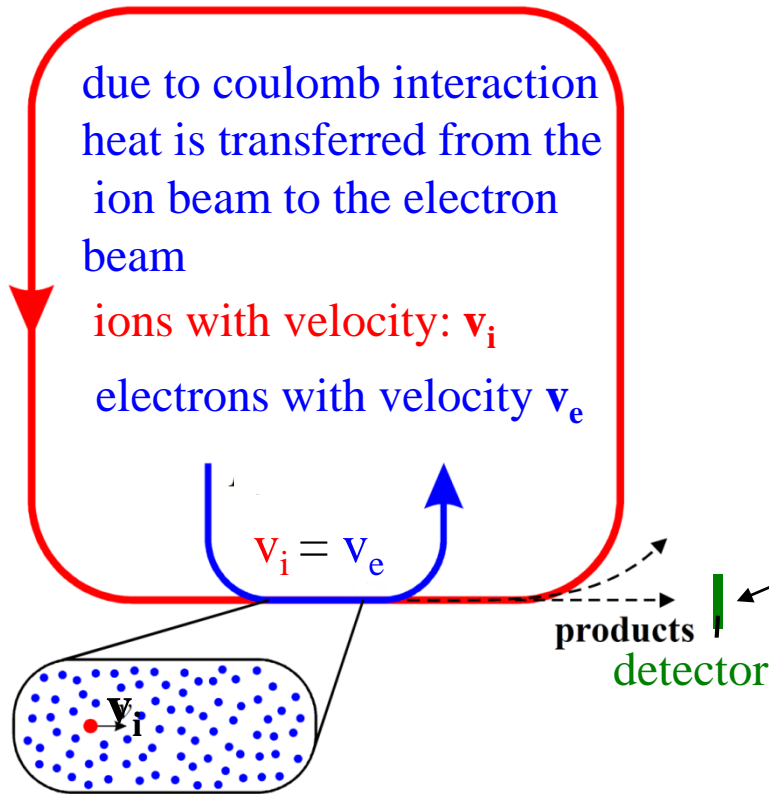


MAD8 simulation of the tune values Q_x and Q_y as a function of the quadrupole strength of family 1. In the simulation one of the quadrupole is rotated by 1° around the longitudinal axis.

rotation angle not specified in the CSR design

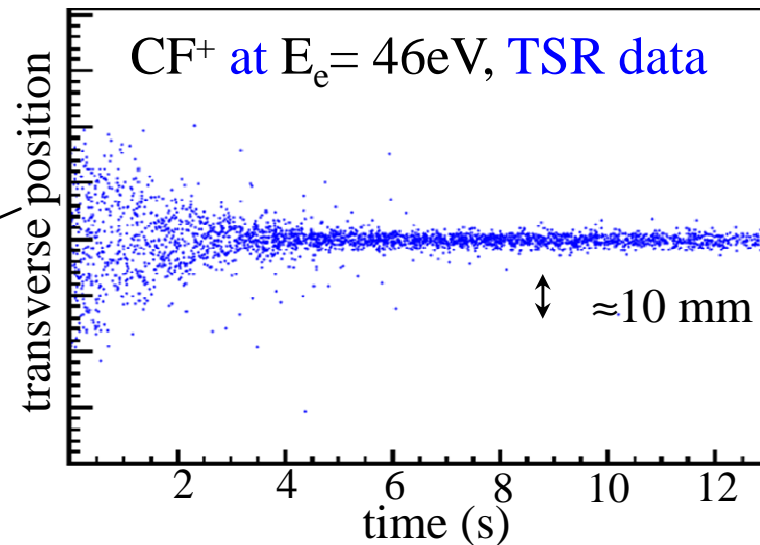
CSR electron cooler – principle

principle of electron cooling:

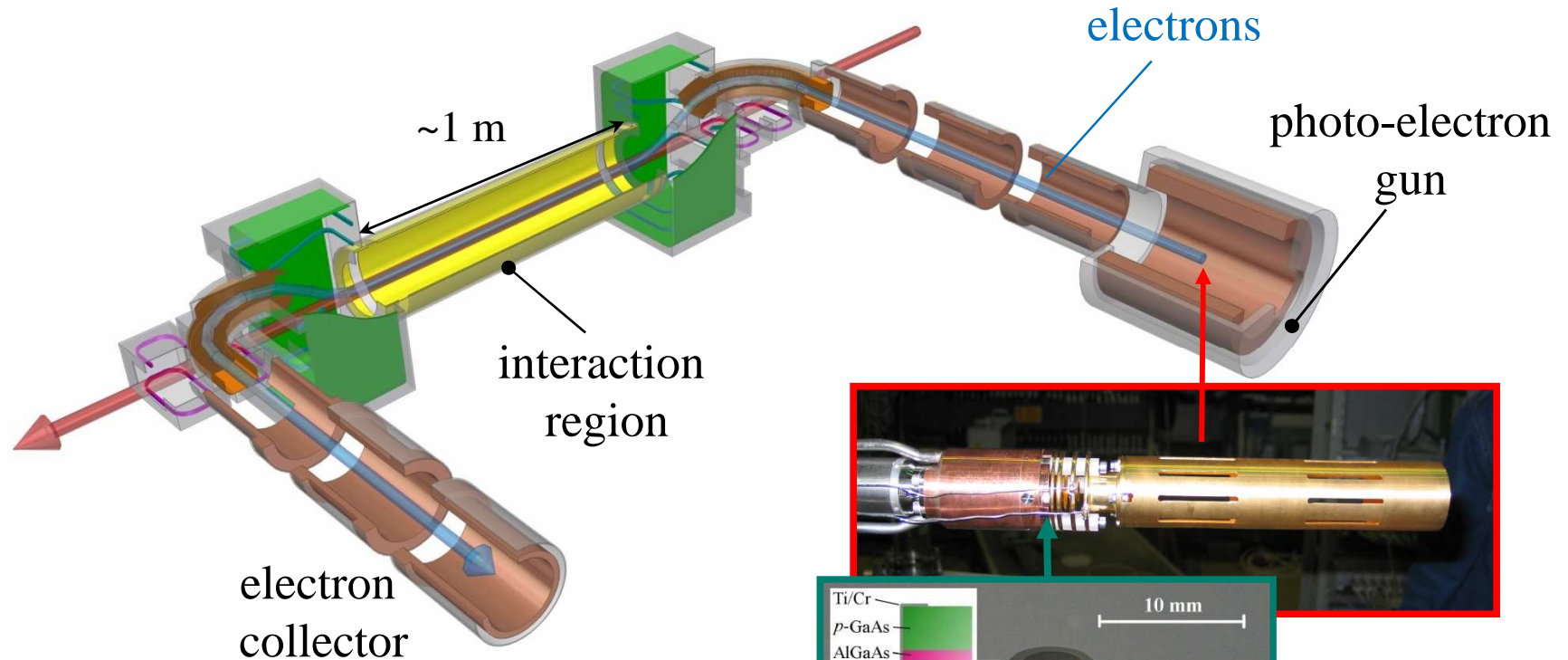


E_e (eV)	ion
163	for 300 keV p^+
~ 10	for most ions
1	for $M_{ion} = 160$ u

electron cooling experiment at the TSR

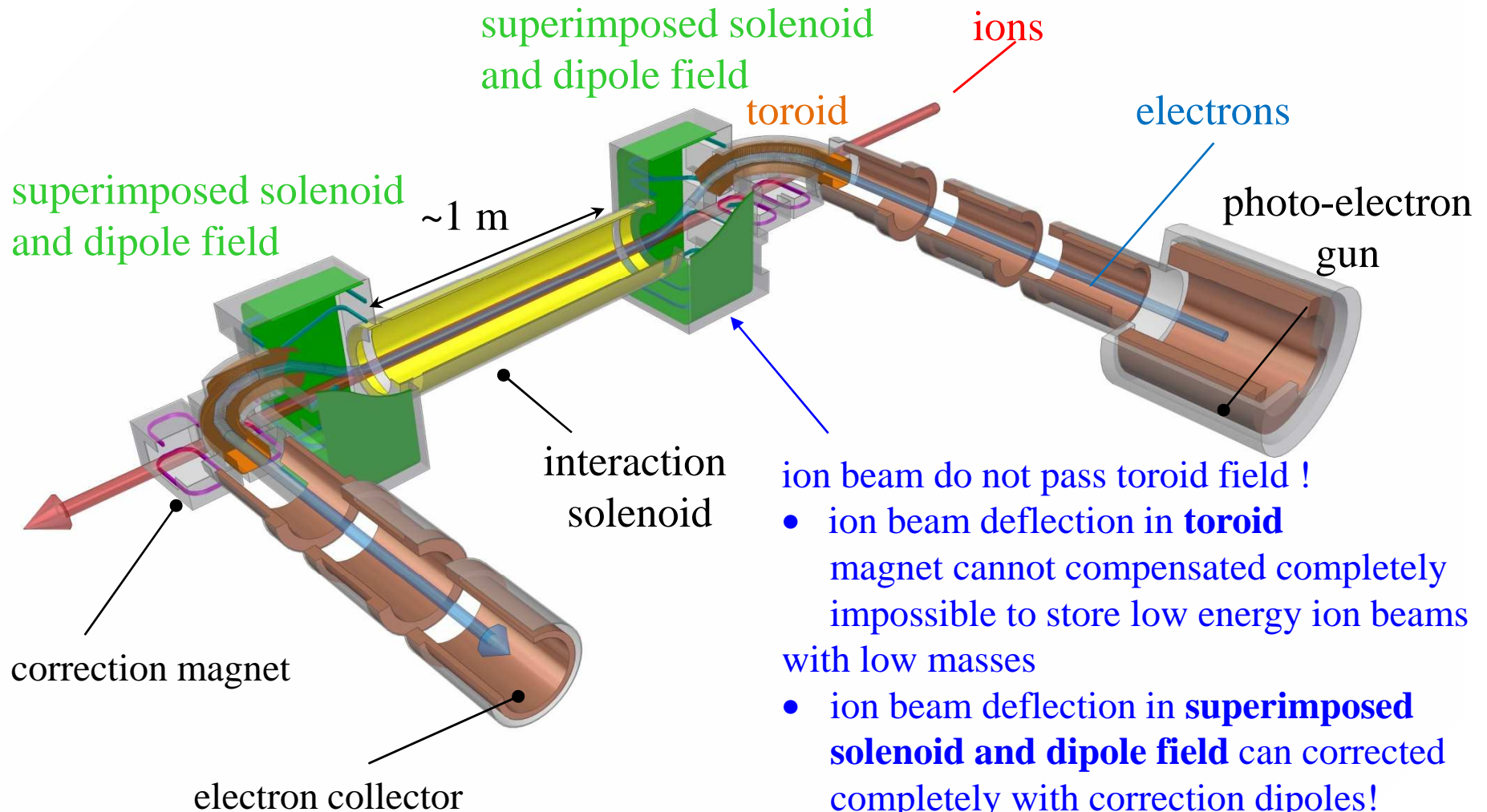


CSR electron cooler – photo-cathode



Shornikov et al., Phys. Rev. ST AB **17**, 042802 (2014)

CSR electron cooler – magnetic guiding field

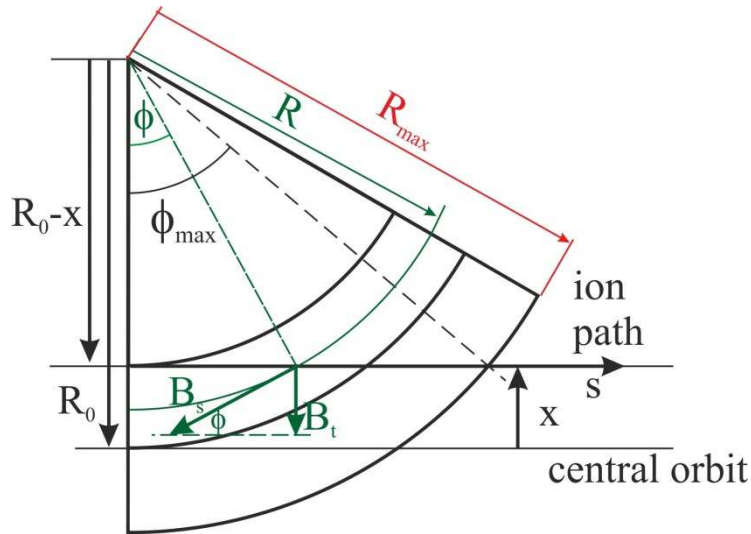


ion beam do not pass toroid field !

- ion beam deflection in **toroid** magnet cannot be compensated completely impossible to store low energy ion beams with low masses
- ion beam deflection in **superimposed solenoid and dipole field** can be corrected completely with correction dipoles!
- very low interaction with the stored ion beam

Ion deflection in one toroid magnet

usual electron cooler: ion beam has to pass an toroid beam



due to interaction with the transverse magnetic field B_t component the ion beam is deflected in the vertical direction:

$$\delta(x) = -\frac{B_0 \cdot R_0}{B\rho} \ln\left(\cos\left(\frac{R_0 - x}{R_{\max}}\right)\right) \quad \text{horizontal deviation}$$

$$= \delta_0 - \frac{B_0}{B\rho} \frac{R_0}{R_{\max}} \tan\left(\frac{R_0}{R_{\max}}\right) \cdot x + \dots$$

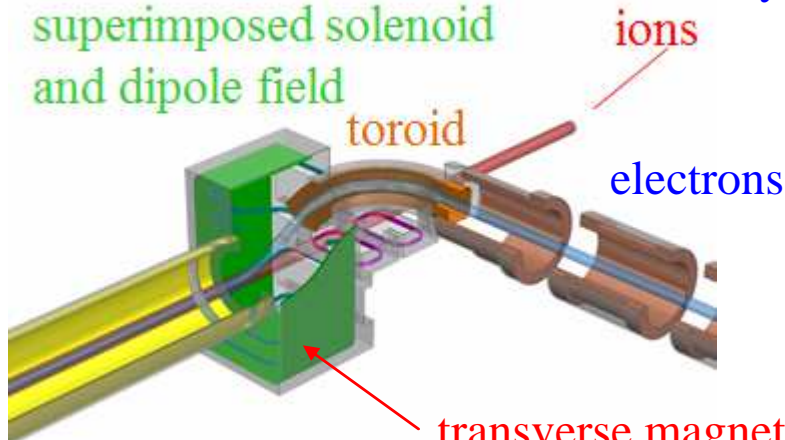
can be compensated by correction magnets

can not compensated by correction magnets

$B\rho$ -beam rigidity

new cooler design

superimposed solenoid and dipole field



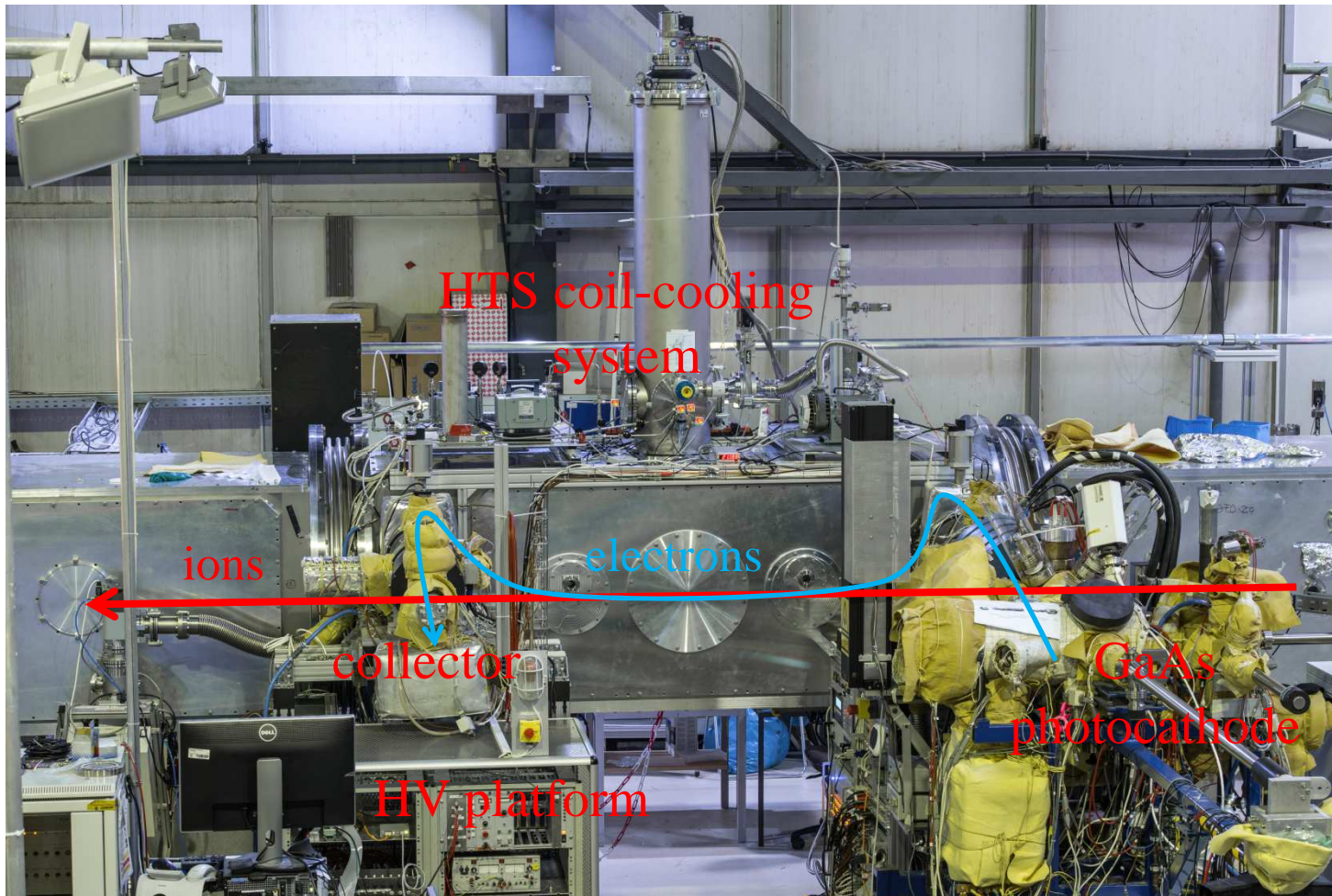
ions with low beam rigidity are kicked out the storage ring !

to avoid the ion loss the ions should not interact with a toroid field

⇒ new electron cooler design

transverse magnetic field B_t do not depend on the horizontal position 66

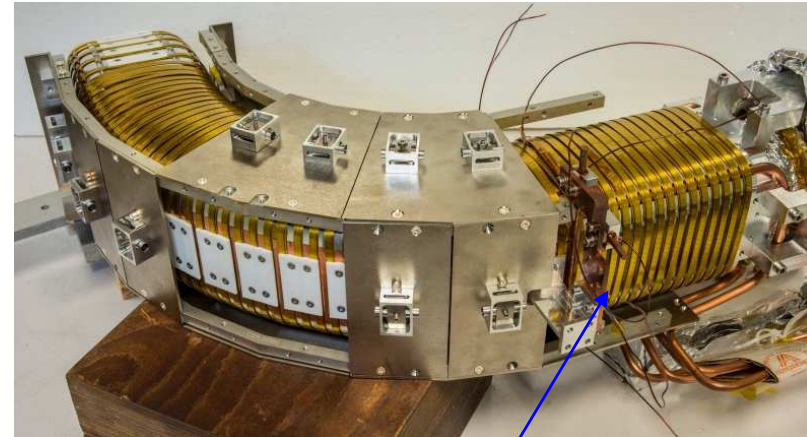
The CSR electron cooler



Magnets of the CSR electron cooler

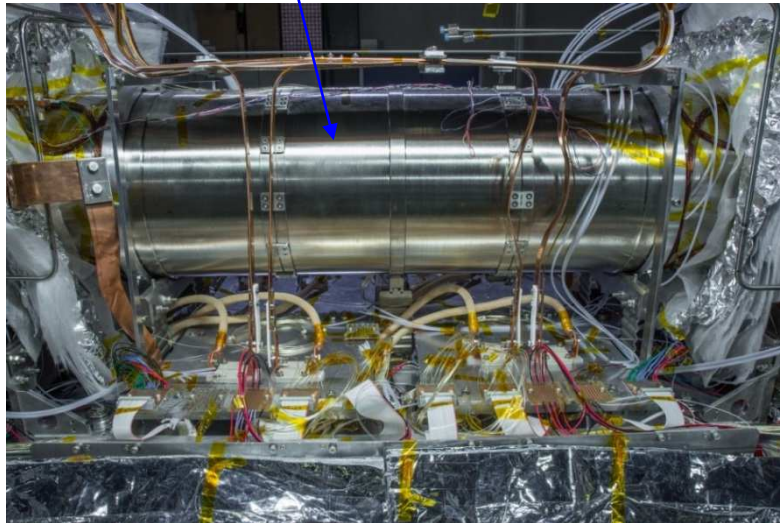
toroid magnet

steering copper coil pairs located inside aluminum body for toroidal drift compensation



high temperature superconductor

iron shield



cooling solenoid

High-temperature superconductor attached onto cooled copper strips distributes ≈ 60 A currents to the magnets

Longitudinal electron cooling of a bunched ion beam

rf system system of the CSR

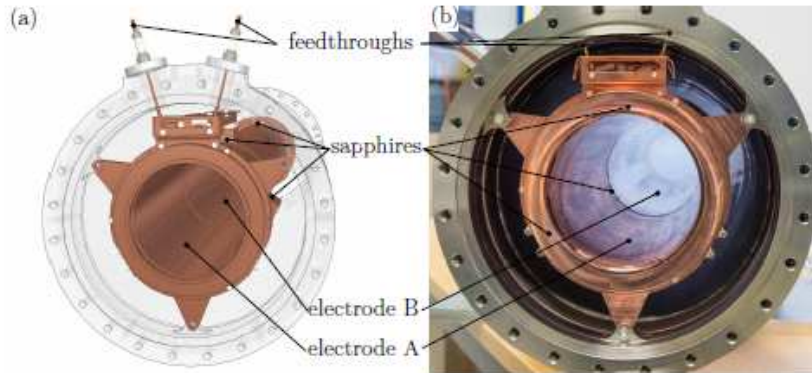


Figure 3.28: The rf system as a (a) CAD-model and (b) photograph mounted in its CSR vacuum chamber. The length of the electrodes A and B are 340 mm and 736 mm, respectively, and the aperture diameter is 100 mm.

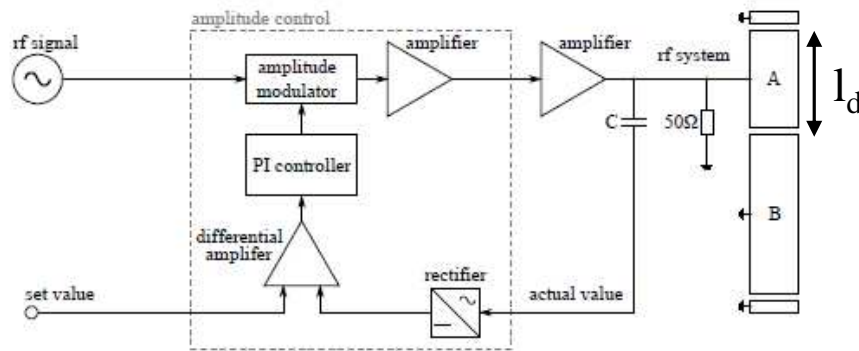


Figure 3.29: Schematic layout of the amplitude regulation system of the rf system.

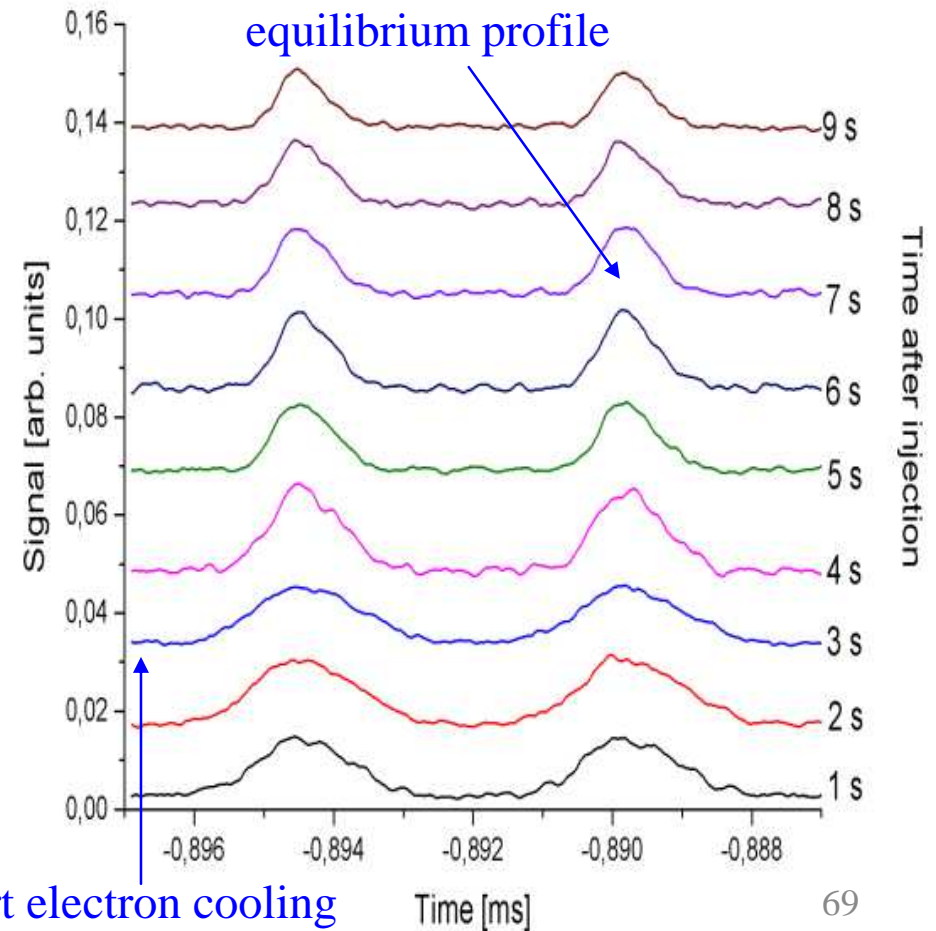
effective voltage:
$$U_{\text{eff}} = 2U_d \sin\left(\frac{\pi h l_d}{C_0}\right)$$

pick-up signal as a function of time

beam: $^{19}\text{F}^{6+}$

ion energy: $E = 1.34 \text{ MeV}$

electron energy: $E_e = 38.7 \text{ eV}$



First electron cooling results of a bunched ion beam

beam width at space charge limit:

$$w = C_0 \frac{\sqrt[3]{3(1 + 2\ln(\frac{R}{r}))I}}{\sqrt[3]{2^4 \pi^2 c^4 \epsilon_0 \gamma^2 h^2 \beta^4 U}}$$

beam: $^{19}\text{F}^{6+}$

ion energy: $E = 1.34 \text{ MeV}$

electron energy: $E_e = 38.7 \text{ eV}$

ion current: $I \approx 300 \text{ nA}$

ion number: $N \approx 10^6 \text{ particles}$

Solenoid field: 100 Gauss

rf bunching frequency = 2nd

(h=2) harmonic of revolution

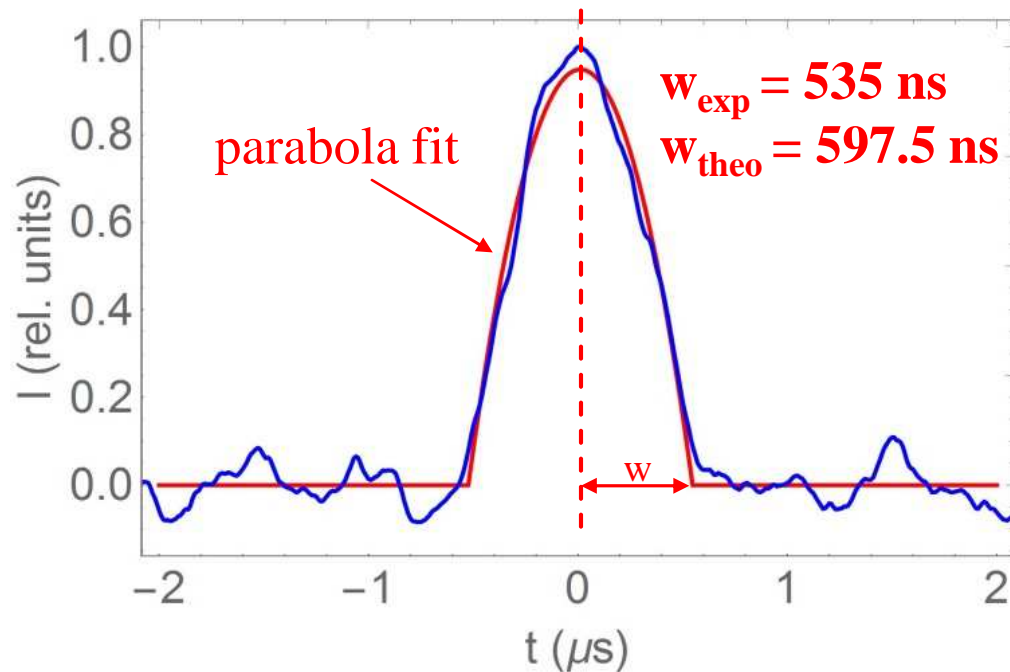
frequency = 214 kHz

drifttube voltage: $U_d = 3.25 \text{ V}$

effective bunch voltage: $U_{\text{eff}} = 0.4 \text{ V}$

$$U = U_{\text{eff}} = 2U_d \sin\left(\frac{\pi h l_d}{C_0}\right)$$

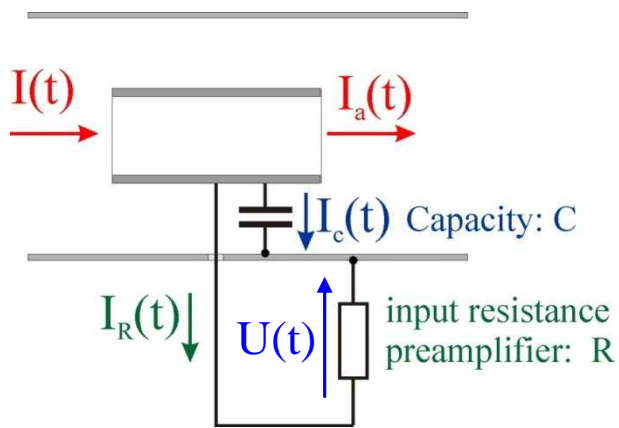
Equilibrium longitudinal beam profile



10 sec after injection,
7 sec after cooling

Principle of the longitudinal cooling time measurements

capacitive current pick up



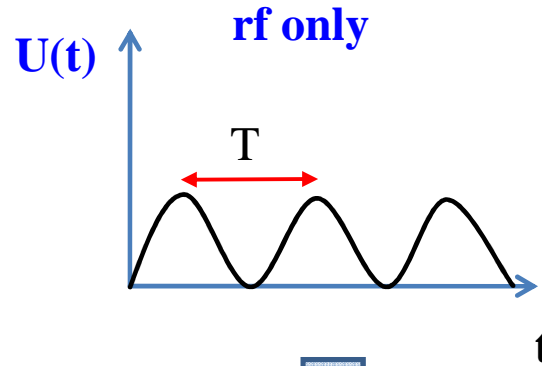
T – RF period

$U(t)$ -pick-up voltage

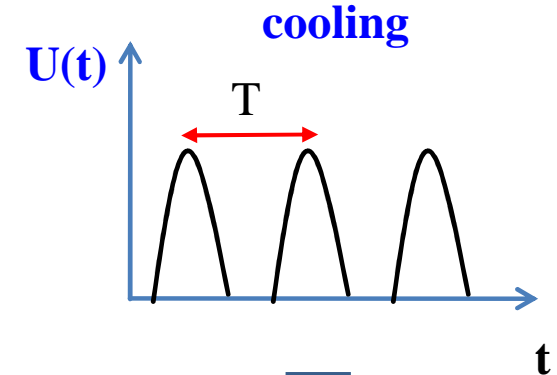
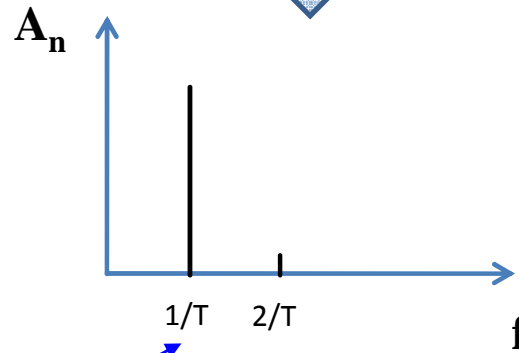
A_n - spectrum

A_2 -second harmonic of the pick-up spectrum

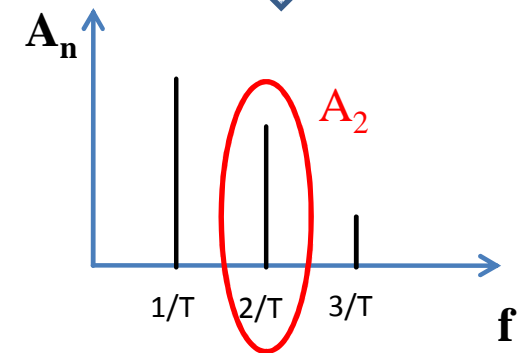
RF frequency



FFT



FFT



measurement:

observation of A_2 as a function of time with a spectrum analyzer in span 0 mode

Longitudinal cooling time of a bunched ion beam

beam: $^{19}\text{F}^{6+}$

ion energy: $E = 1.34 \text{ MeV}$

electron energy: $E_e = 38.7 \text{ eV}$

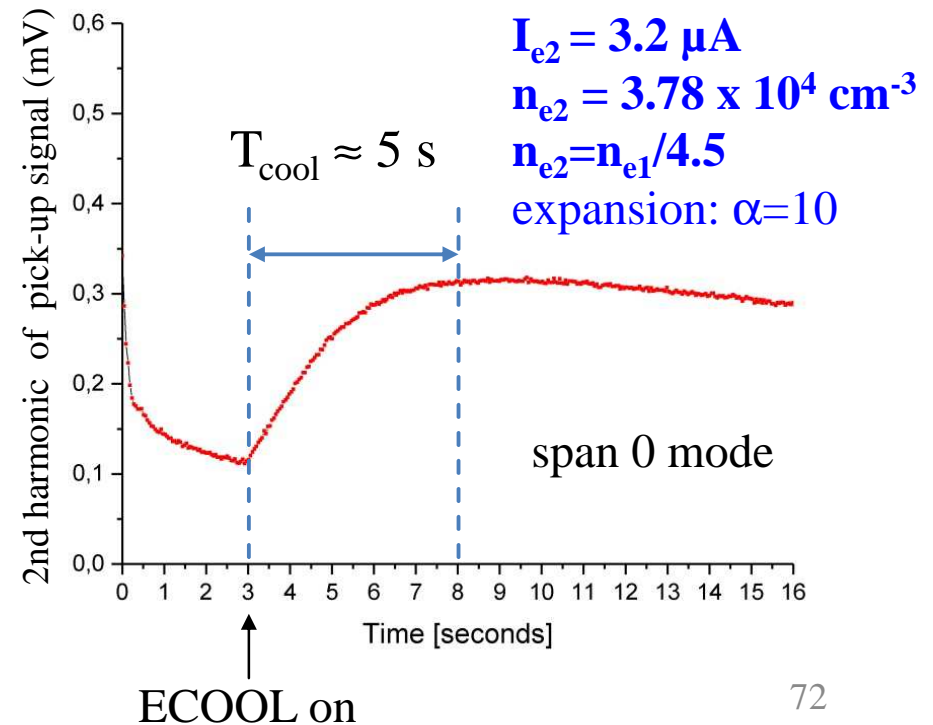
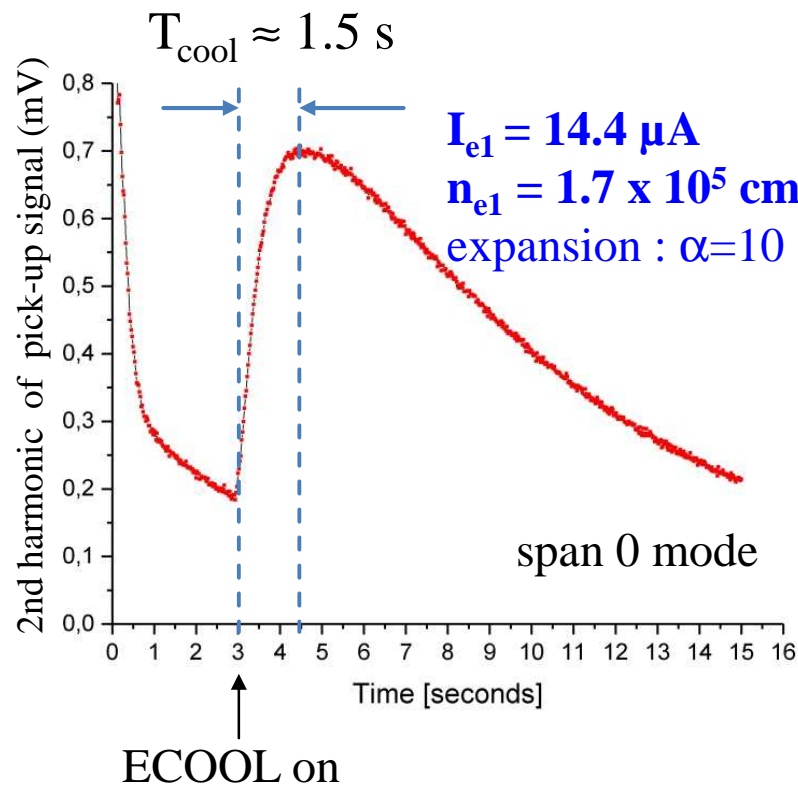
ion current: $I \approx 300 \text{ nA}$

ion number: $N \approx 10^6$ particles

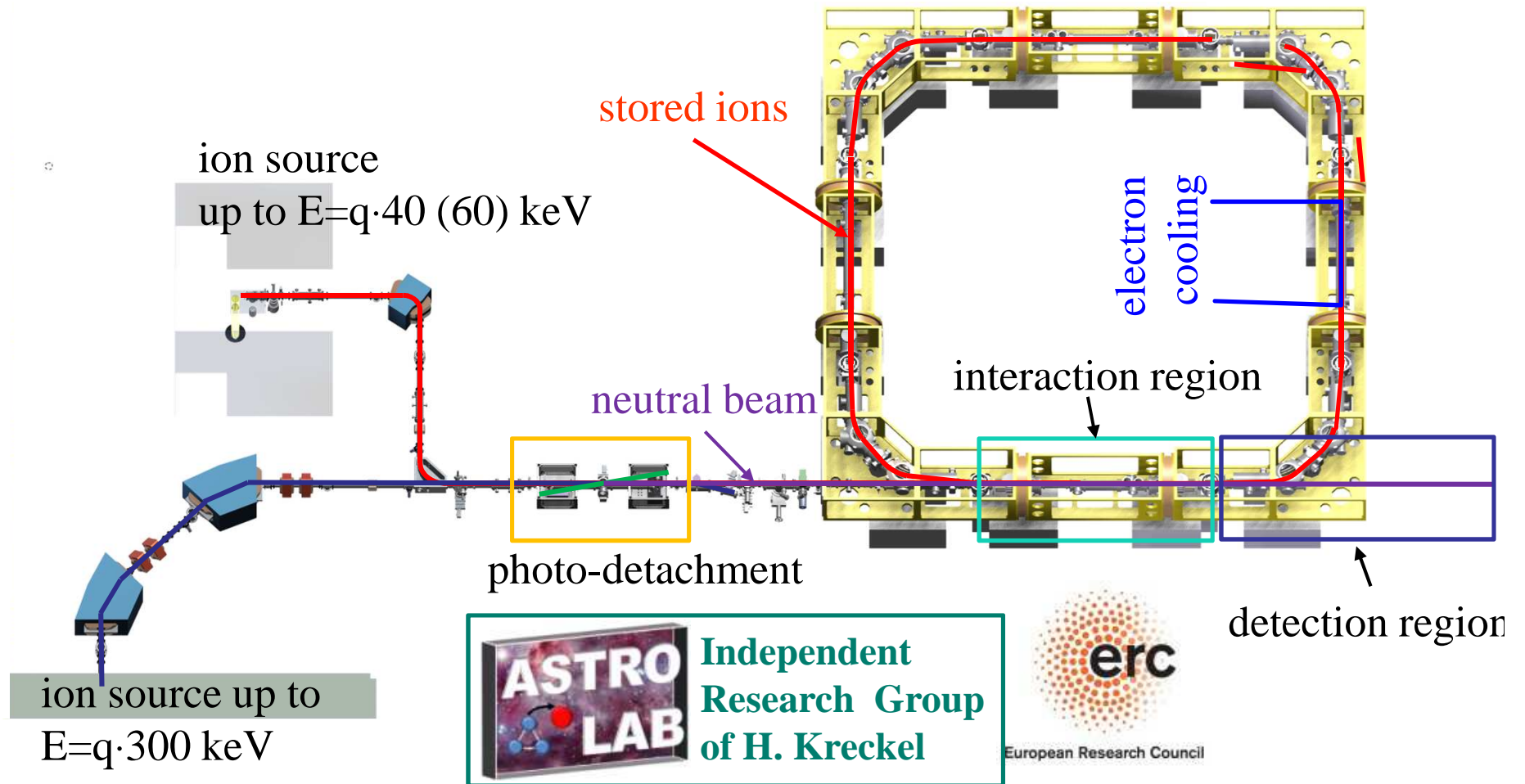
solenoid field: 100 Gauss

rf bunching frequency = 2nd harmonic of revolution frequency = 214 kHz

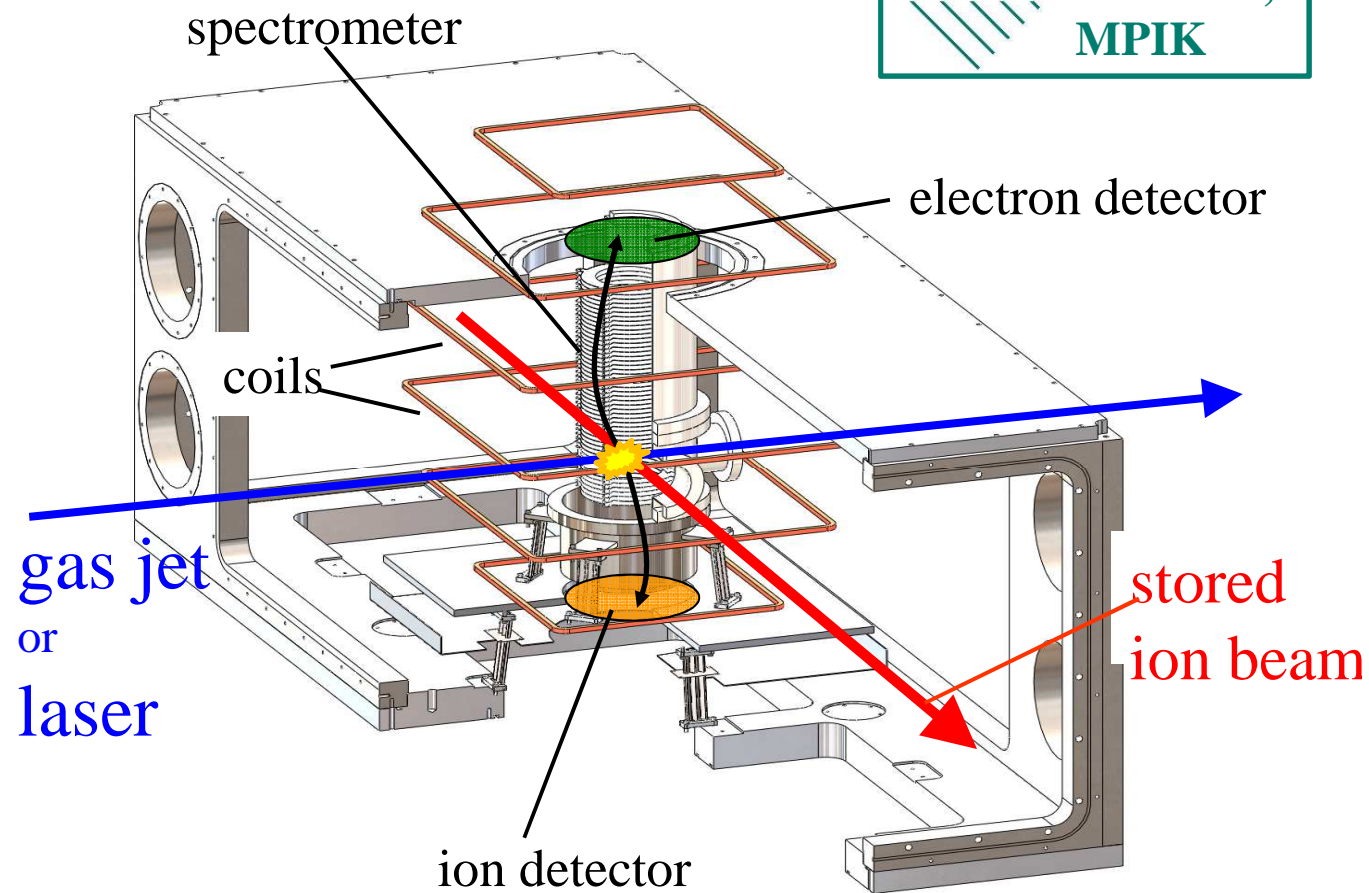
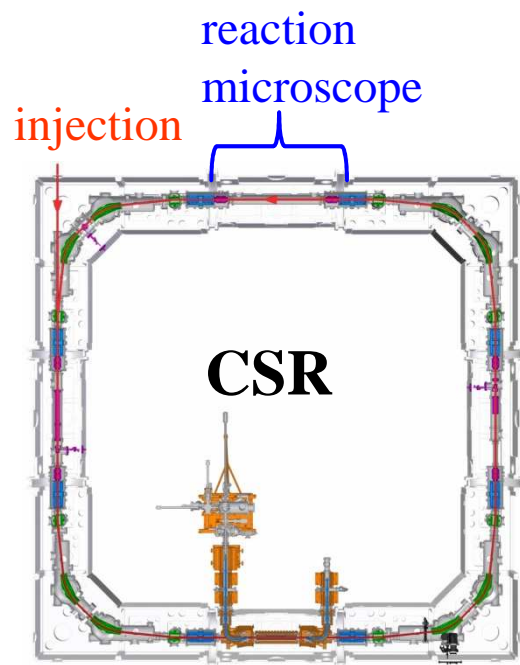
pick-up signal spectrum measured at the second harmonic of the rf frequency ($f=428 \text{ kHz}$)



Merged beam experiments



The reaction microscope



Thanks for your attention!



A. Becker

K. Blaum

C. Breitenfeldt

F. Fellenberger

S. George

J. Göck

M. Grieser

F. Grussie

R. von Hahn

P. Herwig

J. Karthein

C. Krantz

H. Kreckel

S. Kumar S.

M. Lange

J. Lion

S. Lohmann

C. Meyer

P. M. Mishra

O. Novotný

P. O'Connor

R. Repnow

S. Saurabh

S. Schippers

C. D. Schröter

D. Schwalm

L. Schweikhard

K. Spruck

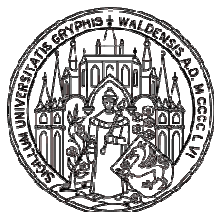
X. Urbain

S. Vogel

P. Wilhelm

A. Wolf

D. Zajfman

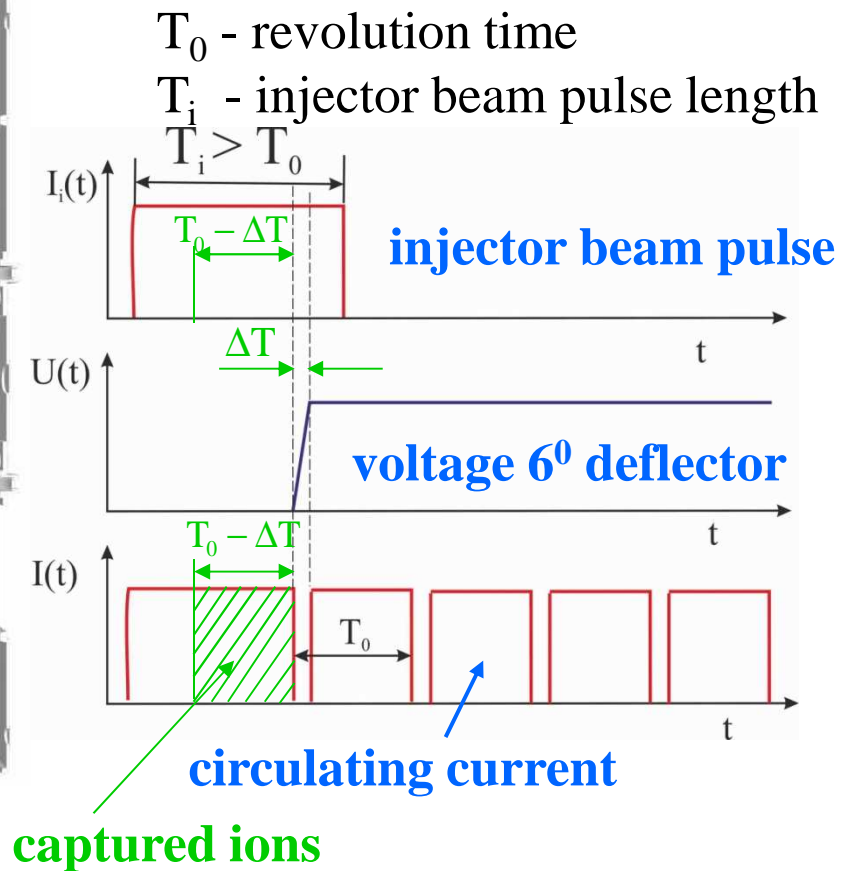
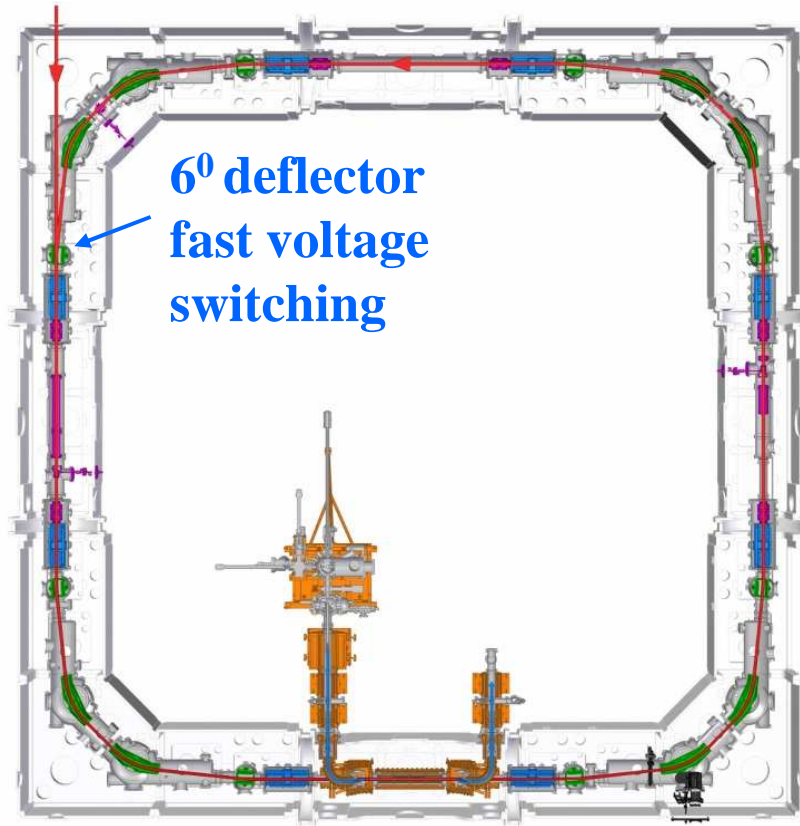


back-up

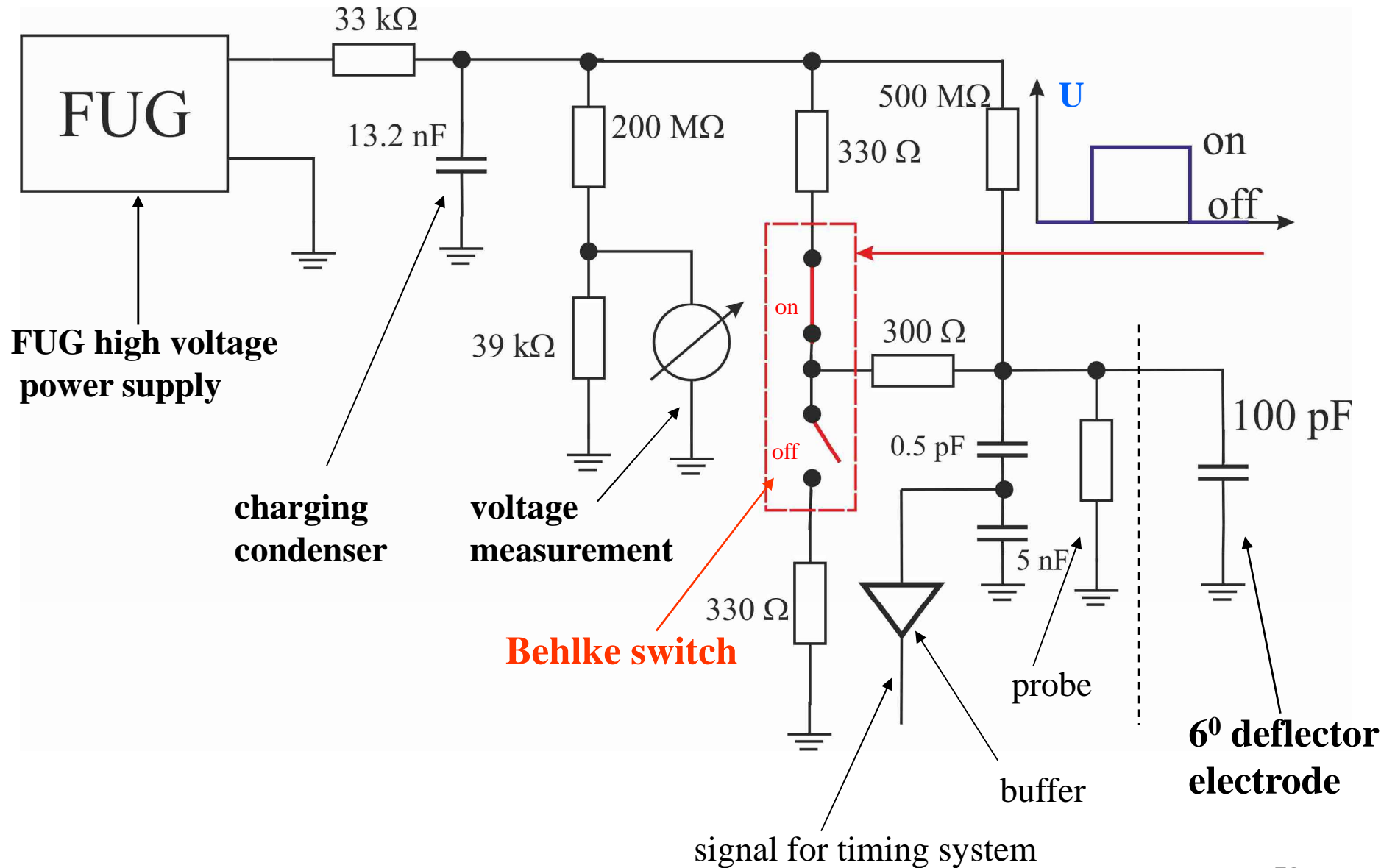
Single turn injection

Single turn injection

pulsed injector
beam

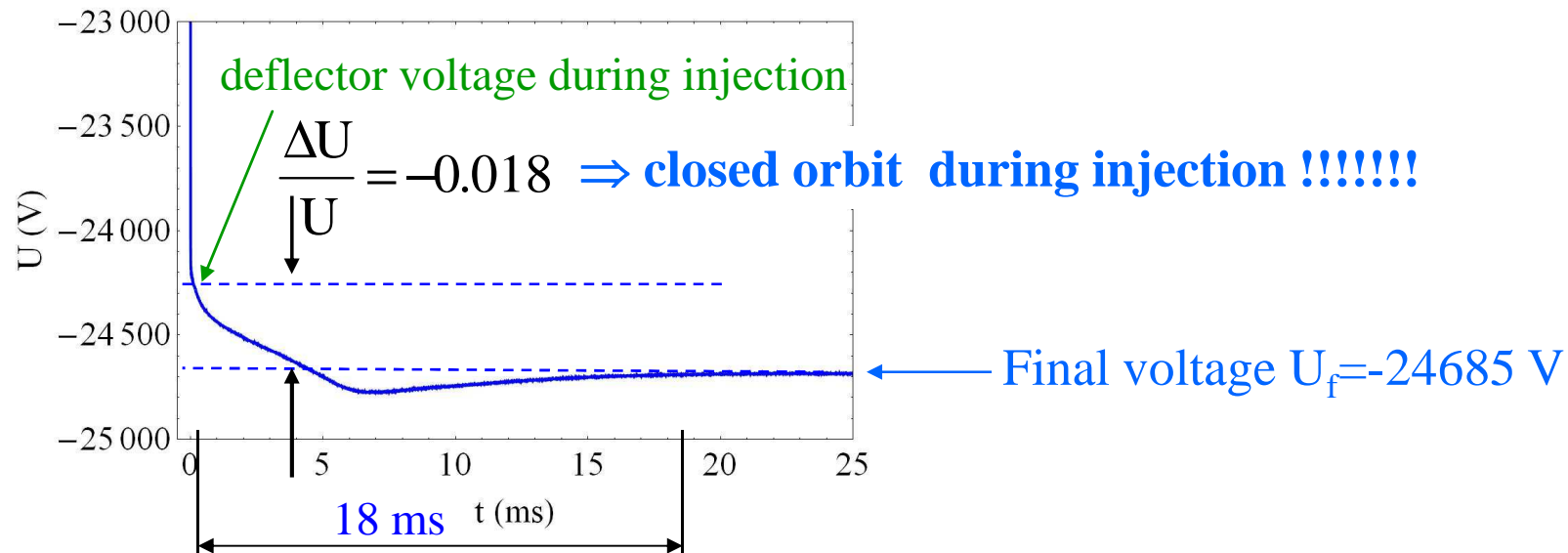
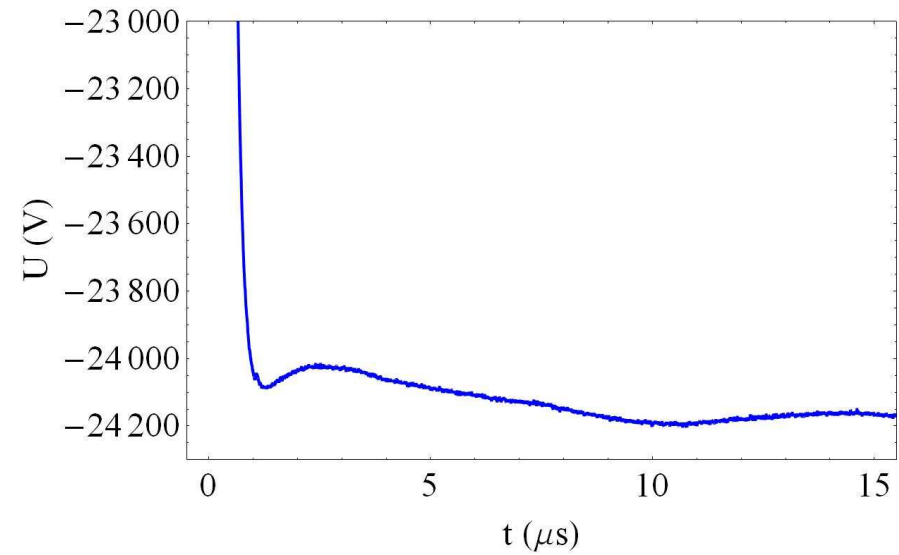
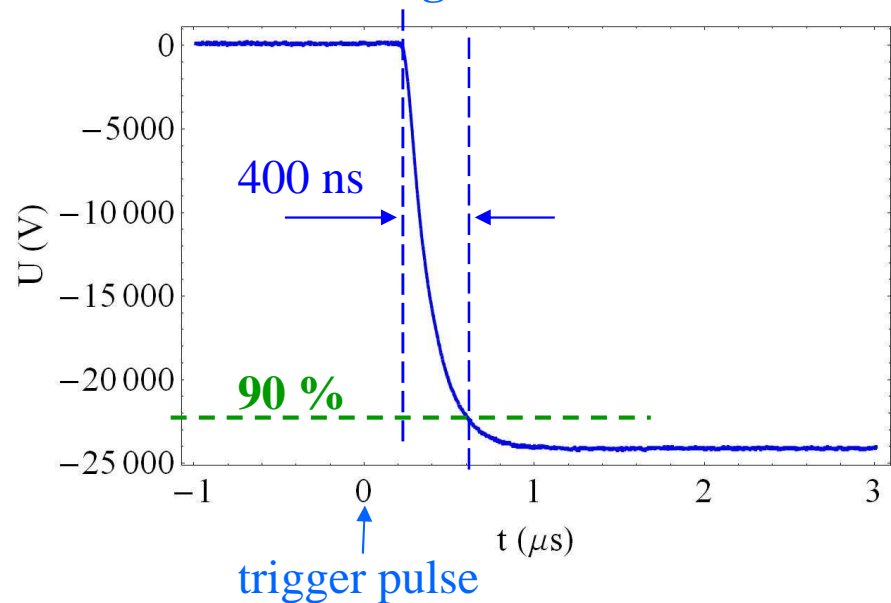


Fast switching of the 6⁰ deflector voltage



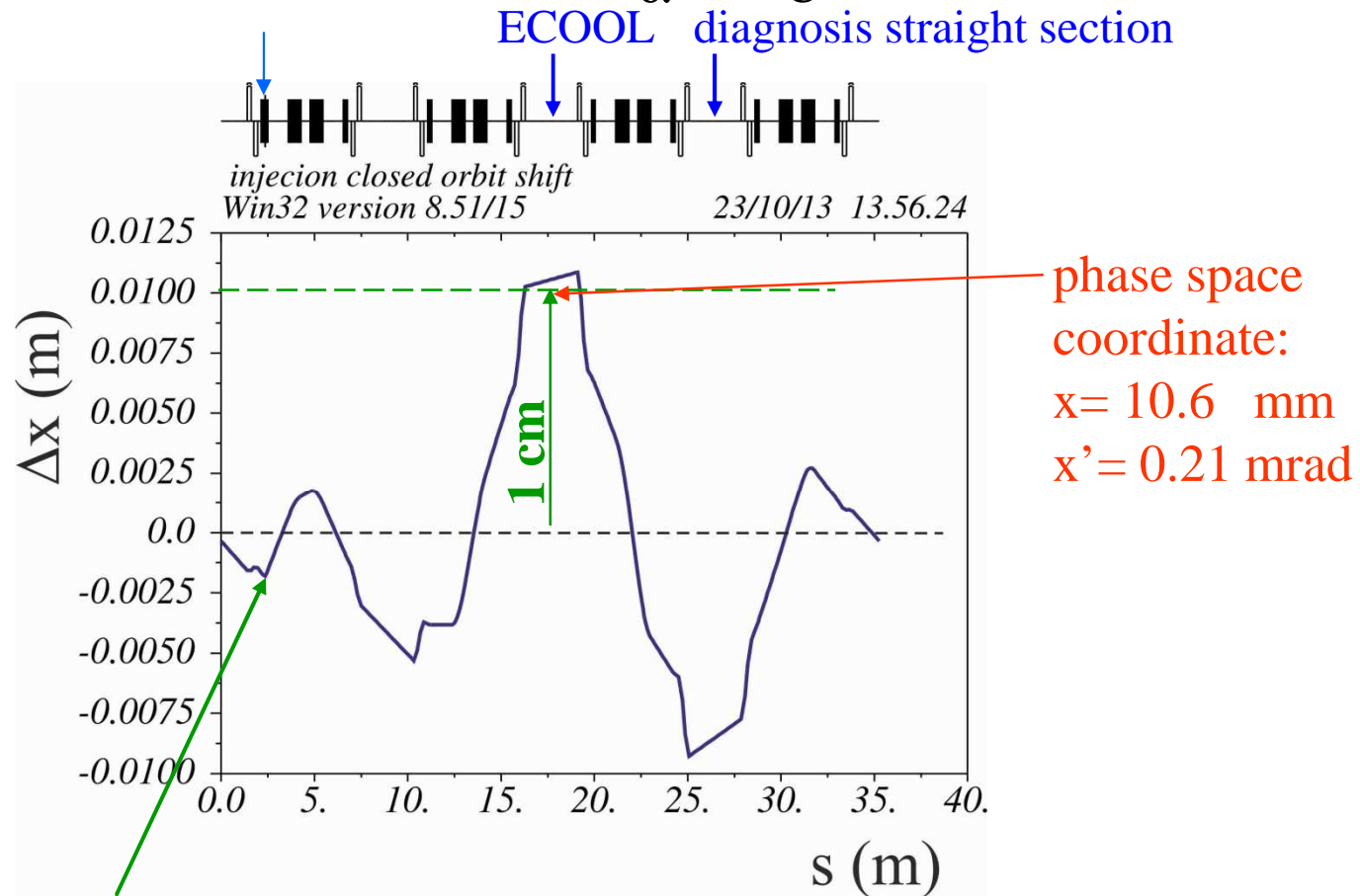
Switching time of Behlke switch

electrode voltage as a function of time



Closed Orbit shift during injection injection

6^o deflector change of the deflection angle by: $\frac{\Delta\alpha}{\alpha} = -\frac{\Delta U}{U} = 0.018$

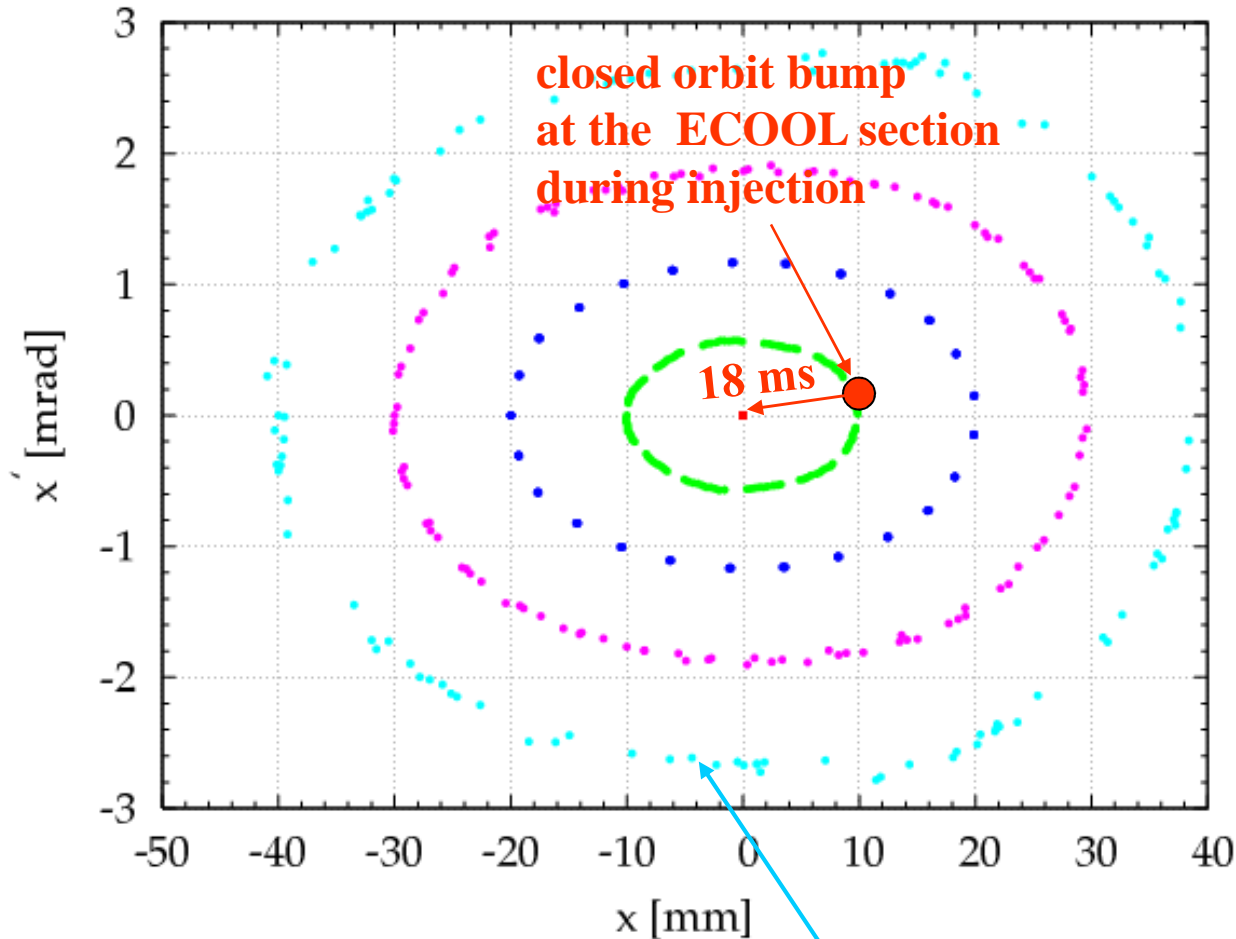


theoretical injection orbit (injector beam), not realizable due to aperture limitations in the transfer line \Rightarrow excitation of dipole oscillations of stored ion beam

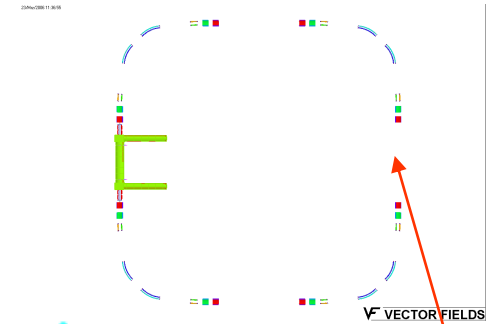
Horizontal dynamical acceptance of the CSR

ECOOOL OFF

Horizontal acceptance at the center of a straight section



$X_i=0$
 $X_i=10$
 $X_i=20$
 $X_i=30$
 $X_i=40$



starting point

maximum beam size in the center of the straight section

$$|x|_{\max} \approx 4\text{cm}$$

ions lost for $x > 4 \text{ cm}$

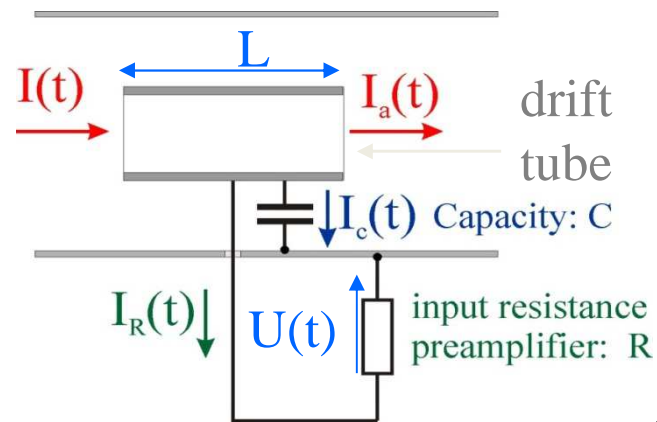
reason: good field region of the quadrupole

dynamical acceptance at center of each straight section

$$A_x = 120 \text{ mm} \cdot \text{mrad}$$

Current pick-up

Pick-up signal of a bunched ion beam



current of the stored ion beam

$$I_a(t) = I(t - \Delta t)$$

↑ after the drift tube ↓ flight time inside the drift tube

node theorem:

$$I(t) = I_a(t) + I_R(t) + I_C(t)$$

$$\Leftrightarrow I(t) = I(t - \Delta t) + I_R(t) + I_C(t)$$

$$I(t - \Delta t) = I(t) - \frac{\partial I}{\partial t} \Delta t = I(t) - \dot{I}(t) \frac{L}{v}$$

With bunch length $l_b \gg L$:

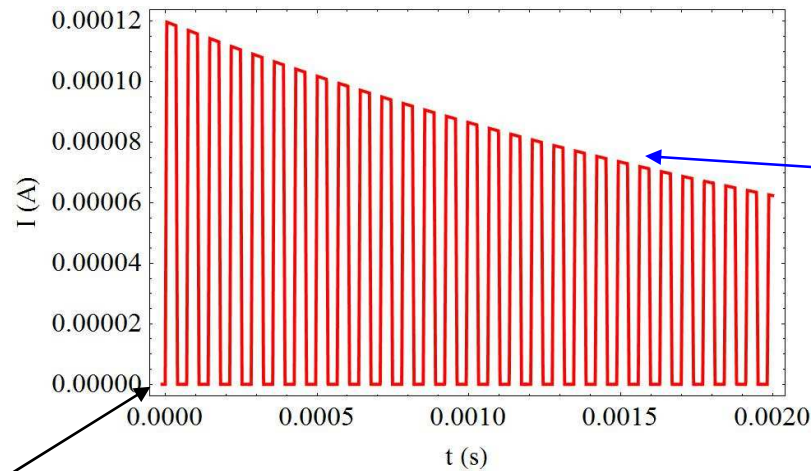
with $I_R(t) = \frac{U}{R}$ and $I_C(t) = C \cdot \dot{U}(t)$ differential equation for drift tube voltage $U(t)$

$$\frac{L}{v} \dot{I}(t) = C \cdot \dot{U}(t) + \frac{U(t)}{R}$$

for $R \rightarrow \infty$ drift tube voltage: $U(t) = \frac{1}{C} \frac{L}{v} I(t) \Rightarrow U(t) \propto I(t)$

Calculated Pick-up signal

circulating beam current

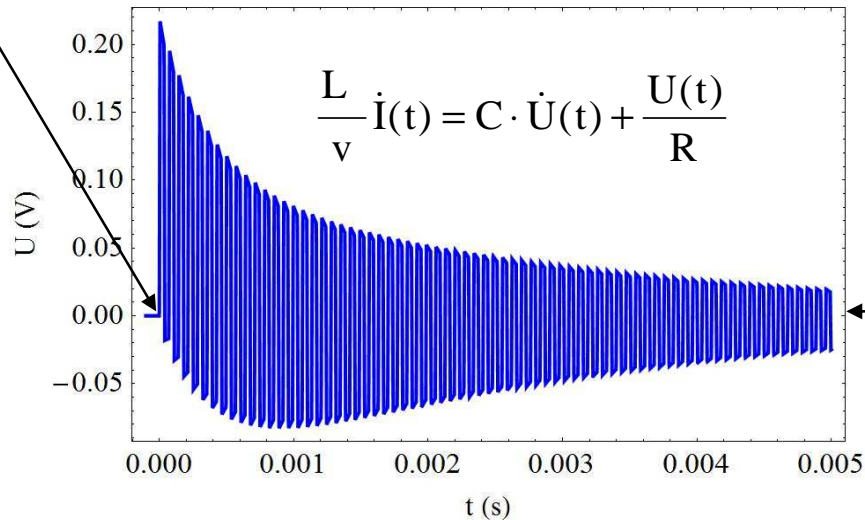


circulating ion pulse
calculated for $p \approx 10^{-7}$ mbar

intensity decrease
due to life-time

injection

pick-up signal

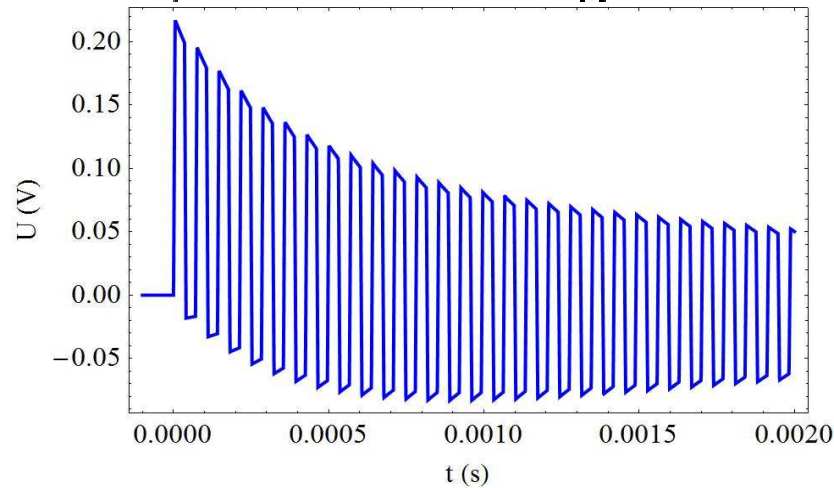


DC part
disappeared

Comparison between calculated and measured pick-up signal

calculated

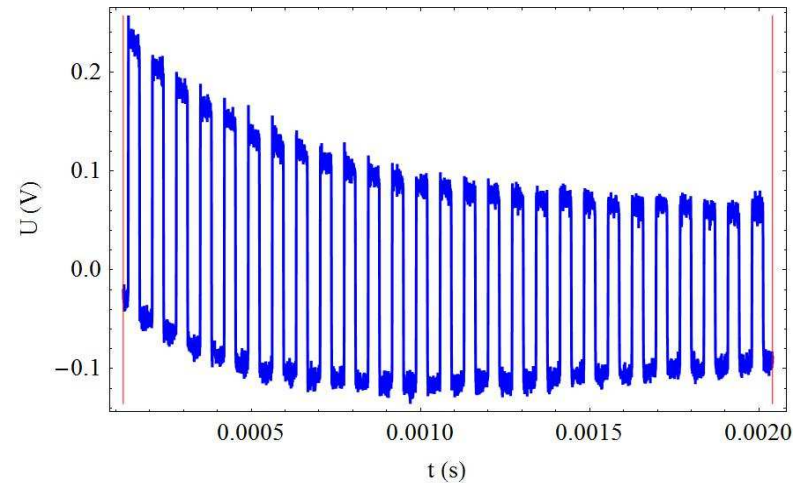
$$\frac{L}{v} \dot{I}(t) = C \cdot \dot{U}(t) + \frac{U(t)}{R}$$



calculated for C=400 pF
and R=1 MΩ

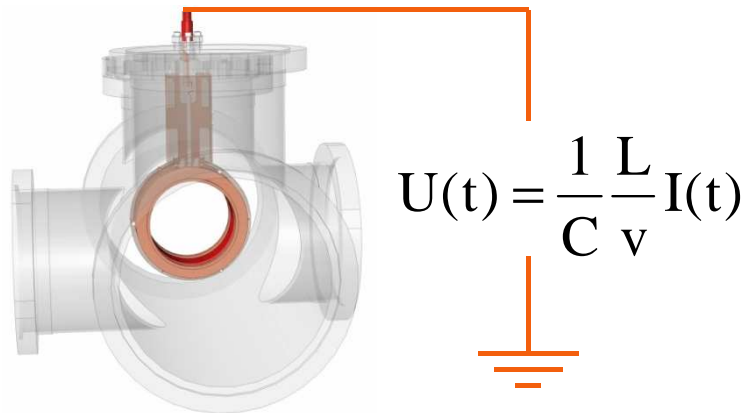
measured

Schottky pick-up used as current pick-up

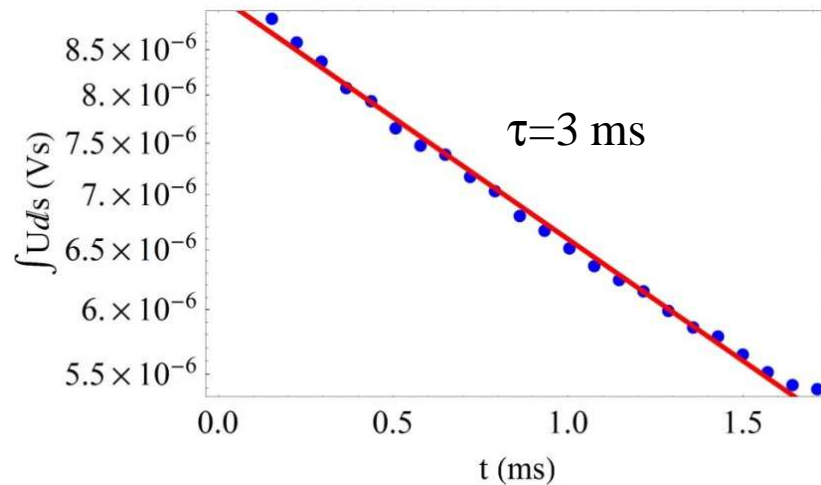
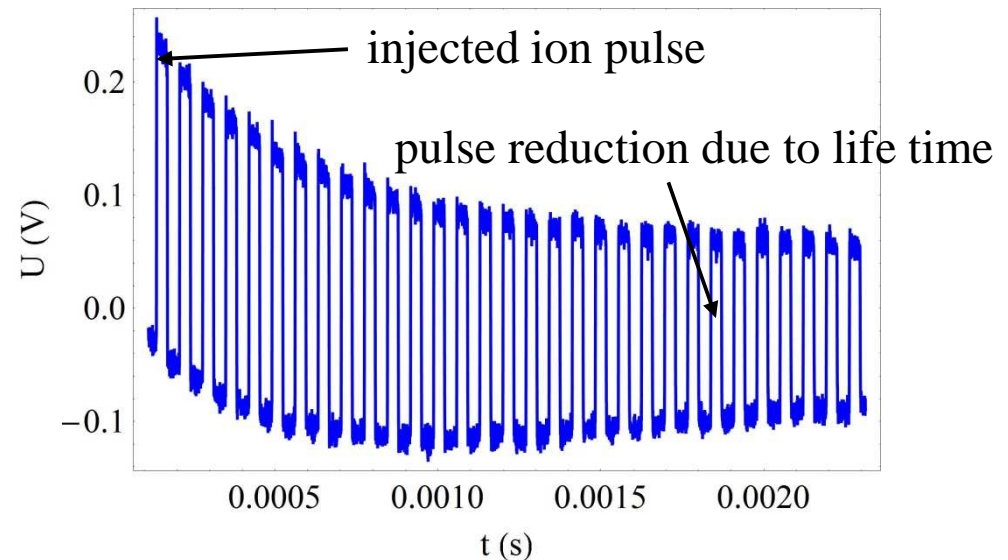


Life time determination with current pick-up

- used to measure the **absolute number** of the injected ion number (pulsed current)
- sensitivity 10^6 singly charged ions



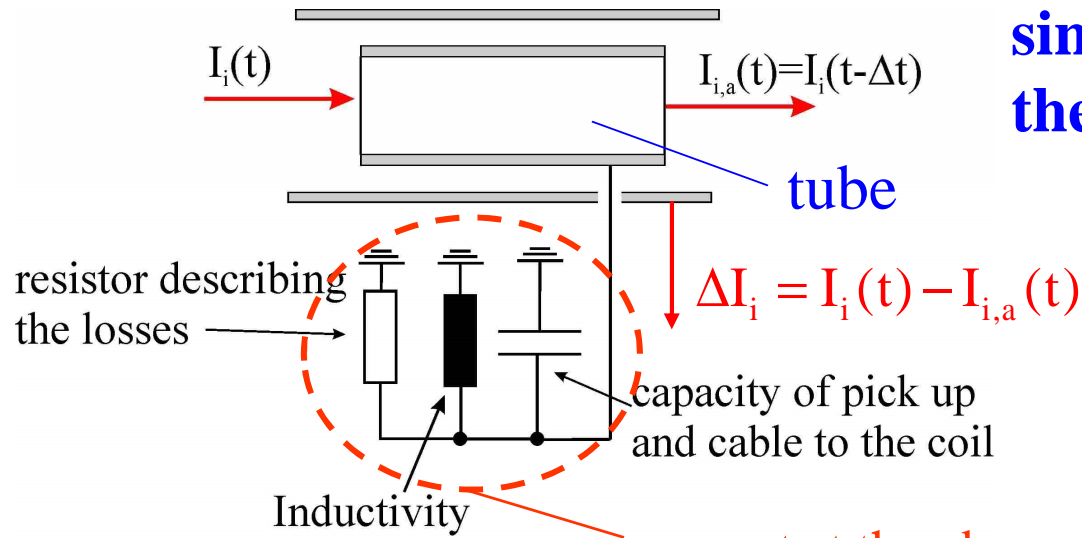
pick-up signal at $\approx 10^{-7}$ mbar
(room temperature) for 50 keV Ar^+ ions



measured lifetime at $\approx 10^{-7}$ mbar
(room temperature operation, **March 2014**)

Schottky-pickup

The Schottky pick up of the CSR



single ion interaction with the Schottky pick up

flying time through the pick up

$$I_i(t) = Q \sum_n \delta(t - nT)$$

$$I_{i,a}(t) = I_i(t - \Delta t) = Q \sum_n \delta(t - nT + \Delta t)$$

$$\Delta t = \frac{L}{v} \quad \begin{array}{l} L - \text{pick up length} \\ v - \text{ion velocity} \end{array}$$

Fourier row

resonant at the observed Schottky band

$$I_i(t) = Q \left(\frac{a_0}{2} + \sum_{n=1}^{\infty} \frac{2}{T} \cos(n \omega_0 t) \right)$$

T - revolution time of the ion

$$I_{i,a}(t) = Q \left(\frac{a_0}{2} + \sum_{n=1}^{\infty} \frac{2}{T} \cos(-n \omega_0 \Delta t) \cdot \cos(n \omega_0 t) + \frac{2}{T} \cdot \sin(-n \omega_0 \Delta t) \sin(n \omega_0 t) \right)$$

current into LC circuit $\Delta I_i(t) = I_i(t) - I_{i,a}(t)$ with $\omega_n = n \omega_0$

$$\Delta I_i(t) = Q \frac{2}{T} \sum_{n=1}^{\infty} \left((1 - \cos(\omega_n \Delta t)) \cos(\omega_n t) + \sin(\omega_n \Delta t) \sin(\omega_n t) \right)$$

Spectrum of the Schottky signal coming from a single ion

$$\Delta t = \frac{L}{v}$$

$$\Delta I_i(t) = Q \frac{2}{T} \sum_{n=1}^{\infty} ((1 - \cos(\omega_n \Delta t)) \cos(\omega_n t) + \sin(\omega_n \Delta t) \sin(\omega_n t))$$

⇒ spectrum of ΔI_i $\omega_n = n \omega_0$

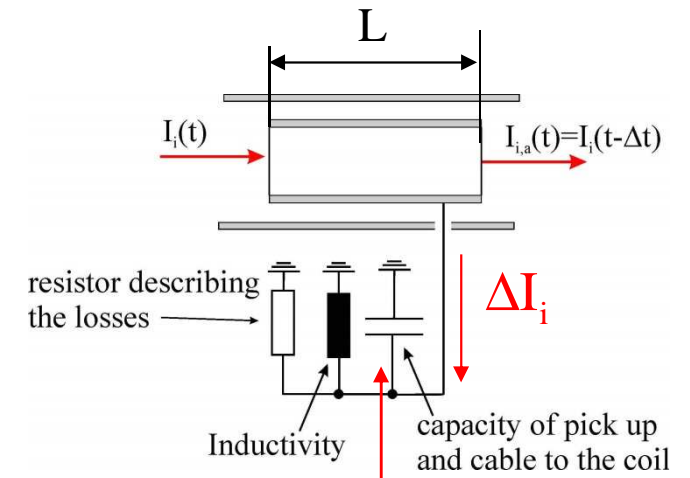
$$\Delta \hat{I}_i(\omega_n) = \frac{2Q}{T} \sqrt{(1 - \cos(\omega_n \Delta t))^2 + \sin^2(\omega_n \Delta t)} = \frac{2\sqrt{2} Q}{T} \sqrt{1 - \cos(\omega_n \Delta t)}$$

$\Delta \hat{I}_i(\omega_n)$ is maximum at $\omega_n \Delta t = \pi, 3\pi, \dots$

$\Delta \hat{I}_i(\omega_n)$ is 0 at $\omega_n \Delta t = m \cdot \pi$ $\Delta t = \frac{L}{v}$

$\omega_n = 2\pi n f_0$ ← revolution frequency of the ion

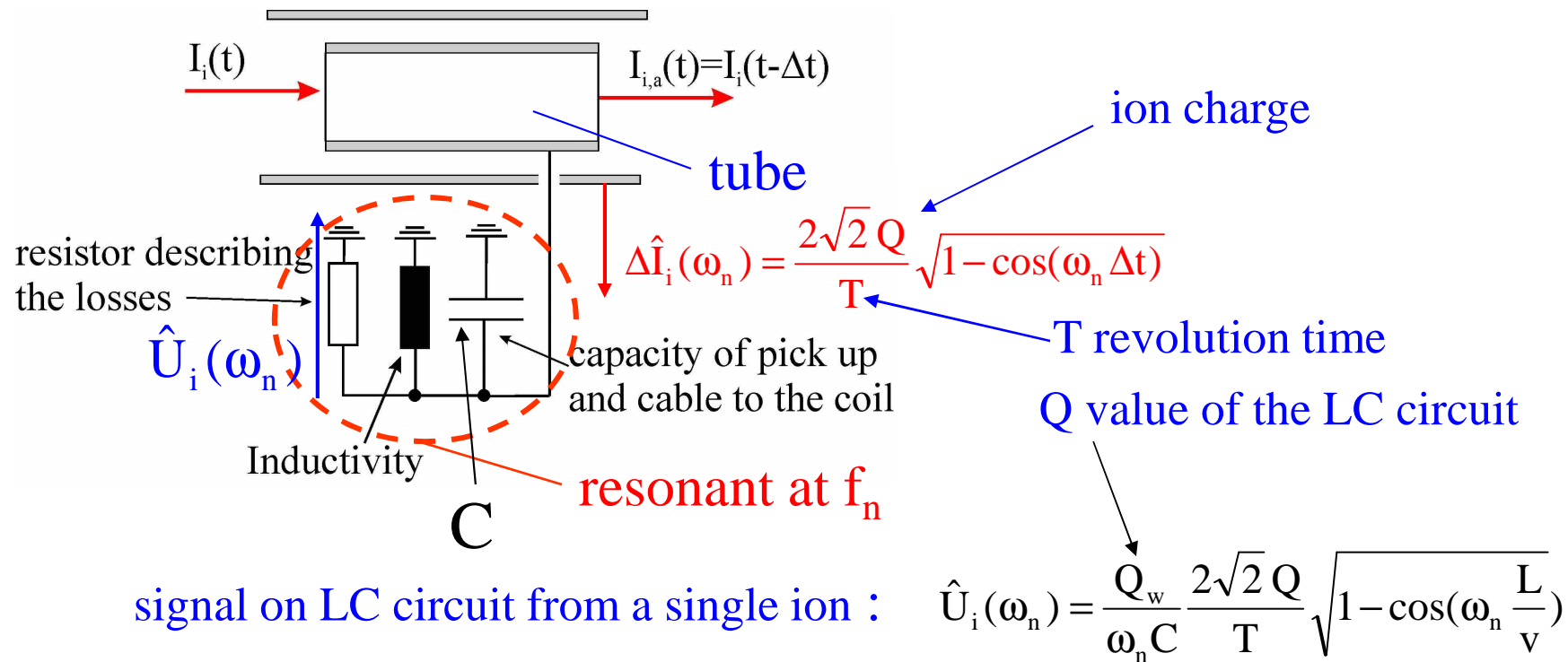
integer number



resonant at f_n

$$f_n = n f_0$$

Spectrum of the Schottky signal coming from a single ion



⇒ signal from a single ion proportion to the Q-value (Q_w) of the LC circuit !

Schottky signal of the ion beam

Schottky signal from a single ion: $\hat{U}_i(\omega_n) = \frac{Q_w}{\omega_n C} \frac{2\sqrt{2} Q}{T} \sqrt{1 - \cos(\omega_n \frac{L}{v})}$

Schottky signal from a ion beam: $\hat{U}(\omega_n) = \sum_{i=1}^N \hat{U}_i(\omega_n) \cos(\varphi_i)$

Schotty Power : $P_0(\omega_n) = \left(\sum_{i=1}^N \hat{U}_i(\omega_n) \cos(\varphi_i) \right)^2$ statistical distributed

hence in the time average: $\overline{\left(\sum_{i=1}^N \cos(\varphi_i) \right)^2} = \frac{N}{2}$

we obtain for the Schottky power:

$$\bar{P}_0(n) = \hat{U}_i^2 \frac{N}{2} = \left(Q_w \frac{\sqrt{2}}{\pi} \frac{1}{n} \frac{Q}{C} \sqrt{1 - \cos(n 2\pi \frac{L}{C_0})} \right)^2 \frac{N}{2}$$

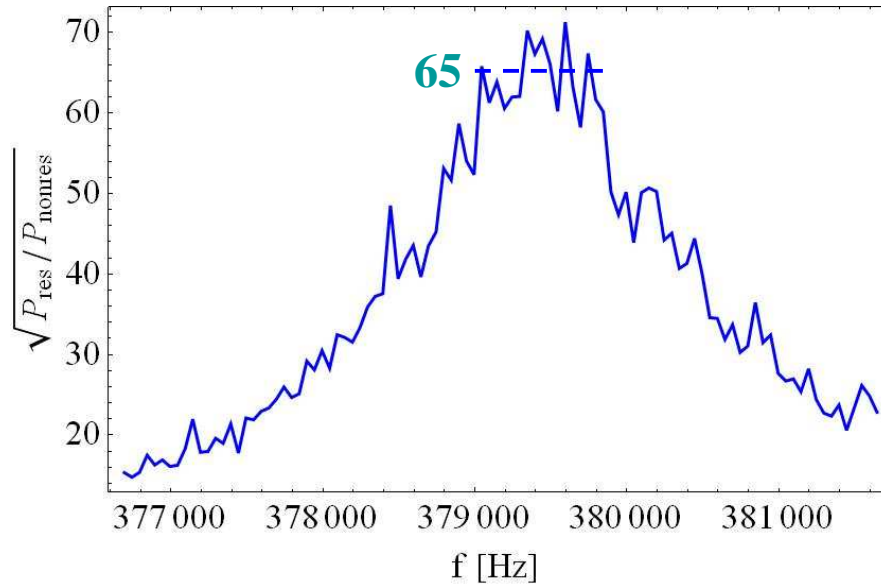
Improvement of noise signal ratio at resonant measurement

P_{res} - noise of preamplifier (resonant measurement)

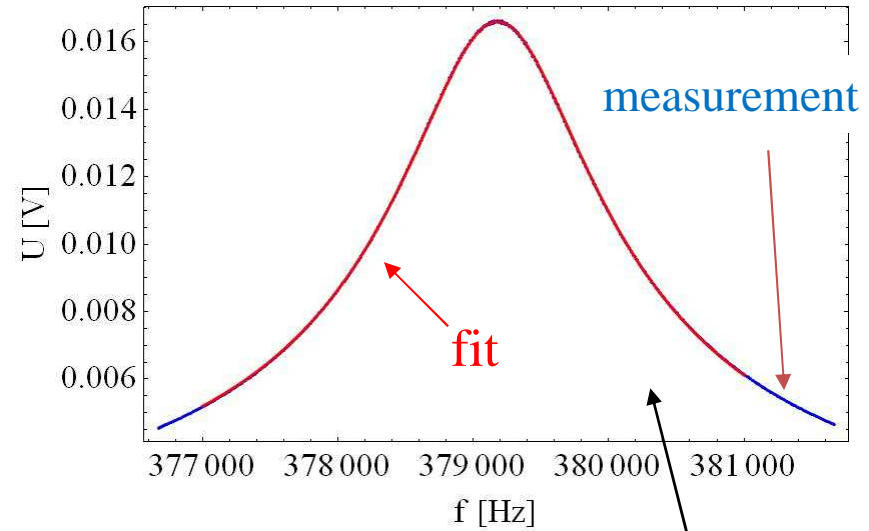
$P_{\text{nonresonant}}$ - noise of pre amplifier (non resonant measurement)

pre amplifier: ULNA

pre amplifier noise



Q_w value measurement



Q_w value : $Q_w=263$

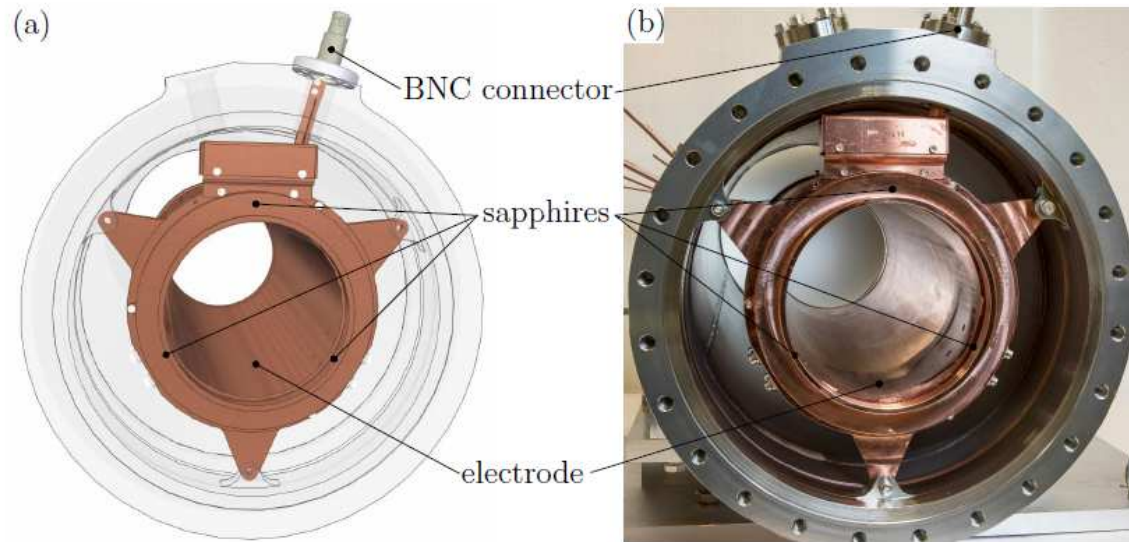
$$\Rightarrow \text{improvement of SNR} = \frac{Q}{\sqrt{P_{\text{res}}/P_{\text{nonres}}}} = \frac{263}{65} = 4$$

detection limit $N \sim \frac{1}{\text{SNR}^2} = \frac{1}{16}$

normal
conducting
coil

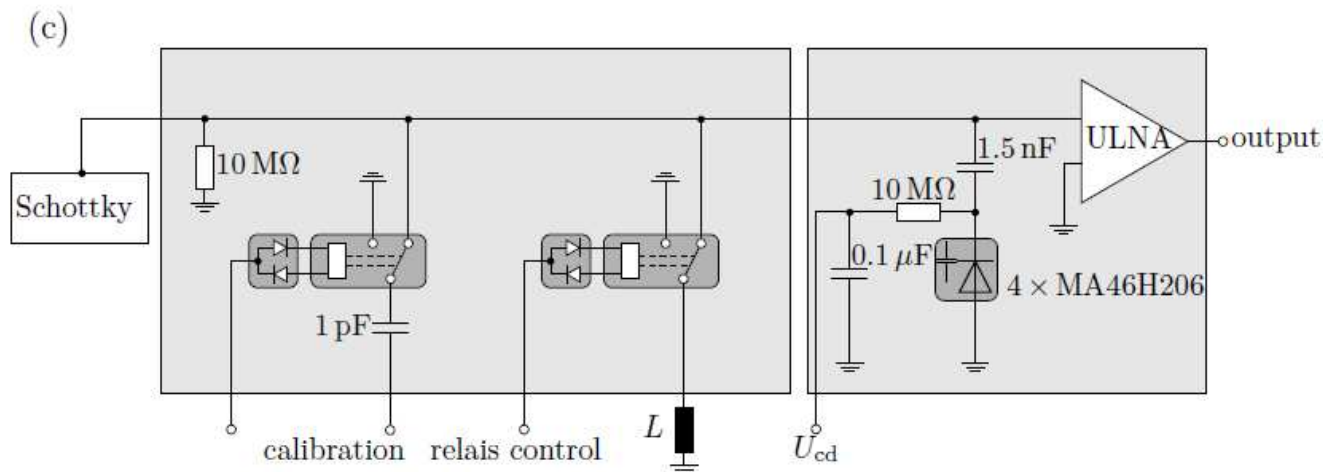
Schottky pick-up of the CSR

52



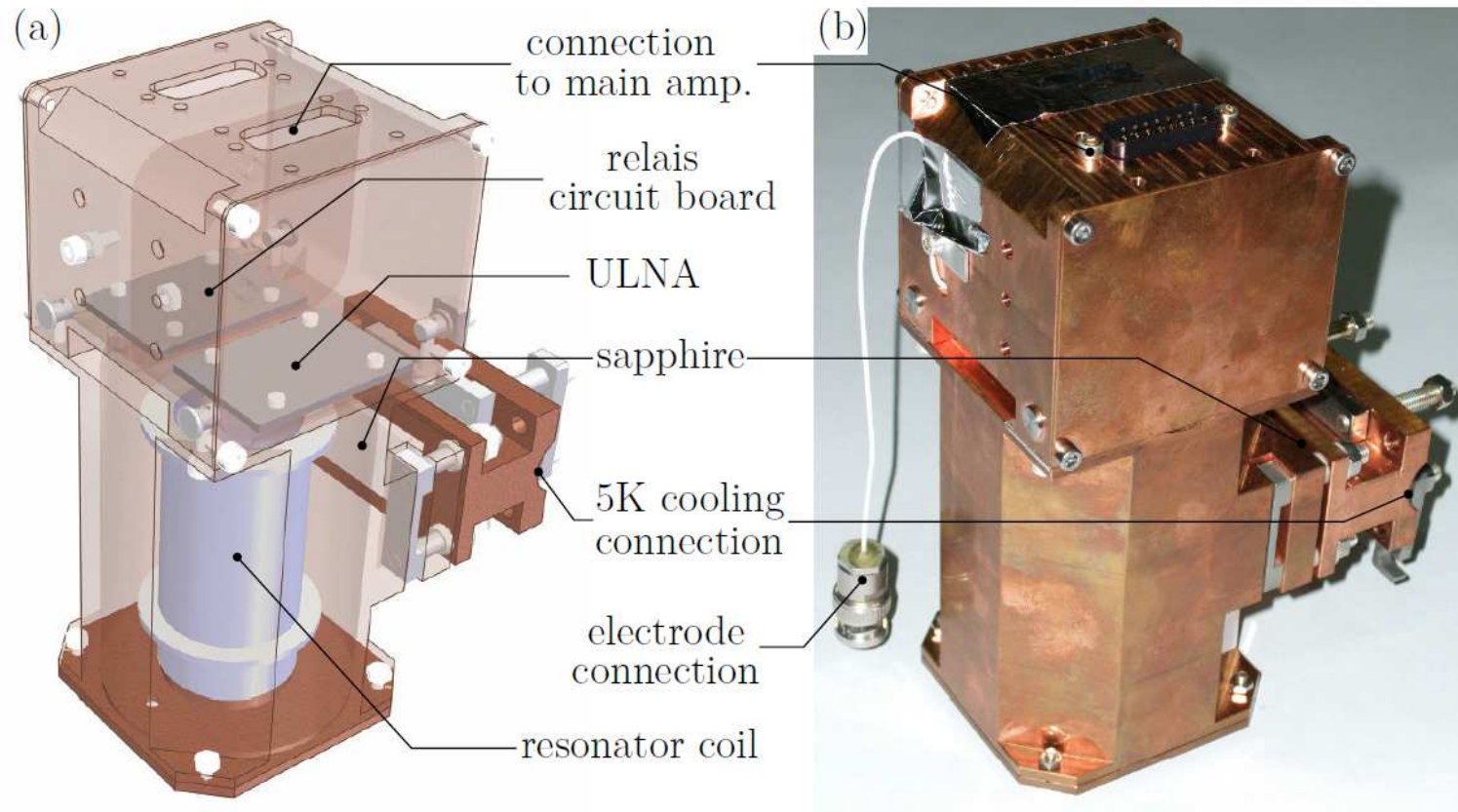
Schottky pick-up

Figure 3.15: The SCHOTTKY pick-up electrode as a (a) CAD-model and (b) photograph mounted in its CSR vacuum chamber. The electrode has a length of 350 mm and aperture diameter of 100 mm.



Layout of the cryogenic electronic of the Schottky pick-up

Cryogenic amplifier box of the Schottky pick-up



CAD-model

Photograph

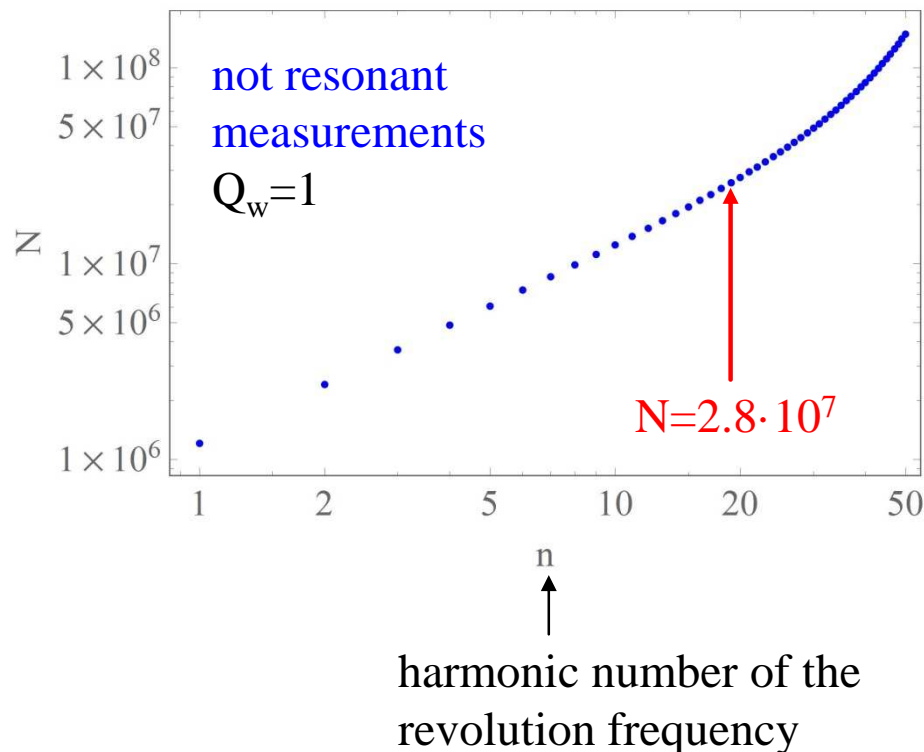
Detection Limit of Schottky pick-up

detection is possible:

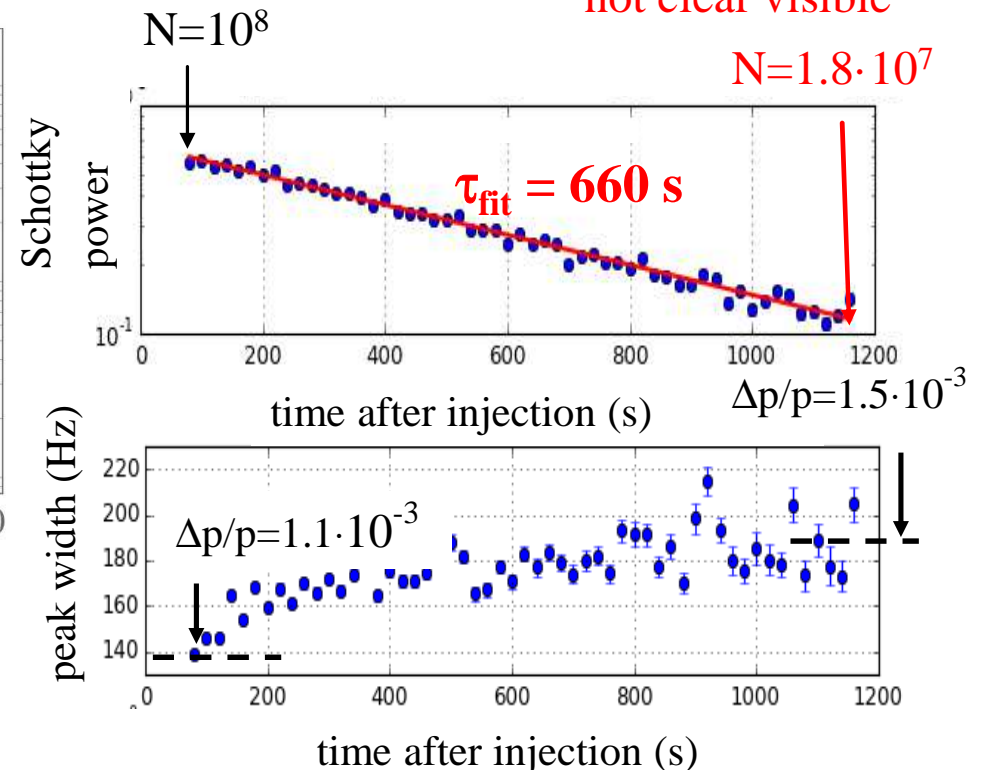
Schottky power > amplifier noise in the Schottky band width:

$$\bar{P}_0(n) = \hat{U}_i^2 \frac{N}{2} > U_n^2 \Delta f_n \quad U_n \approx 1 \text{ nV} / \sqrt{\text{Hz}} \quad \leftarrow \text{noise of pre amplifier}$$

detection limit calculated for Co_2^- (E=60 keV)



Schottky spectrum not clear visible



Some thoughts about the pick-up length L

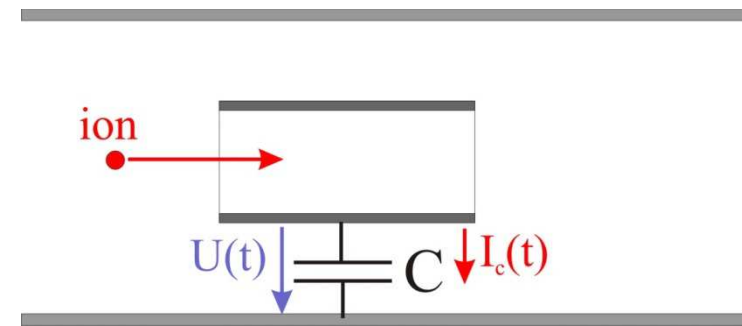
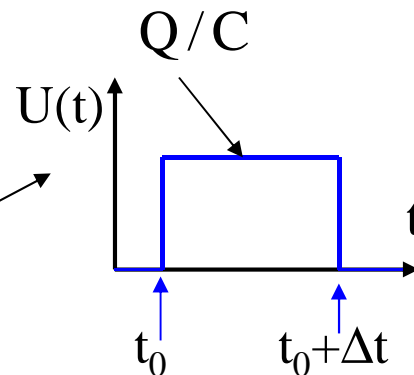
consider pick-up with capacity C

one single ion will produce a voltage during one passage

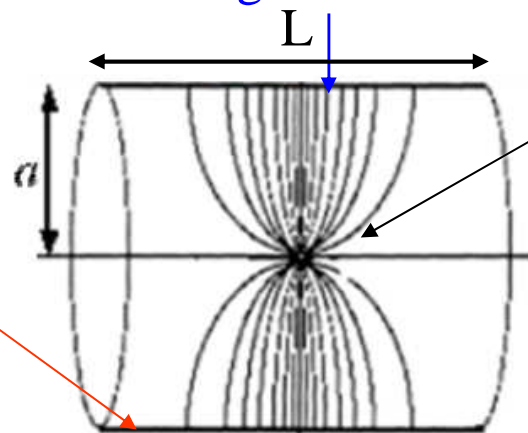
in our simple model

$$I_c(t) = \begin{cases} Q\delta(t-t_0) & t \leq t_0 \\ -Q\delta(t-(t_0+\Delta t)) & t > t_0 \end{cases}$$

$$U(t) = \frac{\int_{t_0}^{t_0+\Delta t} I(t') dt'}{C}$$



induced charge distribution $\Lambda(s)$



ion with charge Q

tube

If $L \gg \sigma_{rms}$

σ_{rms} -RMS value of $\Lambda(s)$

$$\sigma_{rms} = \frac{a}{\gamma\sqrt{2}}$$

radius of the tube
 γ -relativistic γ
CSR: $\gamma=1$

induced charge on the outside of the cylinder

$$Q = \int_{-L/2}^{L/2} \Lambda(s) \cdot ds \Rightarrow U = Q/C$$

ion velocity

voltage rise time: $t_{rise} \approx \frac{\sigma_{rms}}{v}$

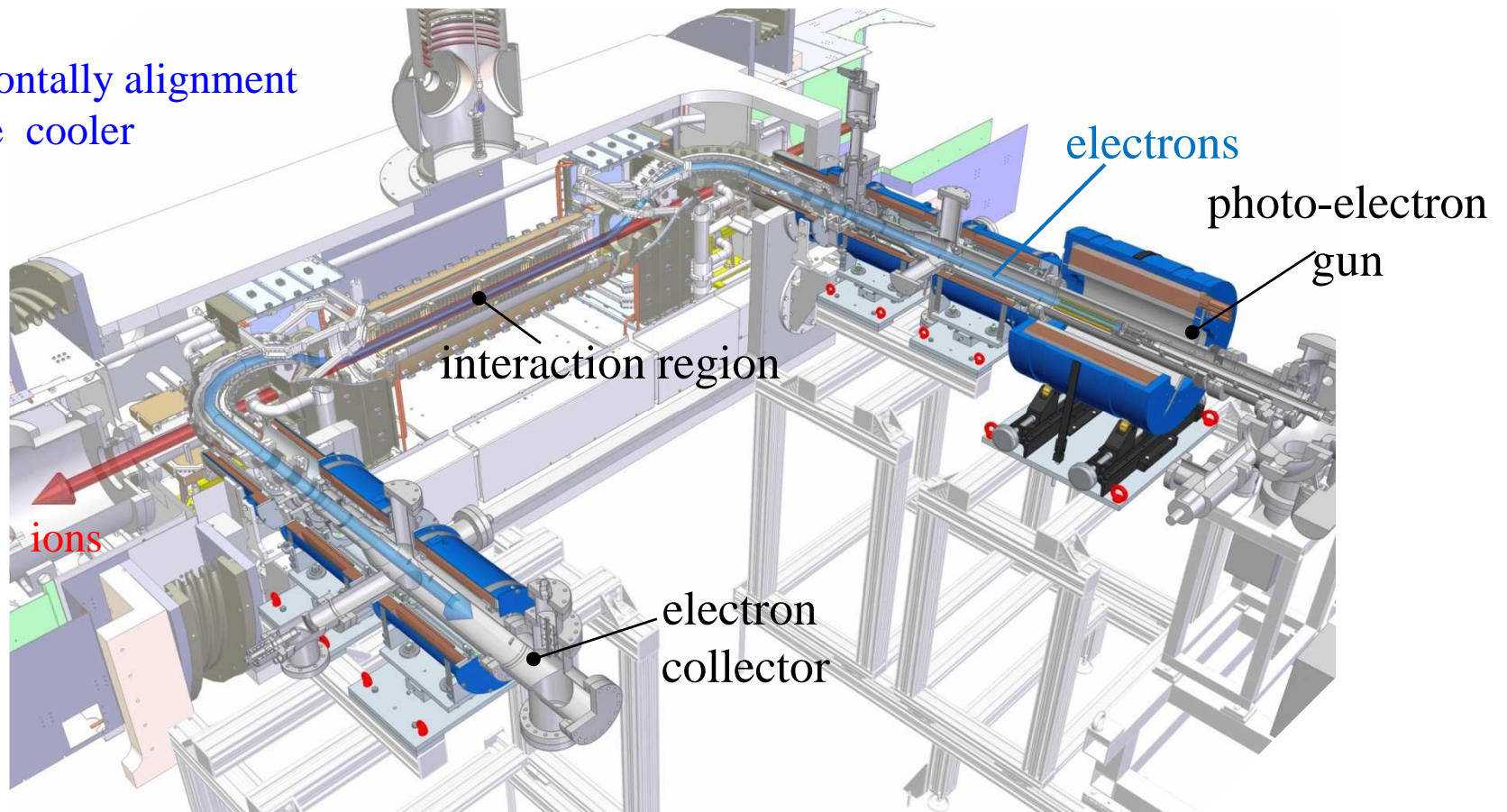
Electrical field lines from a point charge

CSR: $a=5 \text{ cm}$ $L \geq 6 \cdot \sigma_{rms} \approx 20 \text{ cm}$ better $L \approx 35 \text{ cm} \Leftrightarrow L/C_0 = 0.01$

ECOOL

CSR electron cooler – Design

horizontally alignment
of the cooler



Merging and interaction sections of the electron cooler

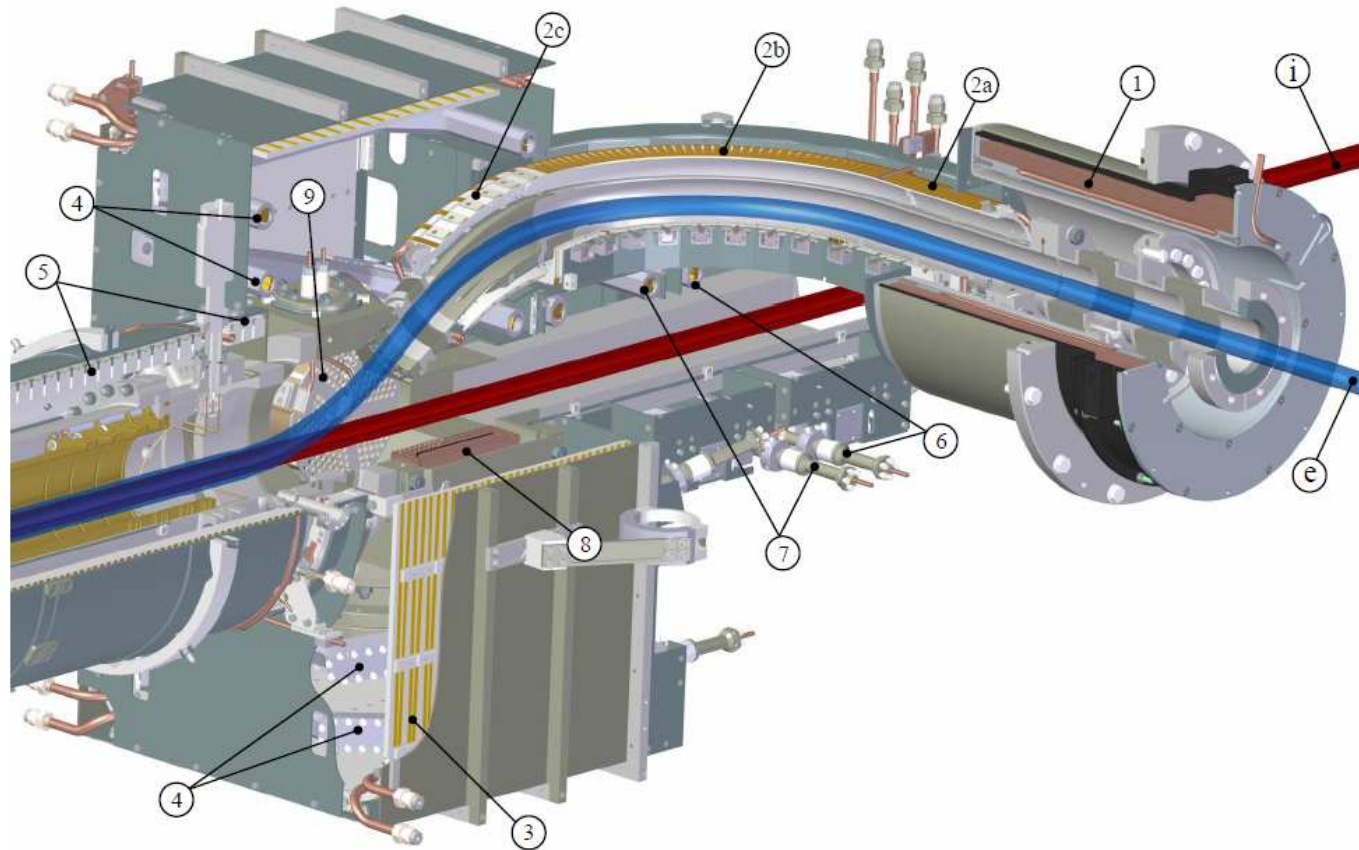


Figure 4.8: Mechanical design of the electron and ion beam merging section with the (e) electron and (i) ion beam, (1) the last low-field guiding magnet, the toroid, consisting of (2a) a solenoidal extension, (2b) the horizontal 90° bend, and (2c) a vertical 30° bending, (3) the longitudinal merging solenoid, (4) four vertical merging coils, (5) the interaction solenoid, (6-7) two pairs of ion beam compensation coils, (8) a charcoal cryopump, and (9) a NEG-pump.

Electron and ion beam Interaction Section

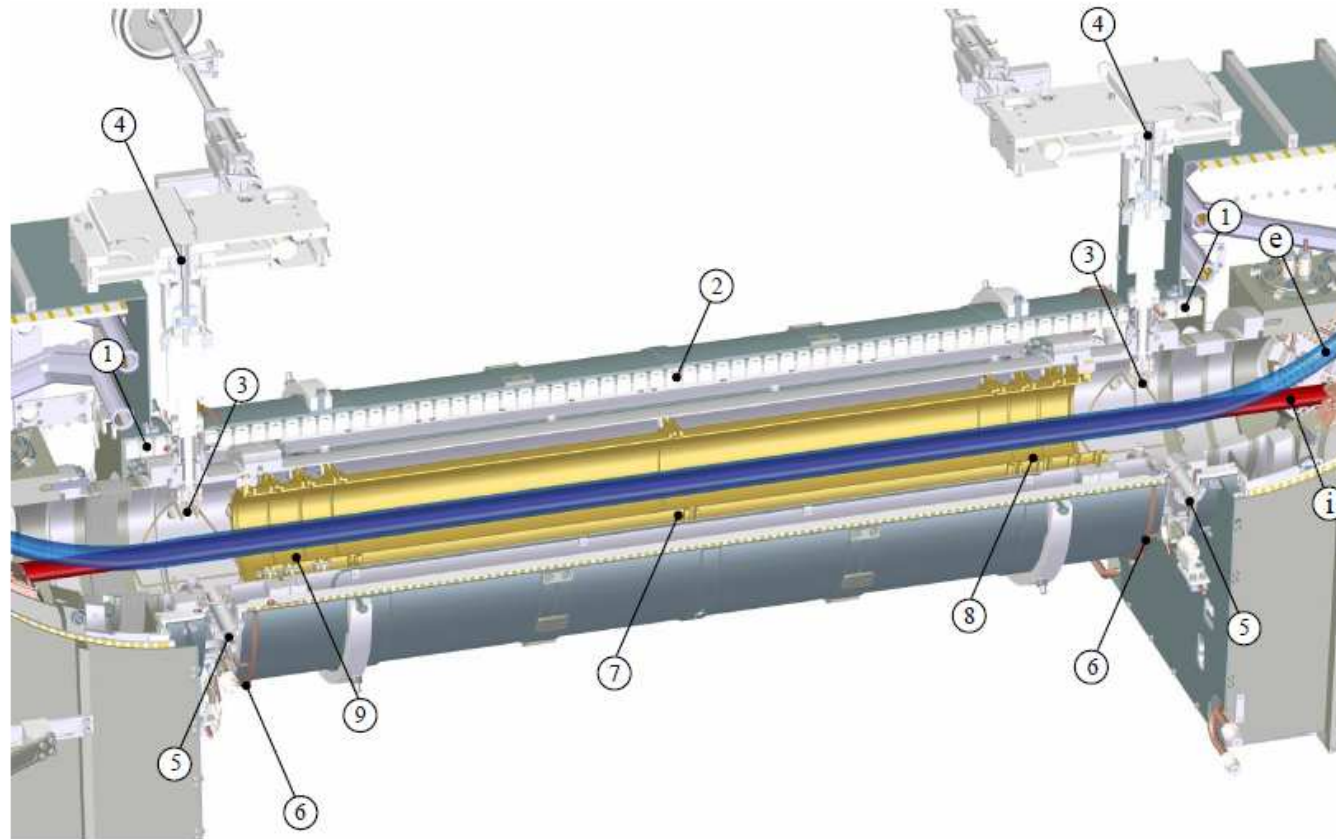


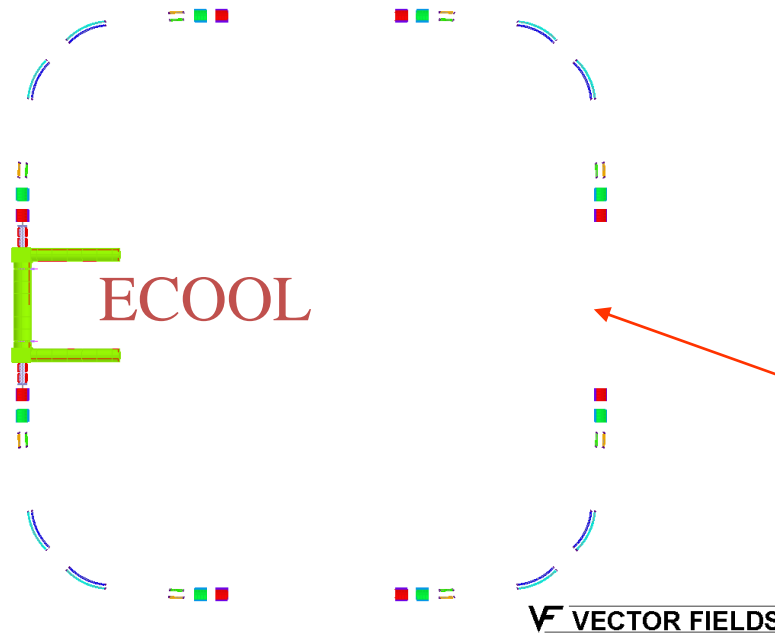
Figure 4.9: Mechanical design of the electron and ion beam interaction section with the (e) electron and (i) ion beam, the interaction solenoid, which is split in (1) two 47 mm and (2) one 944 mm long parts, providing two 34 mm wide gaps for electrical feedthroughs, (3) two wire scanners with (4) their rotational stages, and (5) two crossed laser beam viewports, (6) the transverse steering coils, and (7-9) drift tube consisting of different electrodes.

Acceptance Calculations with TOSCA

Envelope Calculation with TOSCA

Determination of the dynamic acceptance

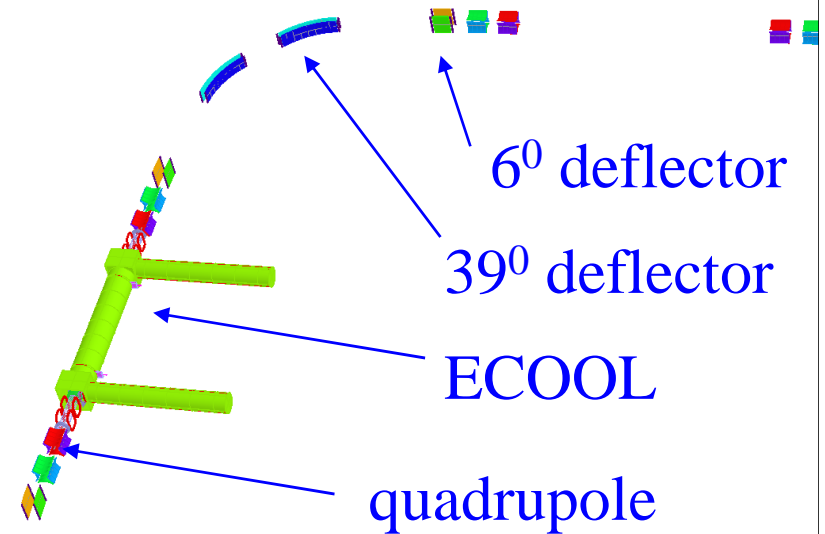
23/Mrz/2006 11:36:55



the hole storage ring was modeled with TOSCA
orbit calculation with real fields
for several hundreds turns

starting point

calculations were done
with and without ECOOL

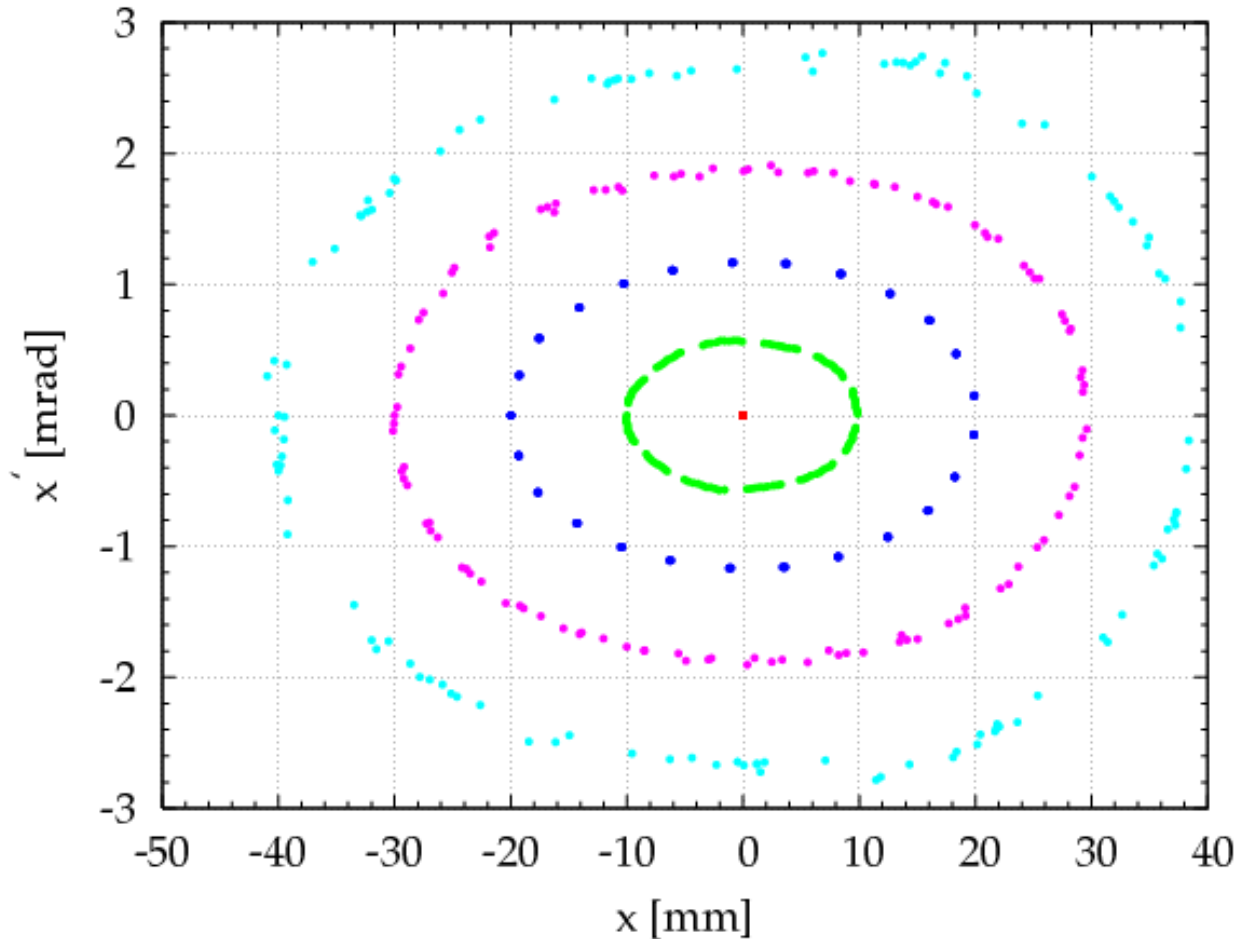


VECTOR FIELDS

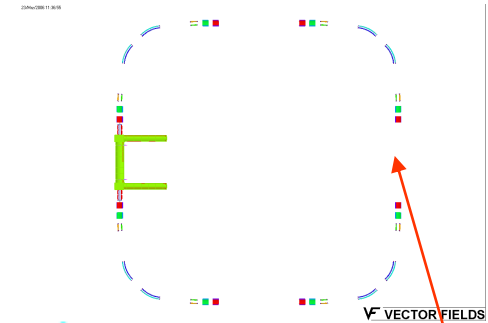
Horizontal Acceptance of the CSR (p 300 keV)

ECOOOL OFF

CSR Horizontal Phase Space Ellipse $E_i=300$ keV



- $X_i=0$
- $X_i=10$
- $X_i=20$
- $X_i=30$
- $X_i=40$



starting point

Maximum Beam Size in the center of the straight section

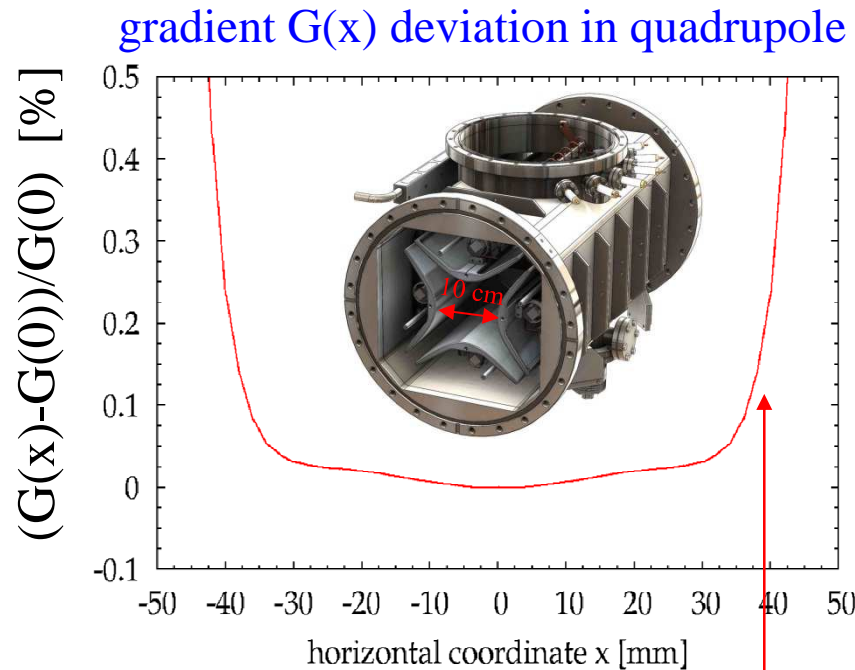
$$|x|_{\max} \approx 4\text{cm}$$

ions lost for $x > 4$ cm

reason: property of the quadrupole

Horizontal acceptance and quadrupole gradient

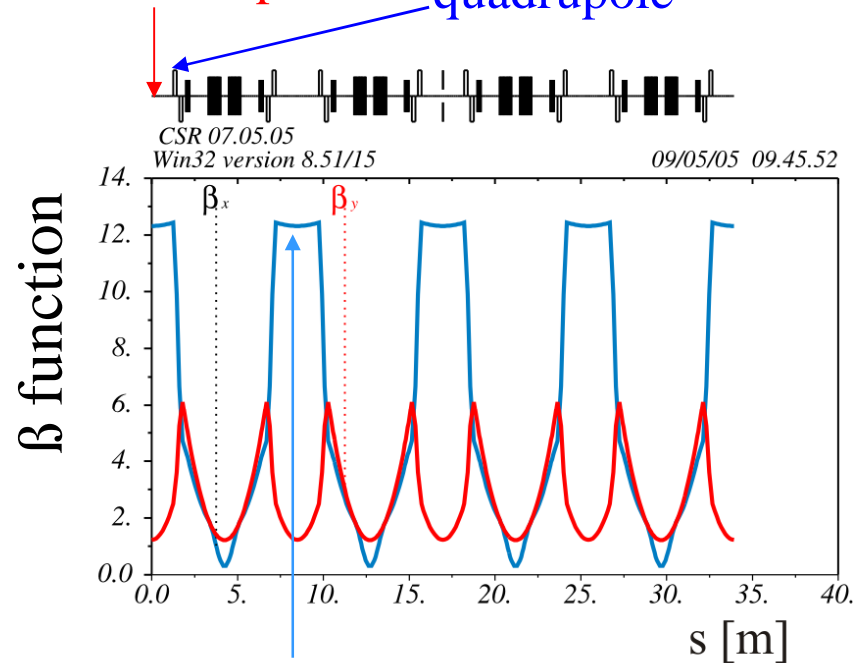
Orbit calculations with real fields: ion lost for $x > 4\text{cm}$



$x = 4\text{ cm}$

if x reaches 4 cm ions see a dramatically change of the quadrupole gradient
 \Rightarrow tune change \Rightarrow ions lost due to resonances

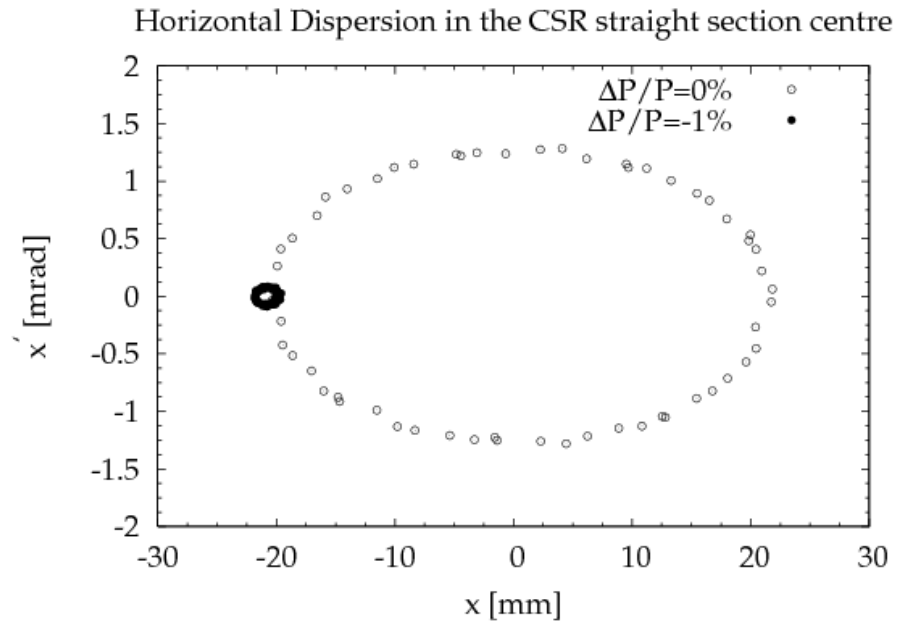
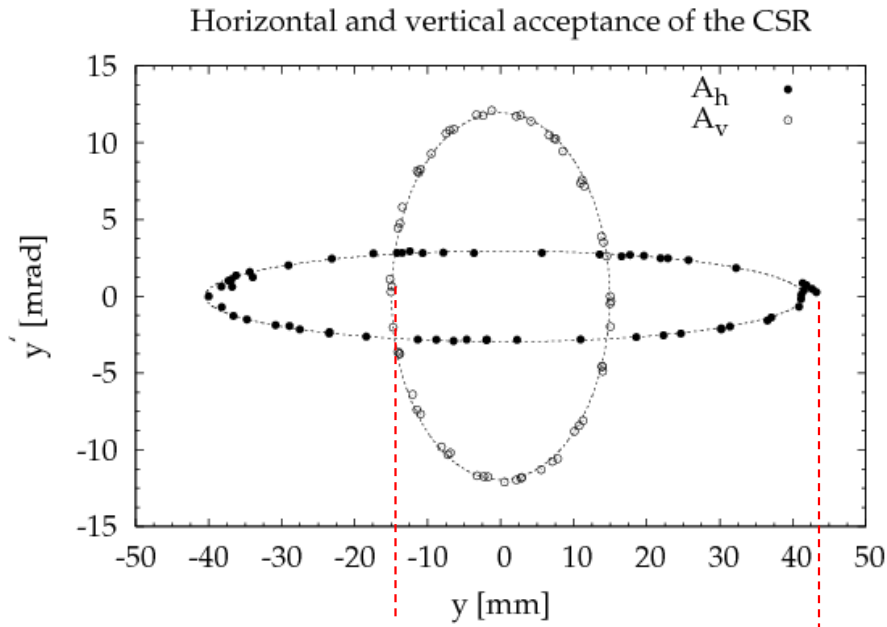
observation point quadrupole



horizontal β_x function

horizontal beam size
 centre straight section
 \approx beam size in quadrupole

Acceptance of the CSR (p 300 keV)



Lattice

± 15 mm

± 40 mm

Horizontal β function

Vertical β function

Dispersion

Acceptance horizontal

Acceptance vertical

Linear

12.3

1.2

2.1

—

Realistic

12.1

1.3

2.1

120

180

m

m

m

mm · mrad

mm · mrad

MAD8 calculations

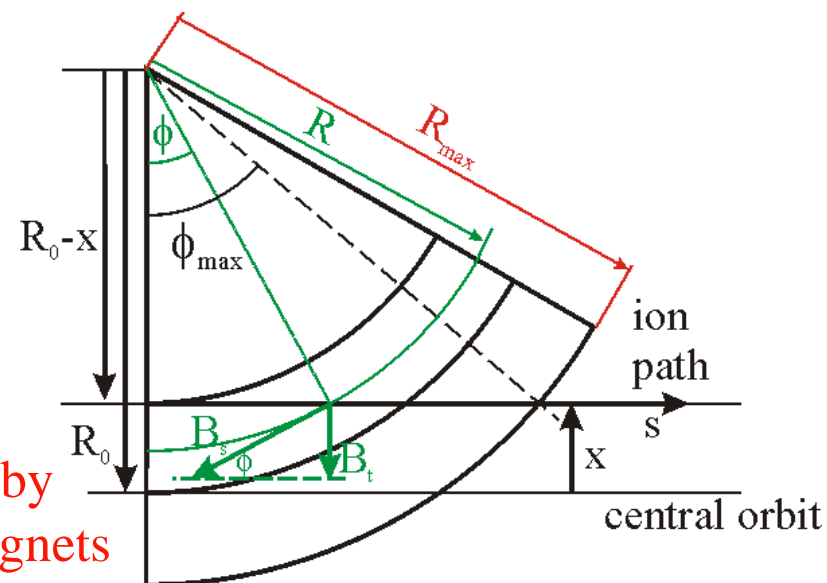
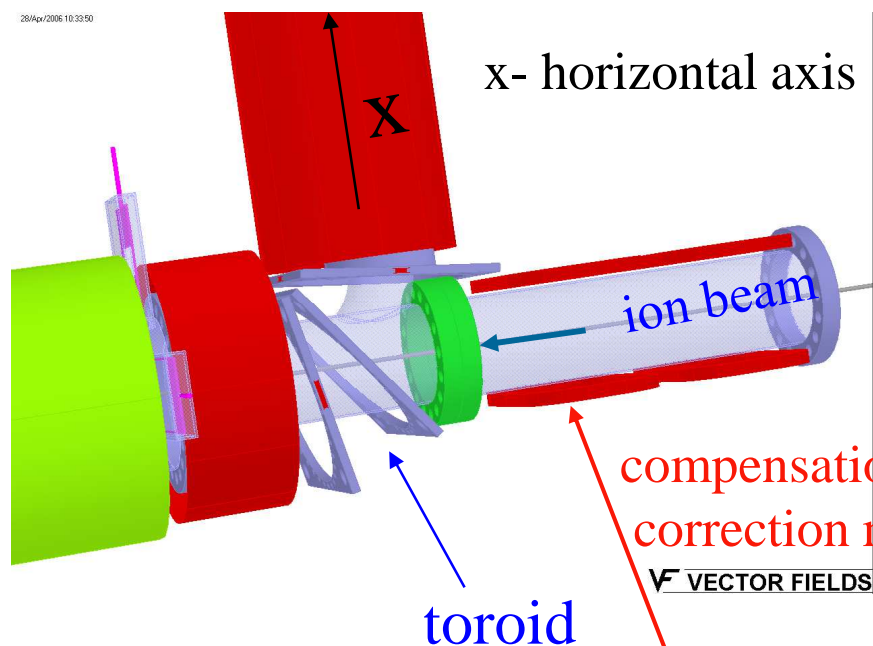
Tosca

Calculation done without ECOOL

First design of the electron cooler

first design of the electron cooler at CSR

vertical ion deflection
in the toroid fields

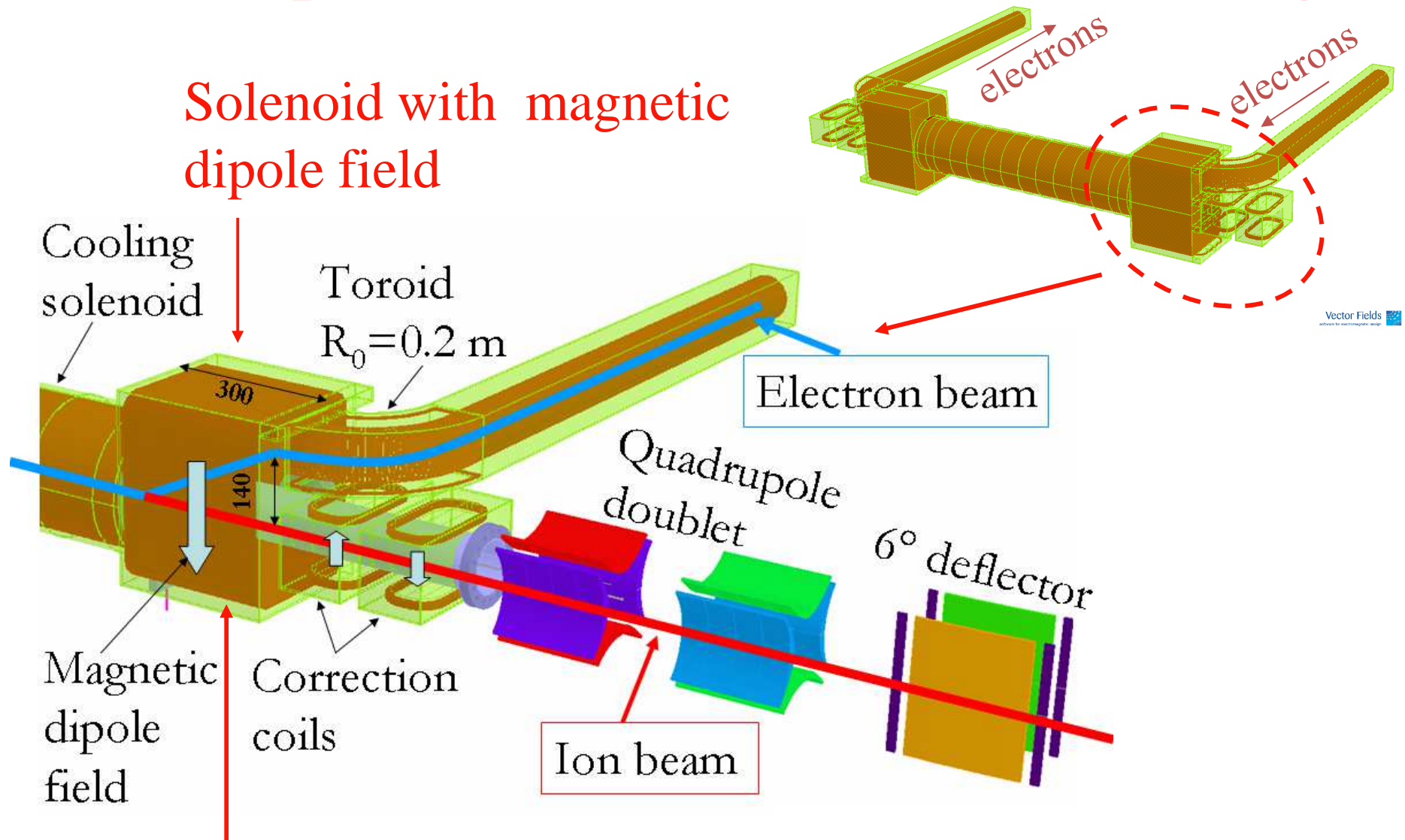


vertical deflection $\delta(x) = \delta(0) - \frac{B_0}{(B \cdot \rho)} \frac{R_0}{R_{\max}} \tan\left(\frac{R_0}{R_{\max}}\right) \cdot x + \dots$

result tracking calculations 20 keV protons can not stored at 30 G ,only
on axis ions stored at 10 G

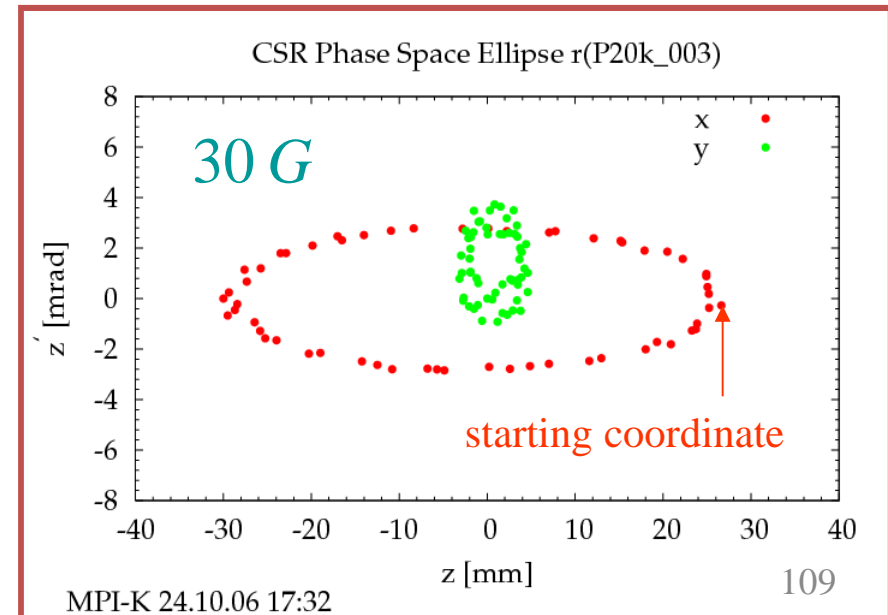
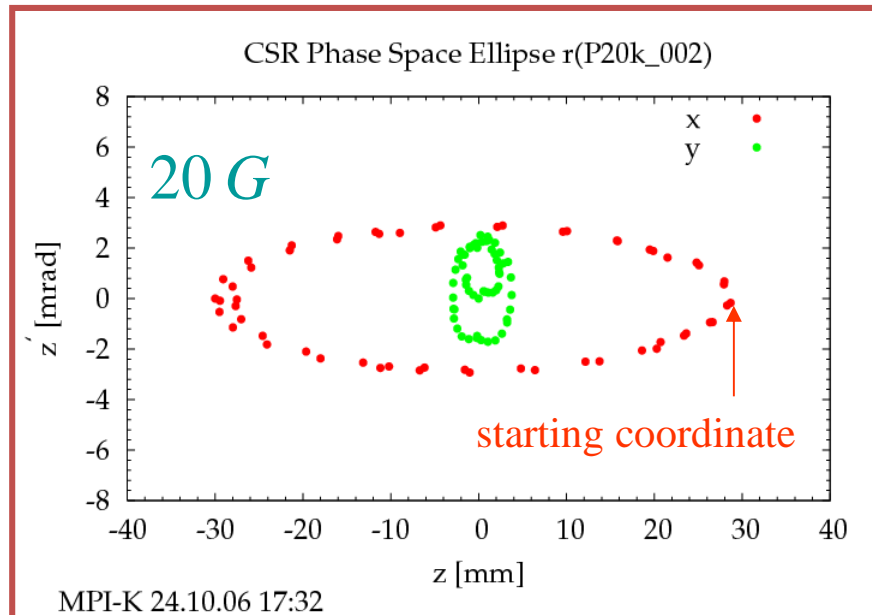
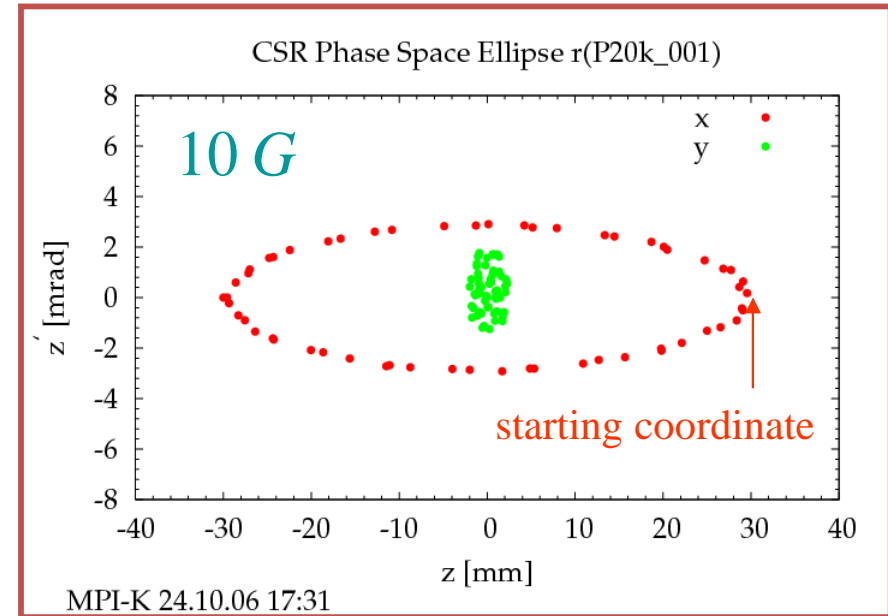
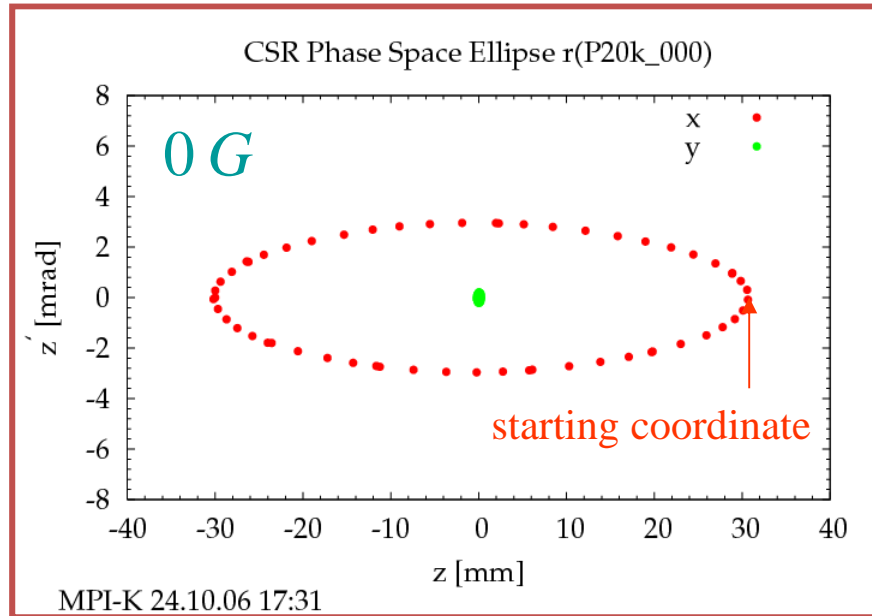
⇒ new electron cooler concept

New Concept for the CSR Electron Cooler/Target



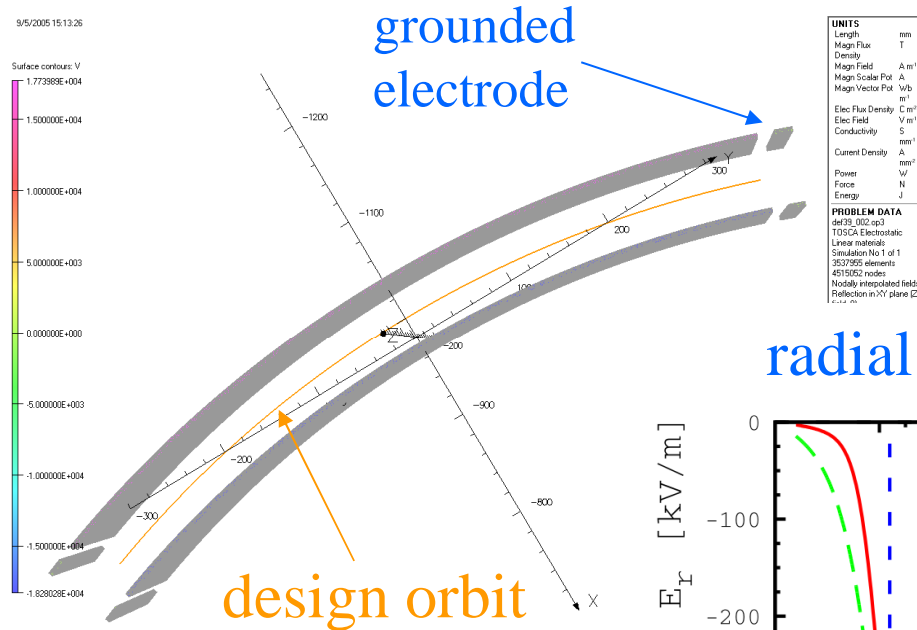
The deflection of low energy ions in the dipole magnetic field can be corrected completely by correction coils.

Ion motion of 20 keV proton with ECOOL



Field Calculations with TOSCA

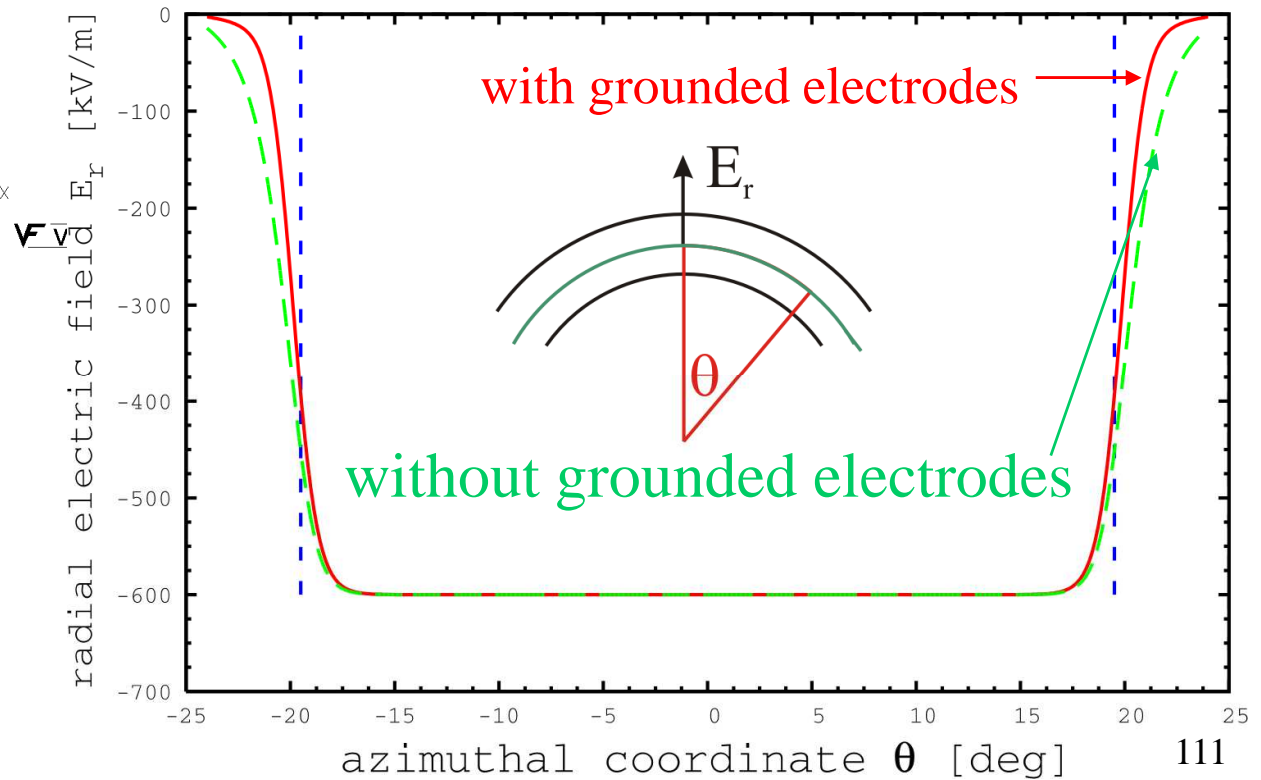
Calculation of the 39° deflector with Opera3D/Tosca



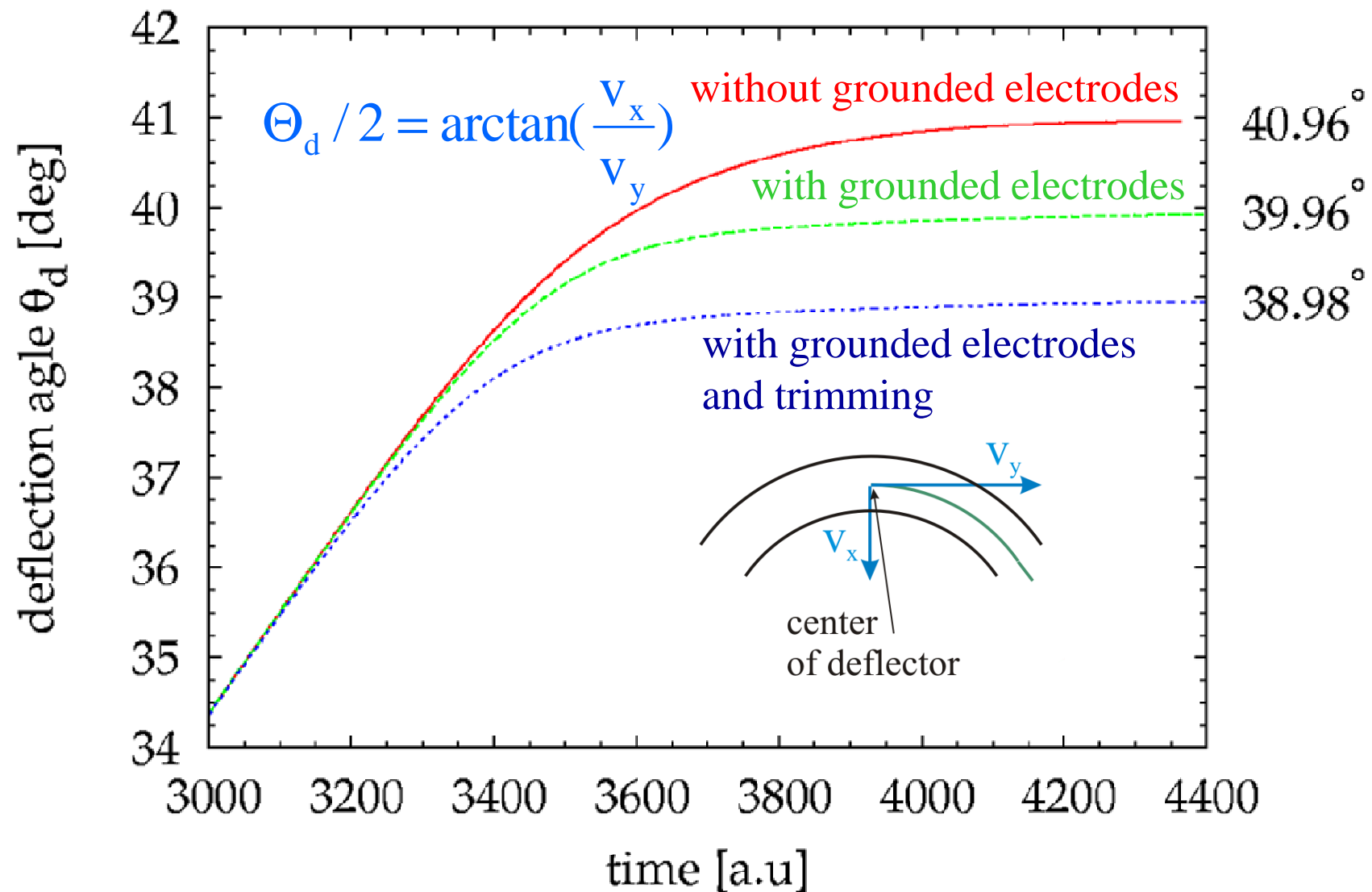
calculation done for ions with $E/Q=300$ kV

radial electric E_r field of the 39° deflector

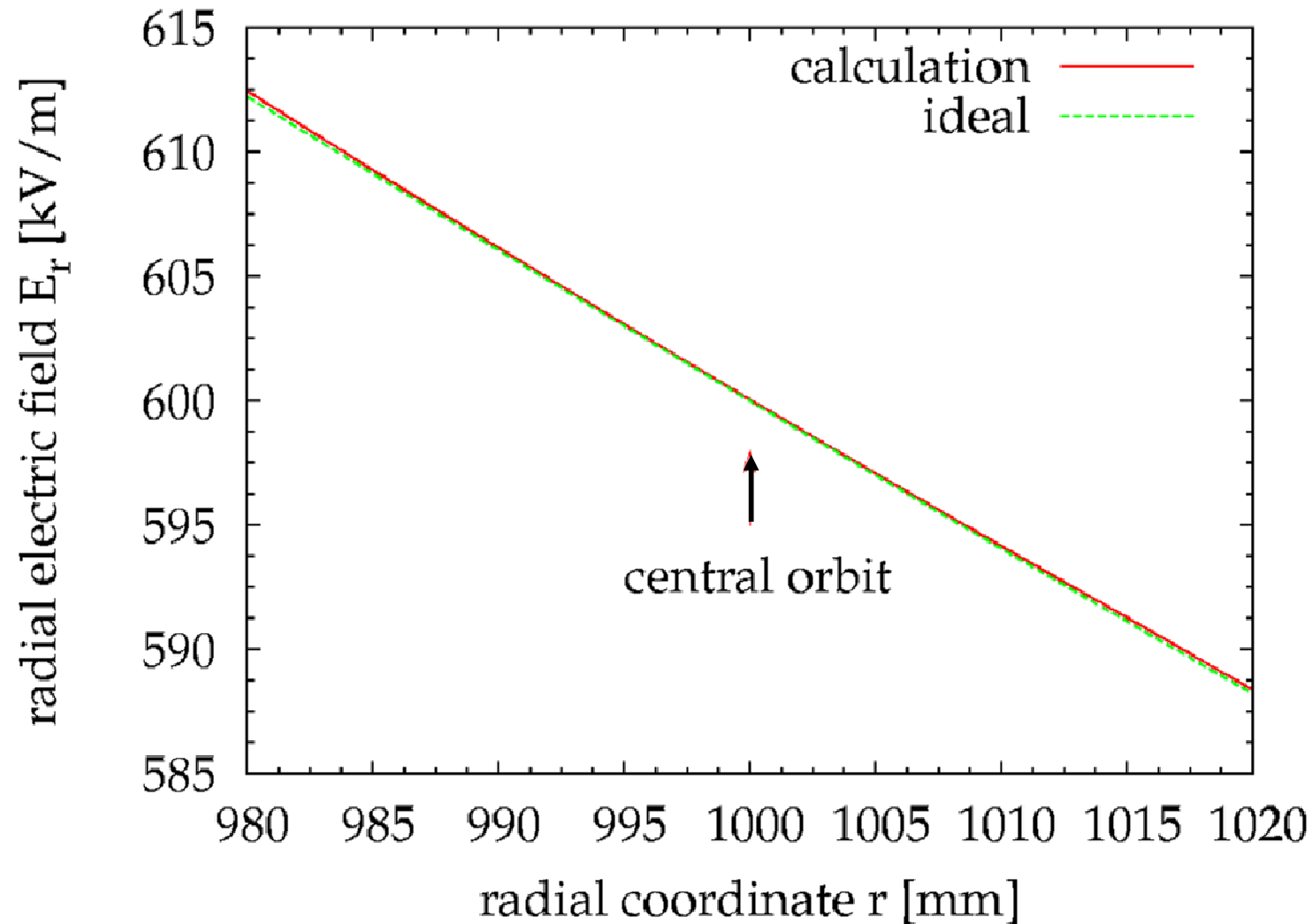
$\theta=39^\circ$
 $r=1$ m
 gap = 6 cm
 height = 16 cm



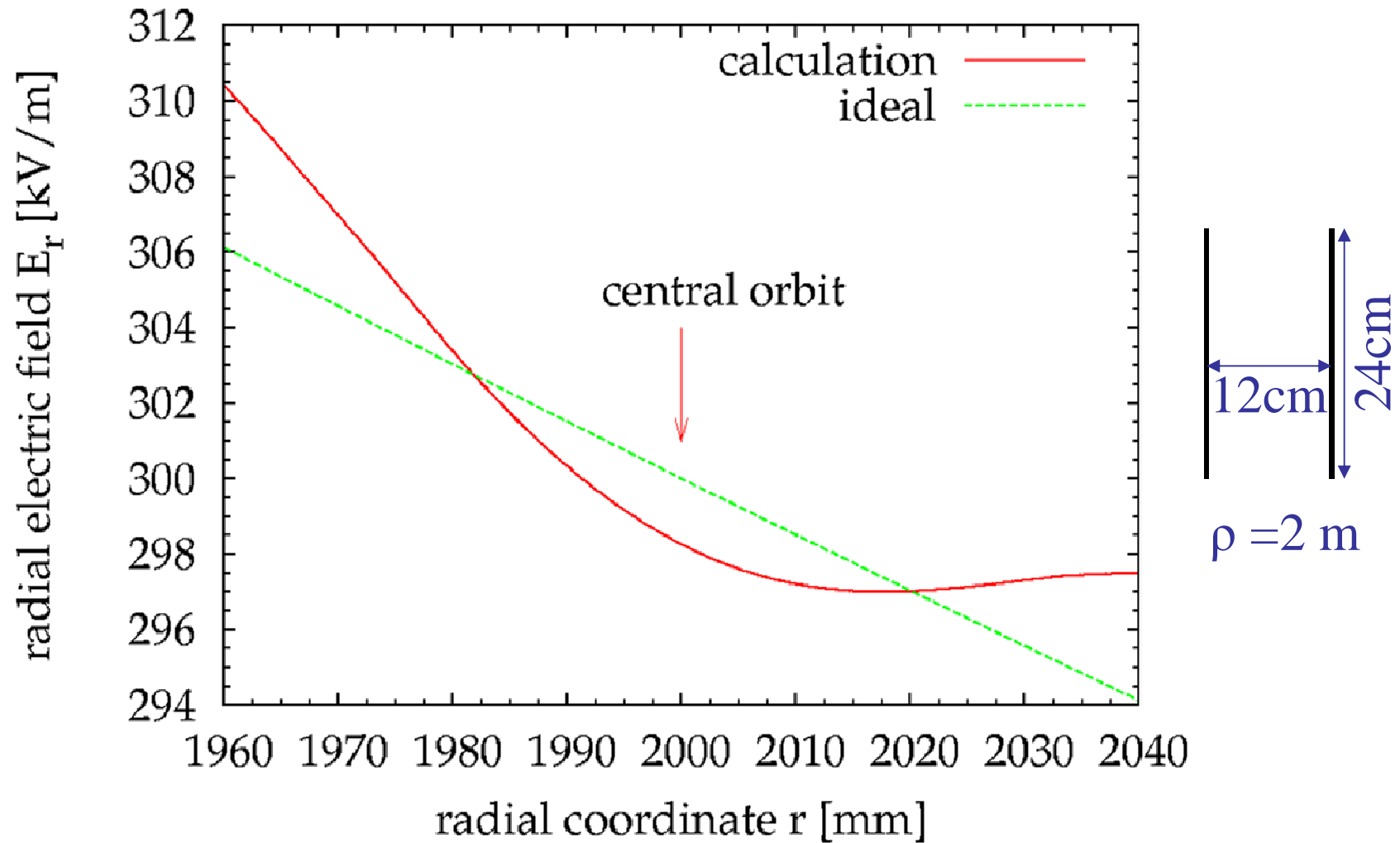
Determination of the deflection angle of 39° deflector



Radial electrical field E_r of the 39° CSR deflector



Radial electrical field E_r of the 6⁰ CSR deflector



All kinds of subjects

Quadrupole strength in MAD8

electrostatic quadrupole

quadrupole strength
in MAD8

$$K_{\text{mad}} = \frac{U}{R_0^2} \frac{Q}{E_0} \frac{L_{\text{eff}}}{L_{\text{MAD}}}$$

$$[K_{\text{mad}}] = \frac{1}{\text{m}^2}$$

U- electrode voltage

E_0 -kinetic energy

Q- ion charge

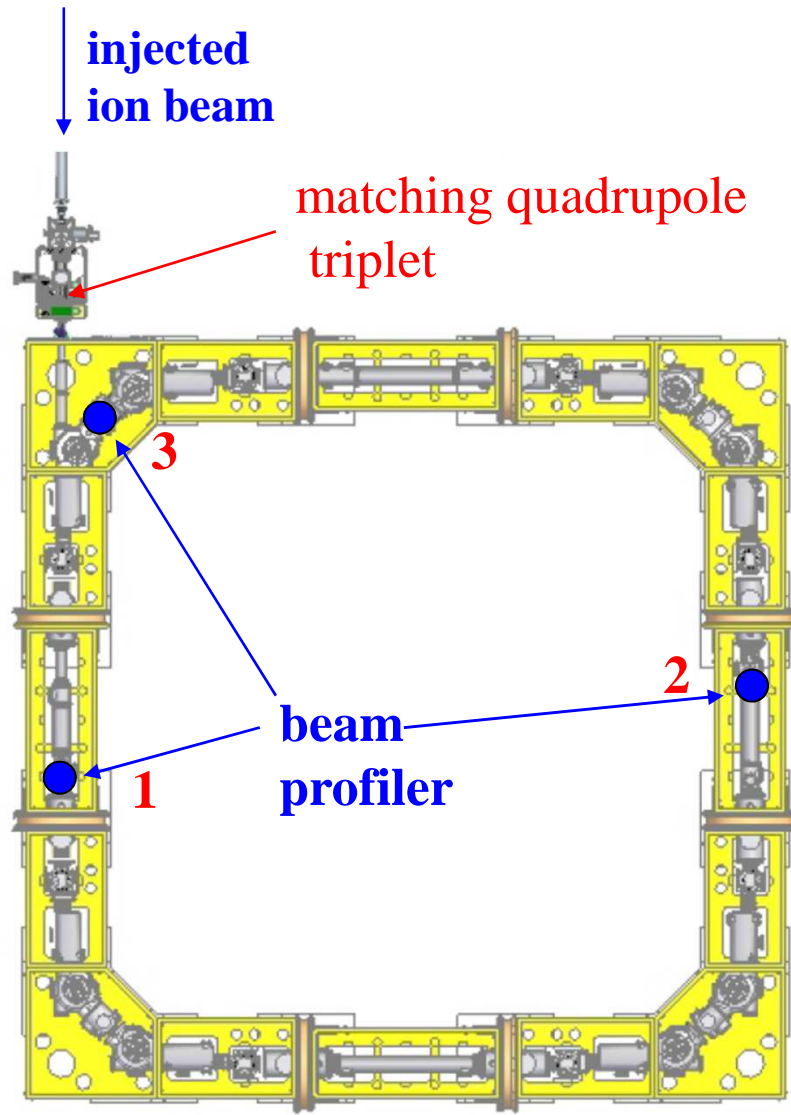
R_0 -aperture radius

L_{eff} -effective length ← determined with TOSCA and tune measurement



in first order transport matrix of an electrostatic quadrupole is the transport matrix of an magnetic quadrupole

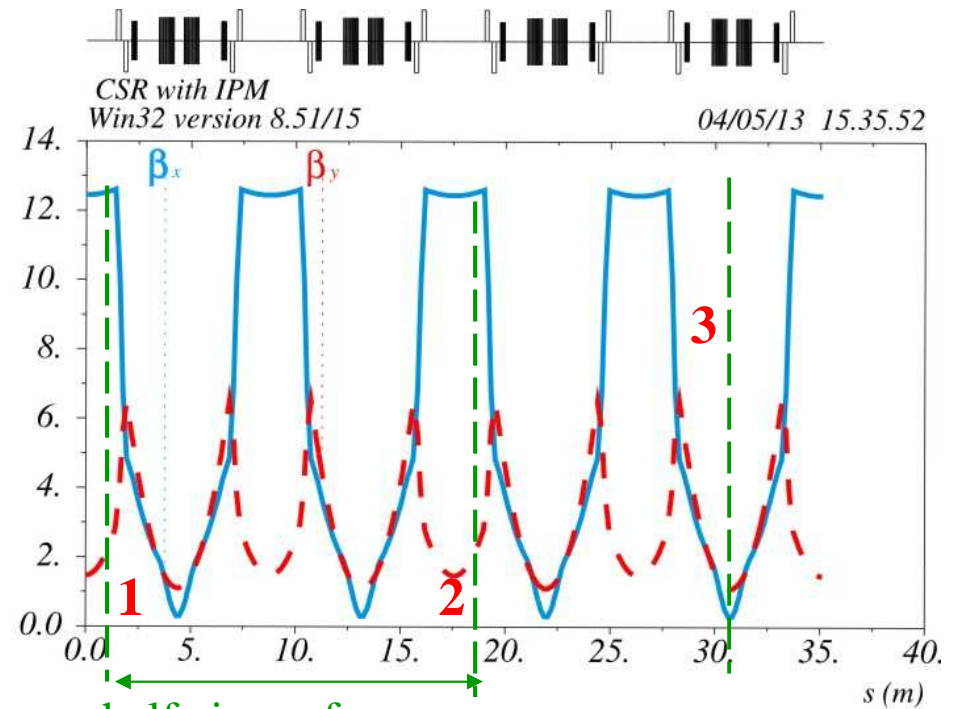
First turn diagnose



beam profile

- used to detect the beam on its first turn
- used to check the matching condition with profiler 1 and 2:
horizontal and vertical beam width at position 1 and 2 should be equal.

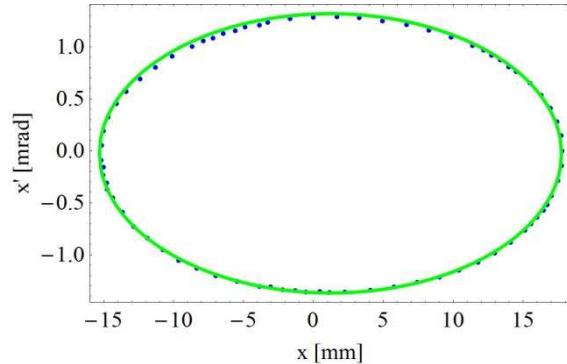
β function of CSR



half circumference =
distance between profiler 1 and 2

First stored ion beam at the CSR

$^{40}\text{Ar}^+$ with $E=20\dots100$ keV

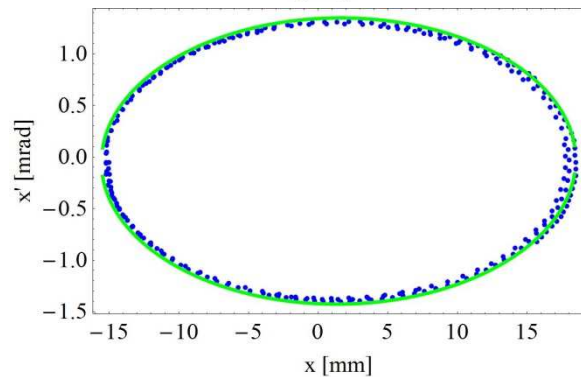


start coordinate: $x=-15$ mm

with earth magnetic field

$E=100$ keV

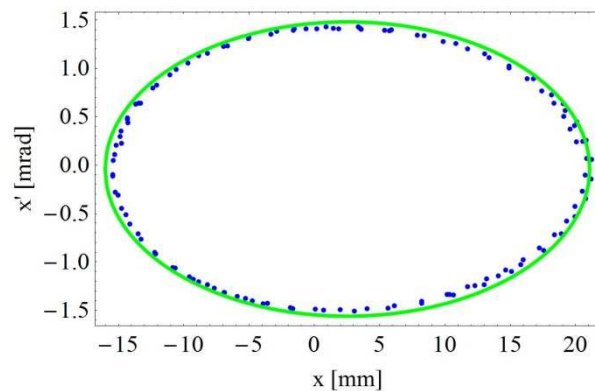
$\Delta x_s=1.22$ mm $\Delta x'_s=-0.0241$ mrad



with earth magnetic field

$E=50$ keV

$\Delta x_s=1.47$ mm $\Delta x'_s=-0.039$ mrad



with earth magnetic field

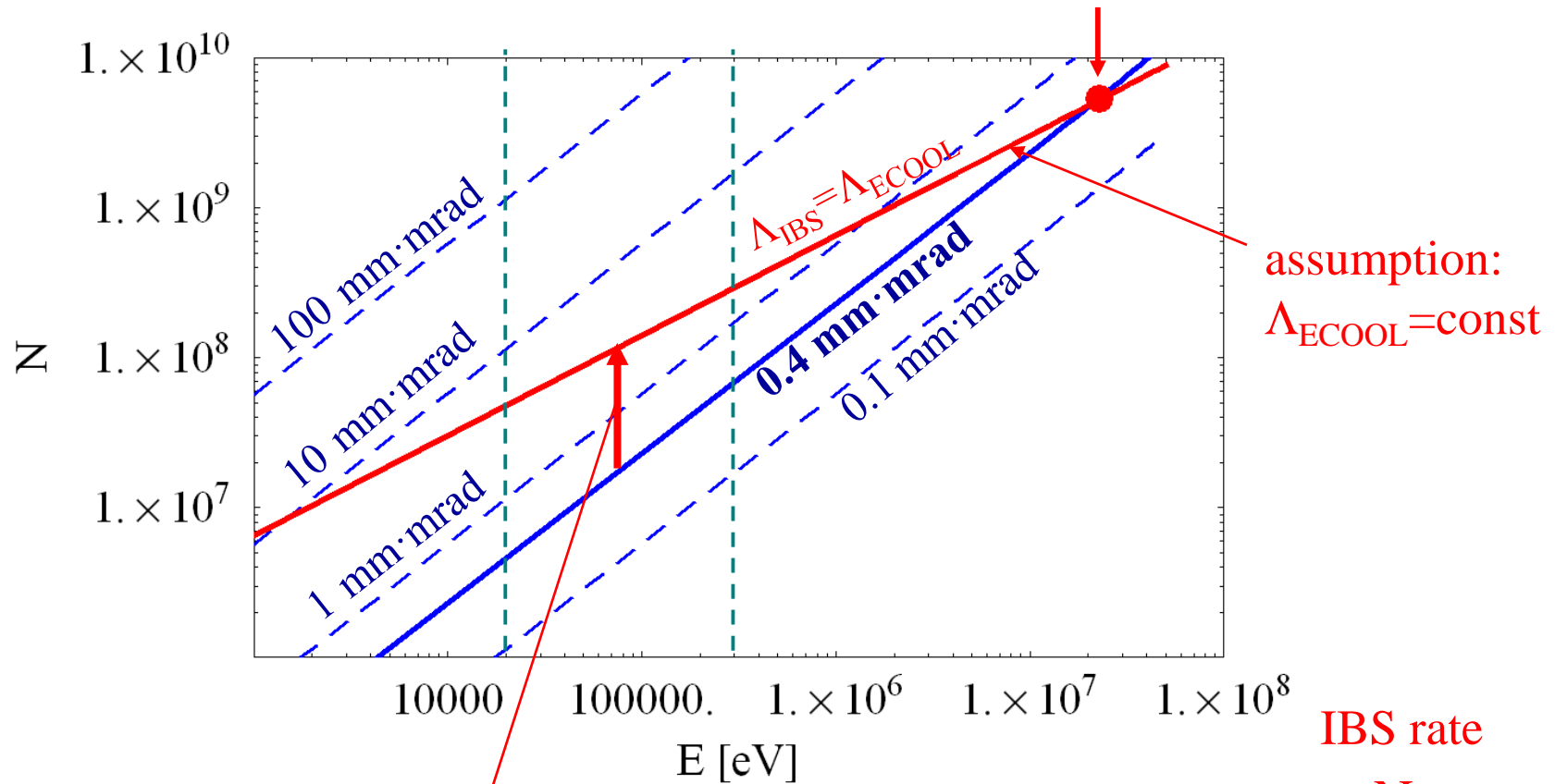
$E=20$ keV

$\Delta x_s=2.53$ mm $\Delta x'_s=-0.04$ mrad

Space charge limit of a cooled stored proton beam

incoherent tune shift:
$$N = \frac{2\pi}{r_p} \cdot B \cdot \beta^2 \cdot \gamma^3 \cdot \varepsilon \cdot (-\Delta Q)$$

TSR: $N=5.3 \cdot 10^9$ $E=23$ MeV $\varepsilon=0.4$ mm·mrad $B=1 \Rightarrow -\Delta Q=0.065$



due to large intra beam scattering rates ε is increased

$$\Lambda_{\text{IBS}} \sim \frac{N}{\beta^3 \cdot \varepsilon^2 \cdot \Delta p / p \cdot L_B}$$

Tune as function of the quadrupole strength at working point II

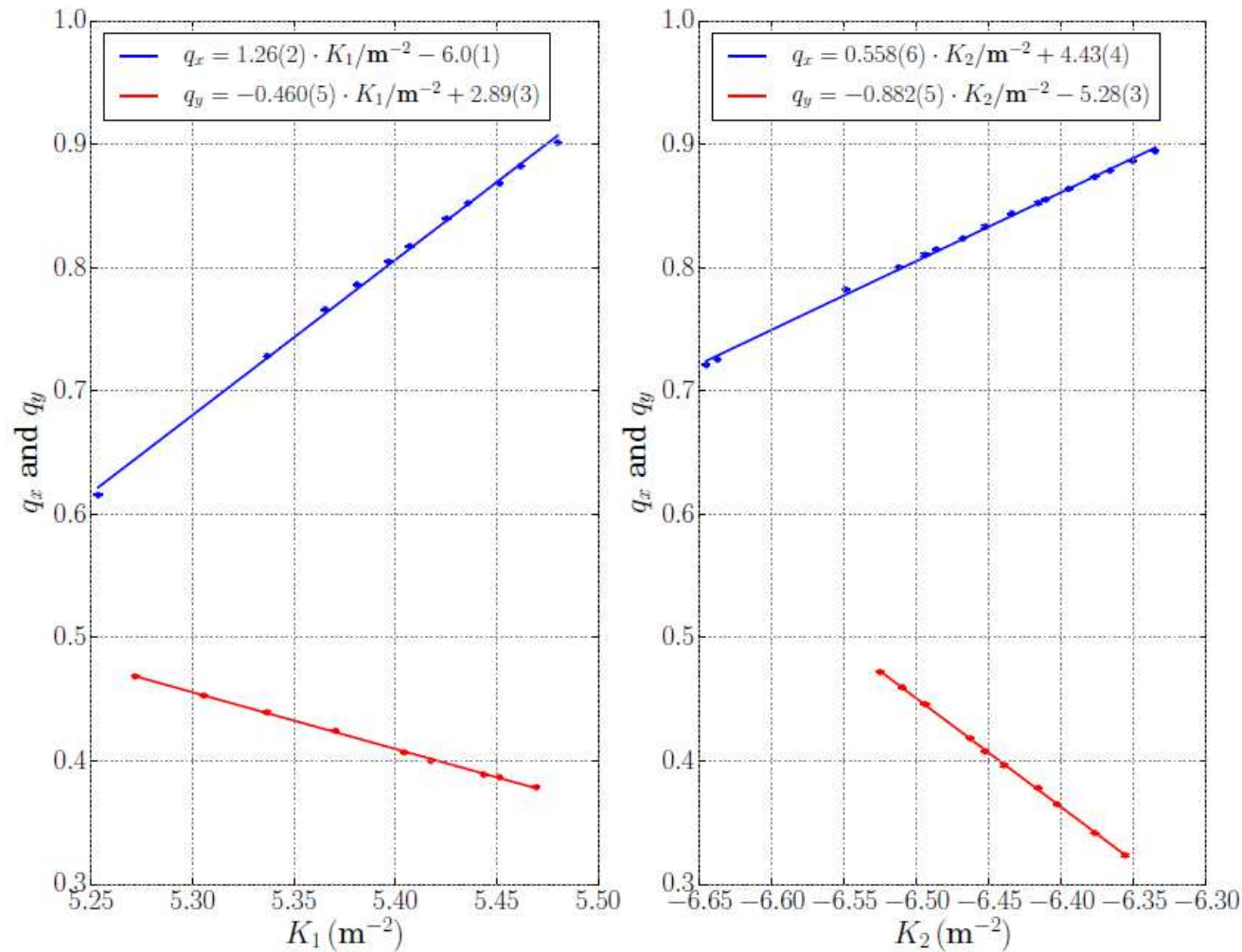


Figure 5.19: Measured fractional tune values q_x (blue) and q_y (red) as functions of the quadrupole strengths of family 1 (left column) with $K_2 = -6.44(9) \text{ m}^{-2}$ and 2 (right column) with $K_1 = 5.43(8) \text{ m}^{-2}$ at the first working point.

Measurement of the momentum compaction factor α_p

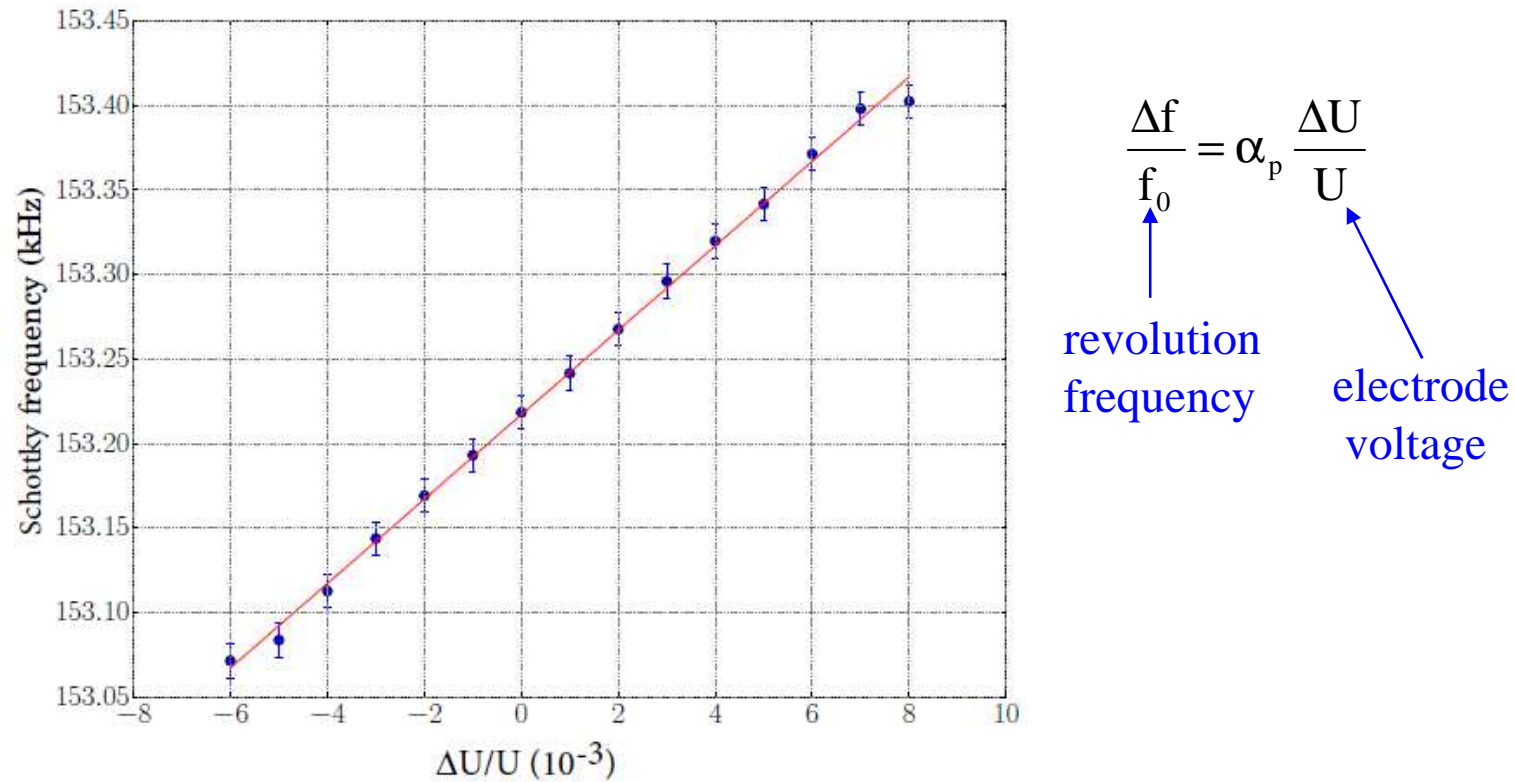
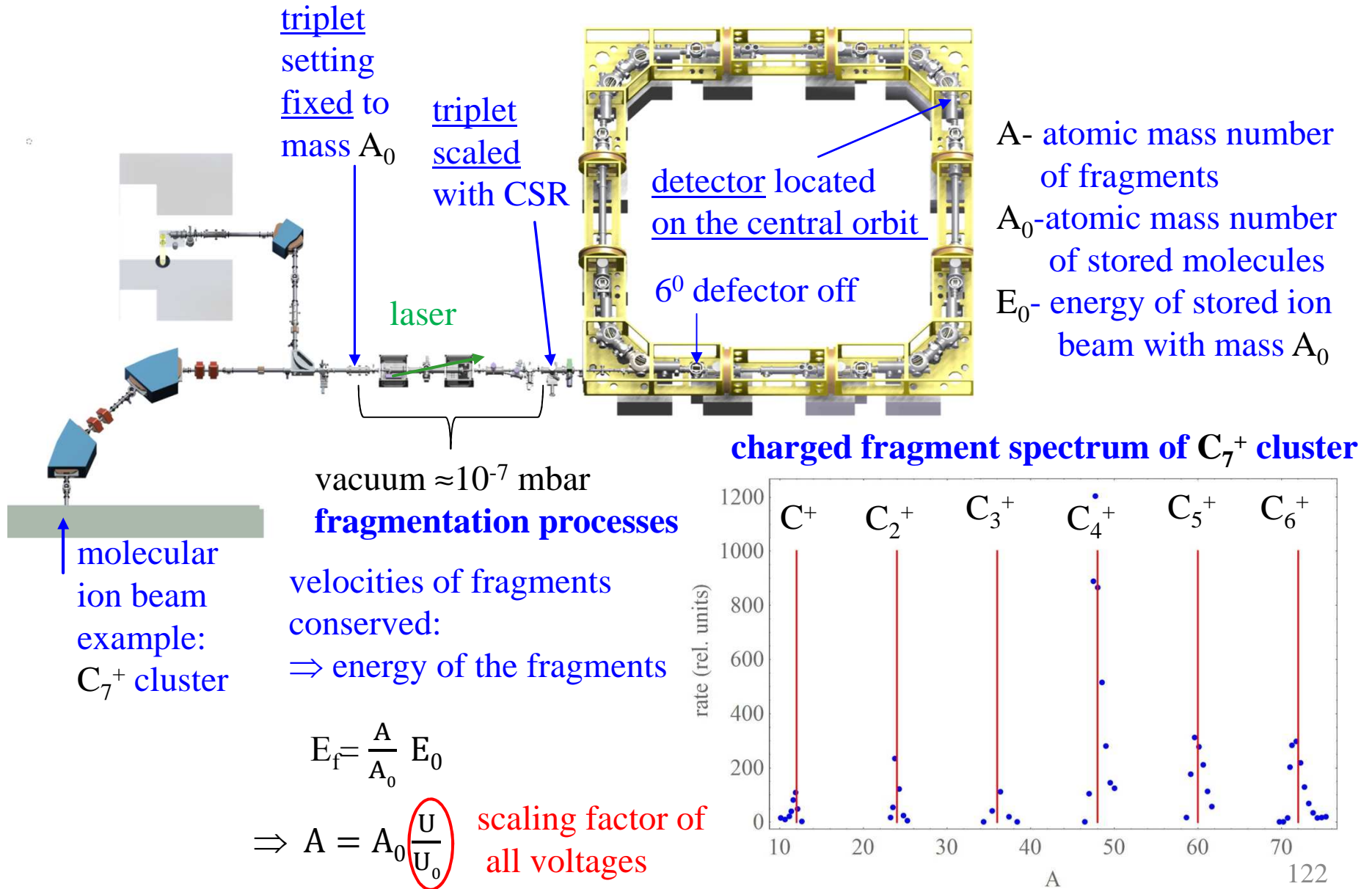


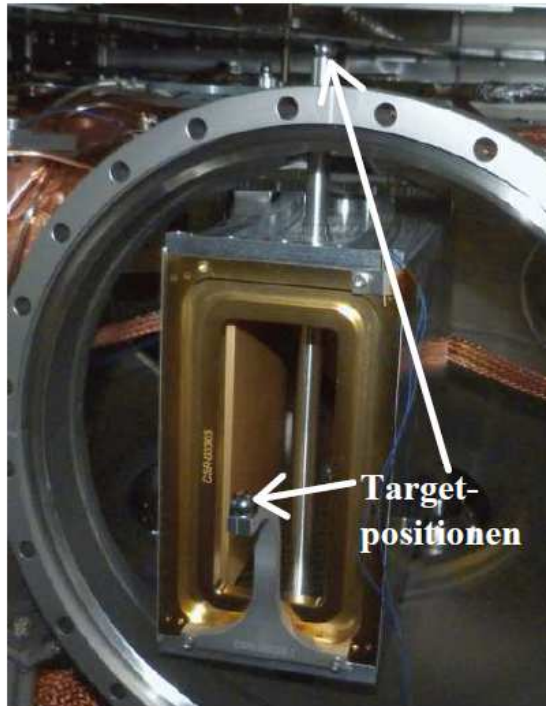
Figure 2. Schottky frequency measured at 10^{th} harmonic of the revolution frequency as a function of the variation of the voltages of all CSR deflectors and quadrupoles expressed by $\Delta U/U_0$.

published in

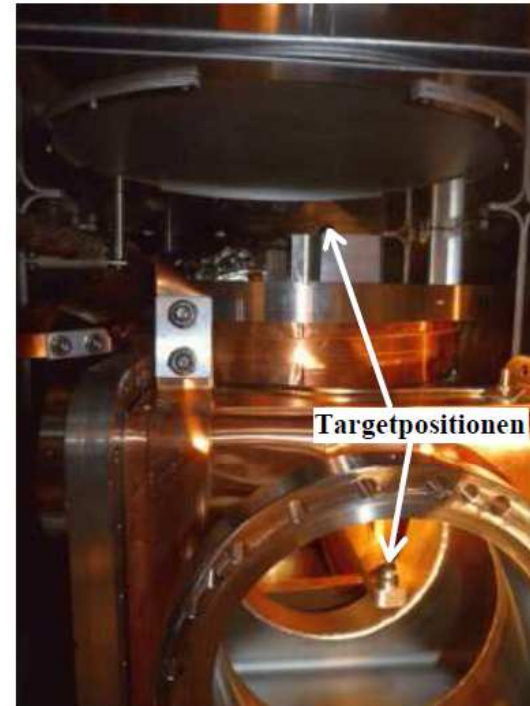
CSR as a mass spectrometer for charge molecular fragments



Laser tracker measurements to measure the position of the elements at warm and cold conditions



(a)



(b)

Abbildung 4.13: Targethalterung zur Vermessung von 39° - a) und 6° -Deflektoren b) im warmen und kalten Zustand.